The Characterisation of Supported Cobalt Catalysts

Fiona. A. Wigzell

Masters Thesis

Department of Chemistry
The University of Glasgow

July 2007

ABSTRACT

The characterisation of a range of supported cobalt catalysts was investigated. The effect of the support as well as the precursor was studied using a combination of characterisation techniques.

Catalysts were prepared via aqueous impregnation of silica, alumina and 99% silica + 1% titania with solutions of cobalt nitrate or acetate. B.E.T analysis showed comparable surface areas for all supports investigated.

The catalysts were subjected to heat treatments in argon, oxygen and hydrogen to examine the effect of the varying supports and precursors. Differences in the temperatures of decomposition and reduction as well as changes in the composition of the evolved gases, revealed that both support and precursor are both important in determining the stability of the system.

Temperature programmed X-ray diffraction was used to determine the phase composition and crystallite size distribution. This confirmed that for all of the catalysts cobalt was present as Co_3O_4 species as the product of decomposition, and furthermore allowed for determination of cobalt species crystallite size at varying temperatures. Weight loss and thermal events associated with decomposition and reduction were followed using a combination of TGA-DSC. On-line mass spectrometry, allowed for identification of evolved gases. Consequently it was shown that decomposition of supported cobalt catalysts was more complex than the bulk cobalt salts. In addition decomposition of cobalt nitrate supported catalysts were found to be endothermic in contrast to the highly exothermic decomposition of cobalt acetate supported catalysts.

AKNOWLEDGEMENTS

First and foremost I should like to express my thanks to Professor S. D. Jackson for his constant help and encouragement throughout the course of this research. I would especially like to thank him for never once being too busy to discuss my work.

My thanks are also due to my colleagues and the technical staff, especially Andy Monaghan for many useful discussions and assistance.

Finally I would like to thank my family and friends for their patience and support.

Declaration

The work contained in this thesis, submitted for the degree of MSc, is my own original work, except where due reference is made to other authors. No material within has been previously submitted for a degree at this or any other university.

Fiona Anne Wigzell

CONTENTS

A FIGURES

B TABLES

1.0 INTRODUCTION

1.1 Heterogeneous catalysis

Catalysts are the keys to the efficiency of most industrial chemical processes. By definition, a catalyst is a substance that increases the rate of approach to equilibrium of a chemical reaction without being substantially consumed in the reaction [1]. It operates by allowing a reaction to follow a different pathway from that of a non-catalysed reaction. A catalyst however does not affect the thermodynamics or the equilibrium position and therefore the Gibbs free energy (ΔG) of the overall reaction is unchanged for both energy profiles. This is illustrated in figure 1.1.

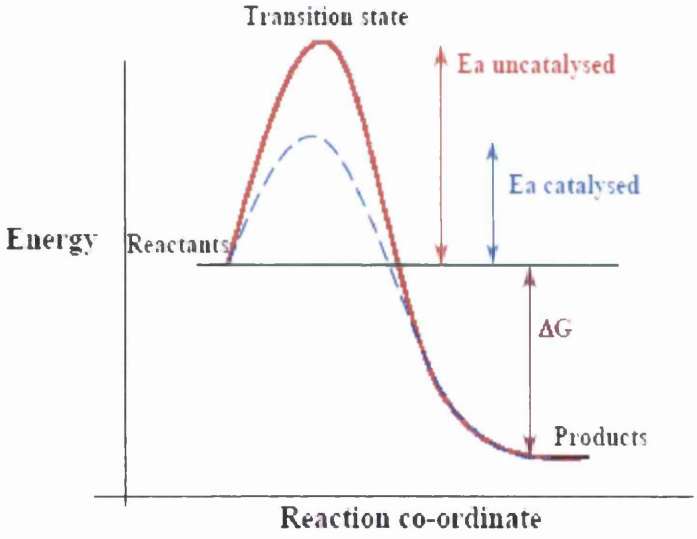

Figure 1.1 Schematic representation of energetics associated with a catalytic reaction [2]

Catalysts fall into two categories, homogeneous in which the catalyst is in the same phase as the components of the reaction and heterogeneous where the catalyst is in a different phase from the components of the reaction. Heterogeneous catalysis makes up the majority of industrially catalysed processes, and is fundamental to the production of fuels and plastics. In heterogeneous catalysis a surface is provided for the molecules to attach and react on. A simplified diagram of the molecular level processes involved are illustrated in Figure 1.2. The first step involves the diffusion of the gas phase onto the metal surface

where they may bond (adsorption) in a molecular form. Surface diffusion may now occur, depending on the internal bond strength of the molecule. This is followed by surface reaction, often the rate determining step. Finally product desorption occurs, where the product to surface bond is broken [3].

Figure 1.2: Molecular and atomic events during catalytic reaction

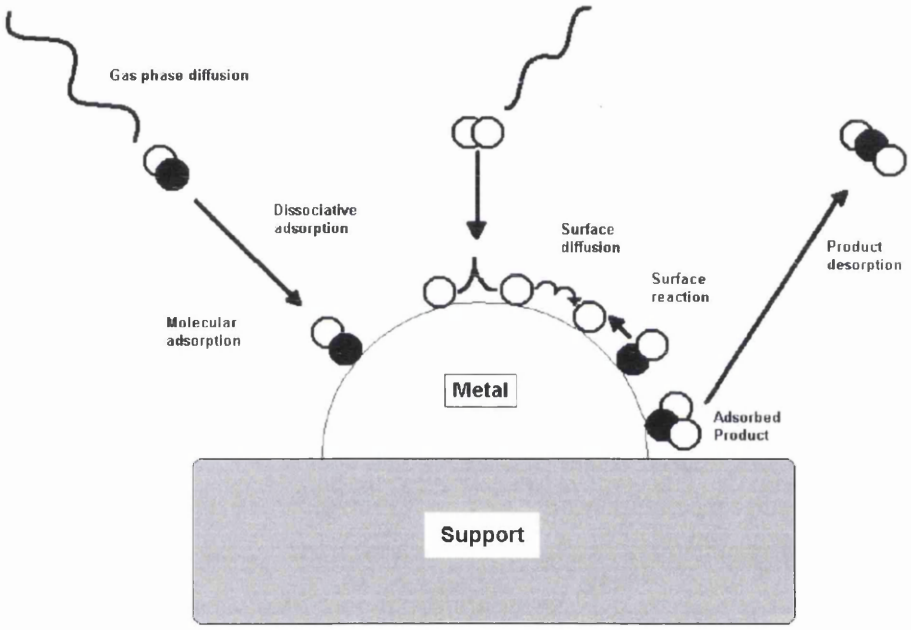

1.2 Cobalt catalysts

Research into cobalt catalysts is an area of importance to industry, due to their extensive application in a range industrial processes. Cobalt catalysts are used in many applications, from decomposition of methanol to Fischer-Tropsch synthesis, mainly due to their high activity and low cost.

1.2.1 Characterization of cobalt catalysts

There is a huge amount of literature available in the scientific press citing the characterisation of cobalt catalysts. There have been many studies examining the structural, chemical as well as electronic properties of these catalysts. These results are obtained using a combination of different methods, the majority of which make use of techniques such as temperature-programmed reduction and oxidation (TPO/TPR), T.E.M, X-ray diffraction (XRD), thermogravimetric analysis and differential scanning calorimetry (TGA-DSC). It has been well documented that the different preparation variables influence the catalysts structure and morphology. The following sections aim to look at the literature concerned with the effect of some of these variables. Rather than quoting every possible reference, key studies have been selected which exemplify typical aspects of cobalt catalyst characterisation.

1.2.1.1 Supports

The role of the support is rather well established. It provides mechanical strength and thermal stability to the cobalt nanoparticles, while facilitating a high cobalt dispersion. A variety of supports are used to prepare cobalt catalysts depending on the properties required; however the bulk of the literature is concerned with high surface area oxide supports, in particular silica, alumina and titania supported cobalt catalysts. The use of supports such as zeolites [4], carbon [5] have also been reported in the literature. There have been many studies into the interaction between the support and the cobalt species. This is due to the fact that the interaction between cobalt species and support can affect the response of cobalt to reduction as well as the dispersion[6]. The choice of the oxide support largely determines the number of active cobalt metal sites stabilized after reduction as well as the percentage of cobalt oxides that can be reduced to cobalt metal. This is due to a difference in the Co-support oxide interaction. A strong Co-support oxide interaction, as occurs in the case of alumina and titania, stabilises small clusters therefore favouring high dispersion, but at the same time decreases their reducibility. On the contrary, a much weaker interaction leading to higher reducibility occurs for the silica supported cobalt catalysts. In this case the cobalt particles tend to appear as large clusters on the support surface. This however, results in a relatively low cobalt dispersion [7-9].

It has been has also been shown that the pore structure of the supports has a significant effect on the cobalt particles produced. Storsæter *et al.* [8] using a variety of techniques, to

investigate the effect the support had on the size, appearance and shape of the cobalt particles. They reported that the cobalt oxide crystallite size was found to increase with increasing pore diameter of support. Similar effects have been observed for cobalt catalysts supported on silicas with increasing mean pore diameters [10].

1.2.1.2 Precursor

There is a variety of precursors used for the preparation of cobalt supported catalysts, these include cobalt EDTA, ammonium cobalt citrate, cobalt acetylacetonate and cobalt chloride [11-13]. The majority of the literature, however, is concerned with the cobalt nitrate and cobalt acetate salts. Giradon *et al.* [14] examined the effect of different precursors using TGA-DSC. They found that the precursor used strongly influences the structure of the supported cobalt species formed. Depending on the exothermicity of cobalt precursor decomposition, the supported cobalt ions either agglomerated to form Co_3O_4, or reacted with the silica support yielding amorphous cobalt silicate. Studies by Martínez *et al.* [12] examined the difference between acetate and nitrate precursors. They reported that although the acetate precursor gave smaller cobalt particles, these small particles then subsequently reacted with the support during thermal treatment. Therefore it has been shown that ideal catalyst precursors are those which produce cobalt oxide particles which while sufficiently large enough to avoid complete reaction with the support are still small enough to exhibit favourable catalytic properties.

1.3 Fischer-Tropsch

Despite cobalt catalysts being used in a variety of industrial applications, the majority of the literature is concerned with their use as Fischer-Tropsch catalysts.

1.3.1 Brief history

Fischer-Tropsch synthesis is a catalytic reaction between CO and H_2. It was discovered by co-workers Franz Fischer and Hanz Tropsch in Germany in the 1920's and yields a variety of products the bulk of which comprise of saturated and unsaturated olefins [15]. Despite being a major scientific breakthrough at the time, the FT process was unable to compete economically with the refining process of crude oil which became important from the 1950's onwards. One exception to this was Sasol in South Africa where embargoes due to apartheid forced the country to look for alternative energy sources. Today a renewed interest in FT technology is mainly due to:

1. Changes in fossil energy reserves
2. Environmental demands to provide 'greener' fuels, in particular the production of sulphur-free diesel fuel
3. The commercialisation of otherwise unmarketable natural gas at remote locations.

This has all led to the recent decisions on major investments by leading petrochemical companies to build large scale plants for example in Qatar. This will inevitably result in a change from crude oil to natural gas as a feedstock for the production of fuels and chemicals in the future. With projects either under construction or in planning it is believed that by the year 2020, 5% of the total production of chemicals could be based on FT technology using methane instead of crude oil refining operations. Adding to this the long-term reserves of coal, the future of Fischer-Tropsch synthesis looks to play a major role in fuel energy scene [16, 17].

1.3.2 Co-based Fischer-Tropsch catalysts

It is well know that all Group VIII transition metals are active for FT synthesis. However, the only metals which have the required Fischer-Tropsch activity for commercial application are composed of Ni, Co, Fe or Ru as the active metal phase [18]. These metals are orders of magnitude more active than the other Group VIII metals.

While there has been much activity in the literature relating to Fe, Ru, and Ni Fischer-Tropsch catalysts, the largest body of papers and patents in the last three decades have dealt with Co-based FT catalysts. This is in an attempt to make more active catalysts with

high wax selectivities (the waxy product then being the feed for hydrocracking), and low water-gas shift activity. Typical the metal loadings of cobalt are between 10-30g of cobalt for 100g of support [19]. Co-based catalysts compositions contain the following components [20]:

1. Co as the primary FT metal
2. A second metal (e.g Ru, Re)
3. An oxidic promoter element (e.g Zirconia)
4. A high surface area oxide support

FT synthesis yields a broad spectrum of from ranging from C1 to C50, the distribution of which is governed by Anderson-Schulz-Flory (ASF) kinetics[19]. The FT reaction involves the following main steps at the catalyst surface:

1. The adsorption and dissociation of CO
2. The adsorption and dissociation of H_2
3. Surface reactions leading to the formation of H_2O and CO_2
4. Reaction of adsorbed carbon and hydrogen to form adsorbed CHx species
5. Primary reactions leading to the desorption of FT products
6. Secondary reactions taking place on the primary products for example due to olefin readsorption

1.3.3 Variables of Co-based Fischer-Tropsch Catalysts

1.3.3.1 Support effect

It was first believed that Fischer-Tropsch reaction rates were not influenced by the nature of the support or by the size of the metal crystallites on the supported catalysts[11]. However it has been pointed out that to produce highly active Fischer-Tropsch catalysts, high cobalt dispersion is required implying the need for both a high surface area and the minimising of the metal-support interactions. The catalyst support has been found to play a major role in influencing the overall hydrocarbon production rate for Fischer-Tropsch synthesis [20]. It is in fact thought that variation in support can have a much more

significant impact on cobalt dispersion and their catalytic performance in FT synthesis than the overall cobalt loading [21].

1.3.3.2 Precursor effect

Since it is cobalt metal that is the active site for Fischer-Tropsch synthesis, the number of active sites and extent of reduction will be crucial in determining the catalytic behaviour of supported cobalt catalysts [12]. Giradon *et al.* [14] investigated the effect of cobalt silica-supported catalysts prepared from acetate and nitrate salts. The highly exothermic nature of the acetate decomposition was found to react with the silica to produce barely reducible cobalt silicate. This is neither active or selective during FT synthesis and can only be reduced at temperatures over 1000°C [12]. Ernst *et al.* [18] examined preparation of Co/SiO_2 catalysts and found that the degree of reduction had a direct effect on the FT selectivity. A higher degree of reduction of cobalt favours production of higher chain hydrocarbons, whereas, the presence of unreduced cobalt that has interacted with the support results in better selectivity to lower molecular weight hydrocarbons.

2.0 PROJECT AIMS

The overall aim of the research was to investigate the effect of the cobalt precursor on the structural and chemical properties of silica, alumina and 99% silica + 1% titania supported cobalt catalysts.

More specifically, to investigate the effect of different precursors and supports on the reduction and decomposition profiles of supported cobalt catalysts during thermal treatment in varying atmospheres.

Also to examine the effectiveness of a multiple characterisation technique approach in determining the particular properties of individual supported cobalt catalysts.

3.0 EXPERIMENTAL

3.1 Catalyst Preparation

Catalysts containing 20 weight % cobalt were prepared by incipient wetness of different supports with aqueous solutions of cobalt nitrate hexahydrate $\{Co(NO_3)_2.6H_2O\}$ and cobalt acetate tetrahydrate $\{Co(CH_3CO_2)_2.4H_2O\}$. The following table shows the supports that were included in the study:-

Table 3.1: Table of catalysts prepared

Code	Catalyst/Support	Precursor	Make of support
CoNS	Co/SiO_2	Nitrate salt	Degussa Aerosil® 200
CoAS	Co/SiO_2	Acetate salt	Degussa Aerosil® 200
CoNA	Co/Alumina	Nitrate salt	Engelhard Al-3992
CoAA	Co/Alumina	Acetate salt	Engelhard Al-3992
CoNST1	Co/ 99% SiO_2 + 1% TiO_2	Nitrate salt	Degussa Aerosil^R-200 Mixed oxide
CoAST1	Co/ 99% SiO_2 + 1% TiO_2	Acetate salt	Degussa Aerosil^R-200 Mixed oxide

Prior to impregnation, the supports were dried in an oven at 100°C overnight. To ensure uniform metal dispersion on the support, the precursor salt was dissolved in a volume of water equal to the support pore volume.

The volume of water necessary to fully saturate a 10g sample of each support was measured, and therefore the support pore volumes determined. For all supports used it was found that the pore volume was around 1 $cm^3.g^{-1}$.

Therefore the metal precursor, cobalt acetate (52.831g) or cobalt nitrate (61.730g) dissolved in 50ml of deionised water was added to the supports (50g) and mixed on a rotary evaporator for 1 hour. After impregnation, excess water was slowly evaporated on a rotary evaporator at 80°C for 30 minutes and the catalyst was dried further in an oven at 100°C overnight.

3.2 Catalyst Characterisation

3.2.1 Hot-stage X-ray Diffraction (XRD)

To obtain information concerning the phase composition and the distribution of the crystallite size of the catalyst, XRD studies were performed using a Siemens D5000 X-ray diffractometer (40kV, 40mA) using monochromatic CuK_α x-ray source (1.5418Å). The scanning range used was $15^\circ < 2\theta < 75^\circ$ with a step size of 0.02° and counting time of 2 secs per step. *In situ* hot-stage comprises of a water cooled, vacuum tight, stainless steel chamber with a beryllium window. Most of the internal fittings were mounted on the front flange, which was inserted into the rear part of the chamber attached to the goniometer. Figure 3.1 shows a schematic of the features relating to the performance of this device:

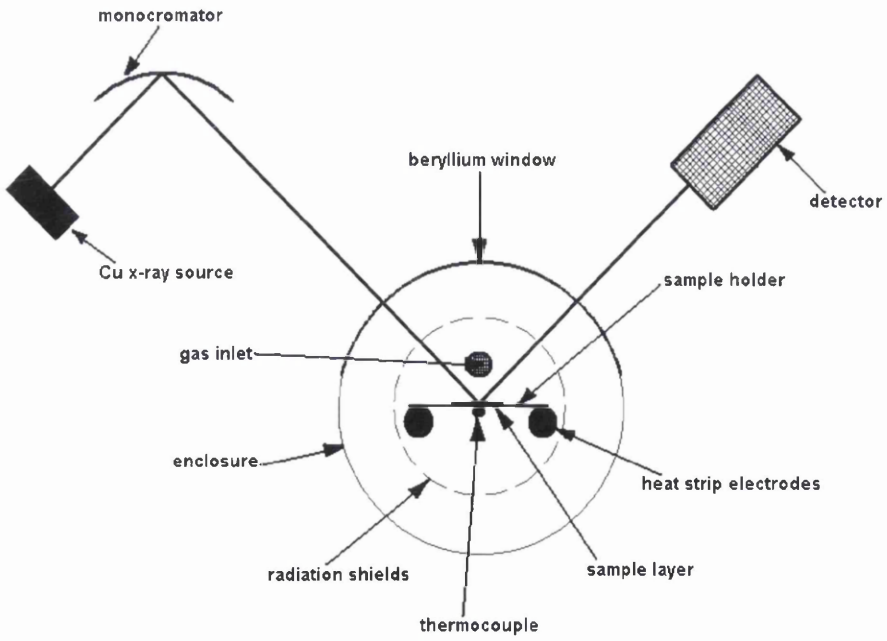

Figure 3.1 : Schematic of hot-stage XRD chamber

The samples were heated at 12° C min^{-1} and scans taken at 30°C, 100°C and then at 100°C increments thereafter to 900°C (with the exception of treatment 2, the sample being heating in oxygen to 500°C before hydrogen to 900°C). At each stage the sample was held for 15 minutes at the desired temperature before the scan was taken, with each scan lasting 115 minutes. For each catalyst this temperature profile was carried out for the following treatments shown in table 3.2. All gases used were supplied by BOC:-

Table 3.2: Table of treatments for catalyst characterisation.

Treatment	1	2	3	4
Gas	2% Oxygen in Argon	2% Oxygen in Argon then Ar 2% Hydrogen in Nitrogen	2% Hydrogen in Nitrogen	Argon
Temp. Ramp (°C)	30 to 900	30 to 500 cool to 30 30 to 900	30 to 900	30 to 900

From the broadening it is possible to determine an average crystallite size by measuring the full width at half maximum (FWHM) of a peak, then applying the Scherrer equation:

$$d = \frac{K\lambda}{B\cos\theta}$$

Equation 3.1 The Scherrer Equation.

where d = particle size diameter / Å

k = constant / 57.29578°

λ = wavelength of X-ray source / 1.5418

B = full width at half maximum / degrees

θ = diffraction angle / degrees

This is only an approximate method since the results can be influenced by various factors such as lattice distortion as well as instrumental parameters.

3.2.2 Thermo-gravimetric analysis [$O_2/H_2/Ar$]

Thermo-gravimetric analysis (TGA) was performed on all catalysts using a combined TGA/DSC SDT Q600 thermal analyser coupled to a ESS mass spectrometer for evolved gas analysis. Fresh sample was heated from 30°C to 1000°C using a heating ramp of 10°C min^{-1}. For each sample this temperature profile was employed using the gases shown in table 2 at a flow rate of 100ml min^{-1}. For mass spectrometric analysis, mass fragments with m/z = 2, 14, 16, 17, 18, 28, 30, 32, 40, 44 and 46 (amu) were followed. The sample loading was typically 10-15mg.

3.2.3 Surface Area Determination

Physisorption of an inert gas (generally nitrogen at 77K) onto a surface and plotting the volume absorbed as a function of equilibrium pressure allows the construction of an isotherm. It is then possible to determine the surface area by applying a linerising mathematical procedure. The approach most commonly used was devised by Brunauer, Emmett and Teller, giving the expression:

$$\frac{P}{V(P_0-P)} = \frac{1}{V_M C} + \frac{(C-1)P}{V_M C P_0}$$

Equation 3.2 **The BET Equation.**

Where V = volume of gas adsorbed at equilibrium pressure P

V_M = volume necessary to form a monolayer

P_0 = saturated vapour pressure of the adsorbent gas at the temperature of measurement

C = constant

Plotting $P/V(P_0-P)$ against P/P_0 yields a straight line, with the slope is given by $(C-1)/V_MC$ and the intercept by $1/V_MC$.

The samples were initially outgassed at 383K in flowing nitrogen overnight to remove any adsorbed species from the surface. Measurements were performed using a Micromeritics Gemini III 2375 Surface Area Analyzer, helium being used as calibrant and nitrogen as adsorbant at 77K. Surface areas were calculated assuming the average cross sectional area of a nitrogen molecule to be $0.162nm^2$. Approximately 0.04g of sample was weighed into a glass tube, with measurements taken of both supports and as prepared catalysts.

4.0 RESULTS

4.1 B.E.T analysis

B.E.T experiments were carried out as described in section 3.2.3, and the data obtained is tabulated below. Although showing some variation, the results show that the three supports had very similar physical properties with comparable surface areas, pore diameters and pore volumes. It is notable that the CoNS catalyst showed the smallest surface area, and that the addition of the cobalt precursor to the support caused a decrease in the overall catalyst surface area.

Table 4.1. BET surfaces areas, average pore diameters and pore volumes for the supports and prepared catalysts.

Catalyst	Surface Area (m^2/g)	Average pore diameter (Å)	Pore volume (cm^3/g)
Silica support	148	203	0.75
CoNS	59	182	0.50
CoAS	92	202	0.46
Alumina support	205	155	0.79
CoNA	132	127	0.42
CoAA	92	143	0.33
99% Silica + 1% Titania support	134	186	0.64
CoNST1	108	177	0.48
CoAST1	124	145	0.45

4.2 Supports

TGA-DSC profiles of all three supports were collected as described in section 3.2.2. This was done in order to confirm that results seen from the catalyst characterisation were due to the effect of the catalyst as a whole and not just the support.

Comparisons of the TGA derivative weight profiles in oxygen obtained for each support are displayed in figure 1 below.

Figure 4.1: TGA weight profiles of silica, alumina and 99% silica + 1% titania supports in oxygen.

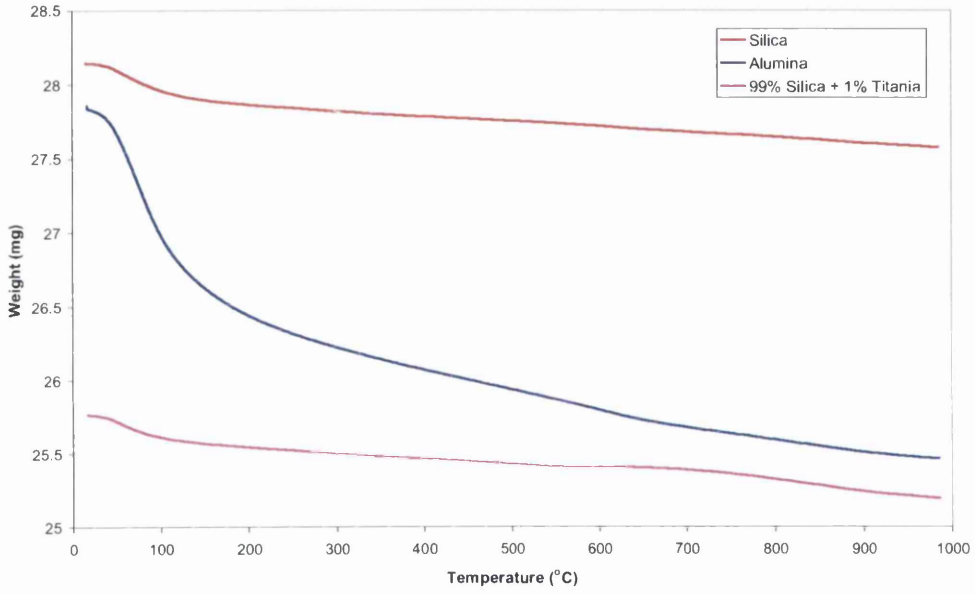

Figure 4.2: TGA derivative weight profiles of silica, alumina and 99% silica + 1% titania supports in oxygen.

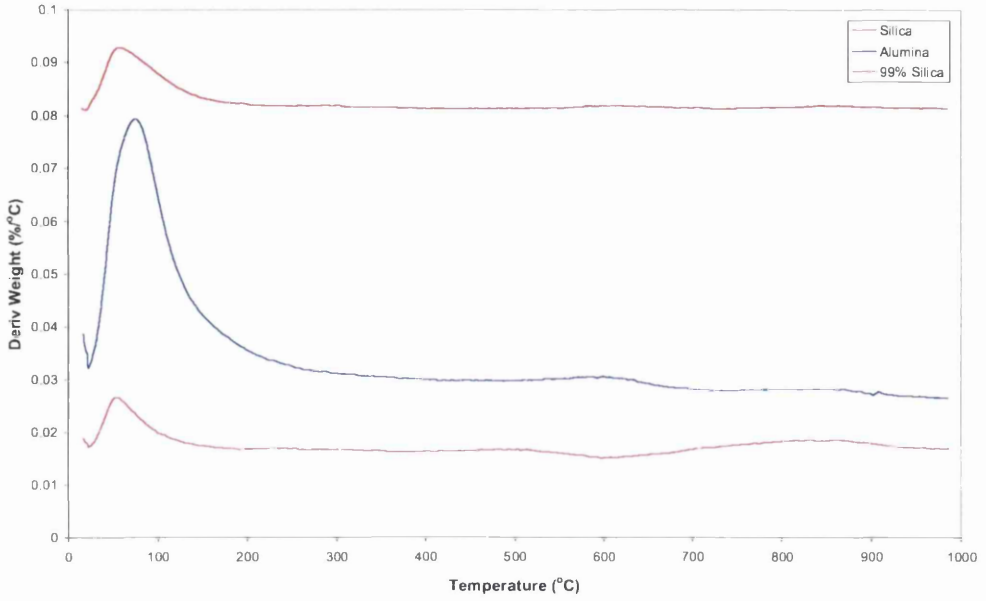

Profiles for each of the catalysts shown in figures 4.1-4.2 each show a significant weight loss region before 100°C. From the corresponding mass spectrometric and heat flow data, it is clear that these weight losses are due to the endothermic desorption of water molecules. The three curves all show several inflections at higher temperatures, however these were not accompanied by any significant change in the heat flow or mass spectrometric data. The total weight loss for theses sample was small, around 8% for the alumina support and 2.5 % for the silica and 99% silica + 1% titania supports.

The TGA-DSC measurements were carried out for all four of the gas treatments. All support results were similar, in that, apart from the loss of water before 100°C, there were no other significant weight losses.

4.3 Cobalt Nitrate

4.3.1 Oxygen (treatment 1)

4.3.1.1 Cobalt nitrate

4.3.1.1.1 Thermogravimetric analysis-Differential Scanning Calorimetry (TGA-DSC)

Figure 4.3: TGA weight and derivative weight profiles for cobalt nitrate in oxygen.

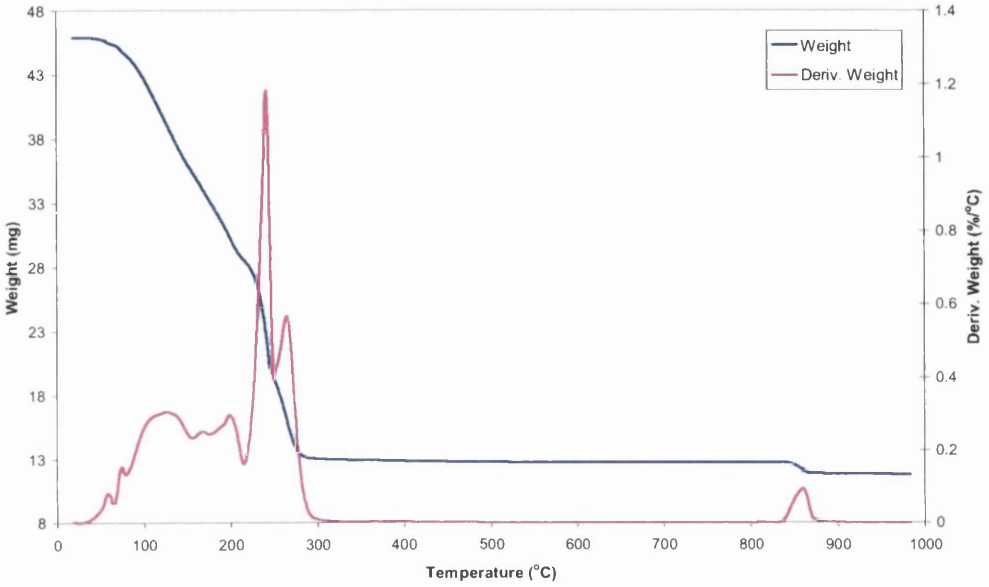

Figure 4.4: TGA-DSC derivative weight and heat flow profiles for cobalt nitrate in oxygen.

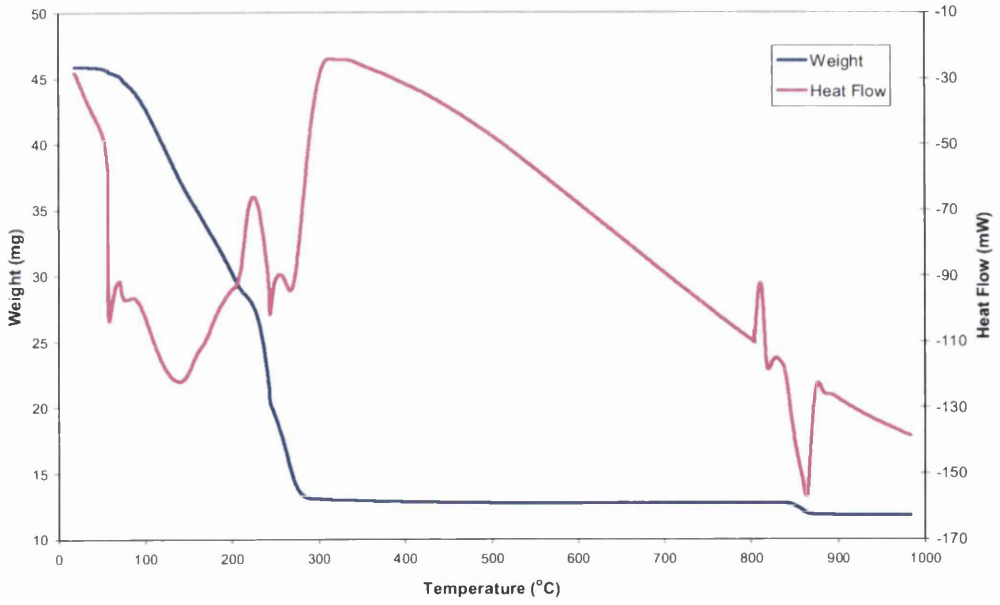

From the weight and derivative weight profiles, the cobalt nitrate decomposition in oxygen mainly occurs as several overlapping events before 400°C. There is a further high temperature weight loss at 862°C. From the heat flow data it can be seen that all the weight losses were endothermic events. The mass spectrometric data shows the decomposition in oxygen occurs via the evolution of water, oxygen, nitrogen monoxide and nitrogen dioxide. Above 500°C, the evolution of oxygen and nitrogen monoxide are detected.

4.3.1.1.2 Mass spectrometric analysis

Figure 4.5: Mass spectrometric data of H_2O (m/z=18) and O_2 (m/z=32) for cobalt nitrate in oxygen.

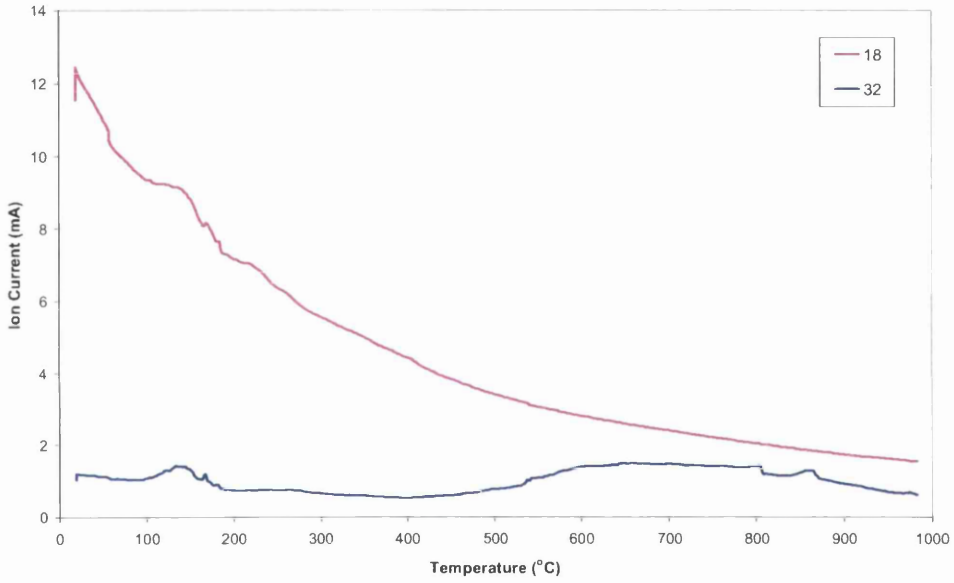

Figure 4.6: Mass spectrometric data of NO (m/z=30) and NO_2 (m/z=46) for cobalt nitrate in oxygen

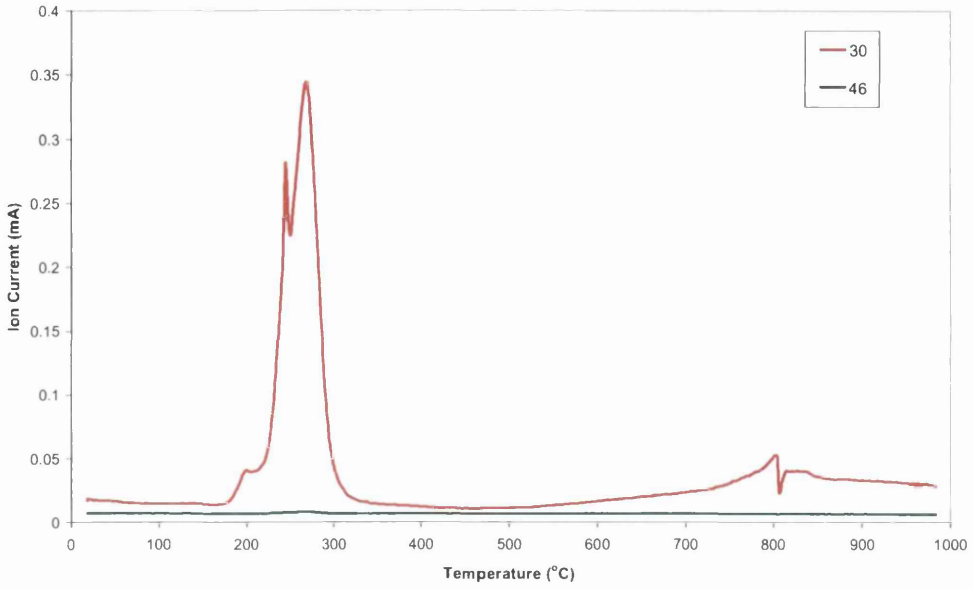

4.3.1.2 Cobalt nitrate supported catalysts

4.3.1.2.1 Thermogravimetric analysis (TGA)

TGA profiles of all three catalysts were collected as described in section 3.2.2. Figures 4.7 and 4.8 present curves for TGA in oxygen for the catalysts prepared from cobalt nitrate on silica, alumina and 99% silica +1 % titania supports.

Figure 4.7: TGA weight profiles of silica, alumina and 99% silica + 1% titania supported cobalt catalysts in oxygen.

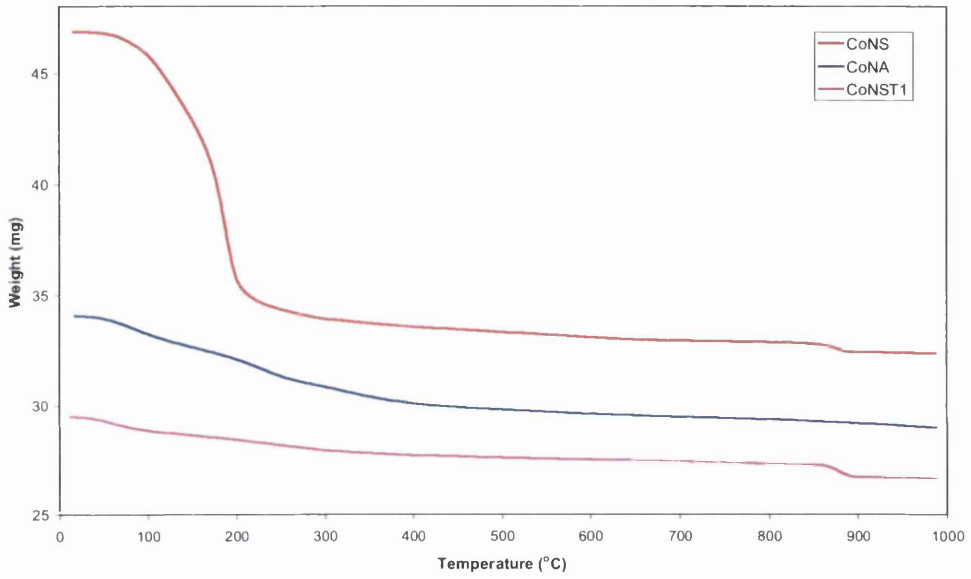

Figure 4.8: TGA derivative weight profiles of silica, alumina and 99% silica + 1% titania supported cobalt catalysts in oxygen.

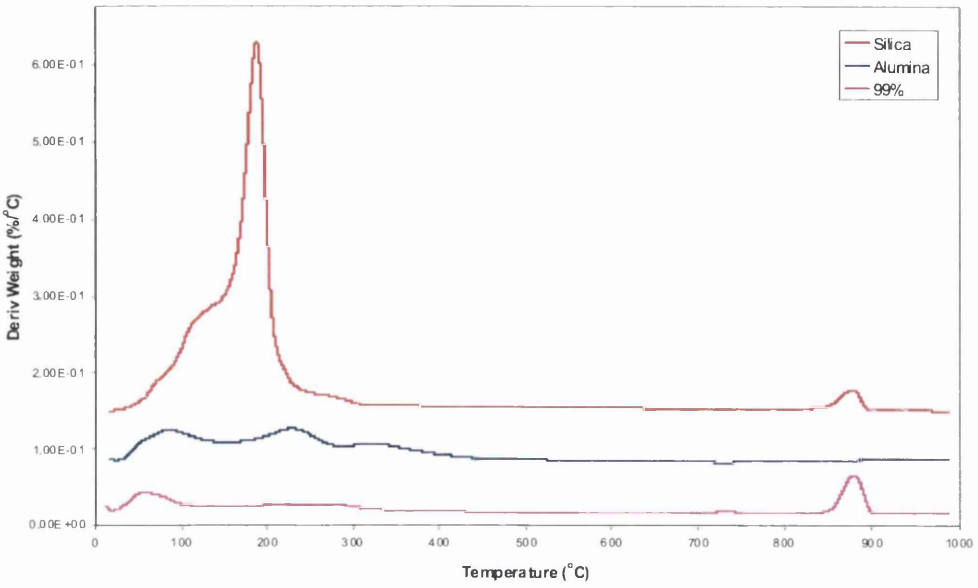

The derivative weight loss curves shown exhibit several inflections between 0-400°C. These are thought to be due to the desorption of water molecules in the cobalt hydrate shell and to the decomposition of the nitrate anion. For two of the curves shown in figures 4.7 and 4.8, CoNS and CoNST1, there is another distinctive weight loss region at around 880°C. Since this peak is not seen in CoNA or in the supports alone it is presumed to be associated with the interaction of the cobalt nitrate with the silica.

4.3.1.2.2 Differential Scanning Calorimetry (DSC)

Figure 4.9: DSC heat flow profiles of silica, alumina and 99% silica + 1% titania supported cobalt catalysts in oxygen.

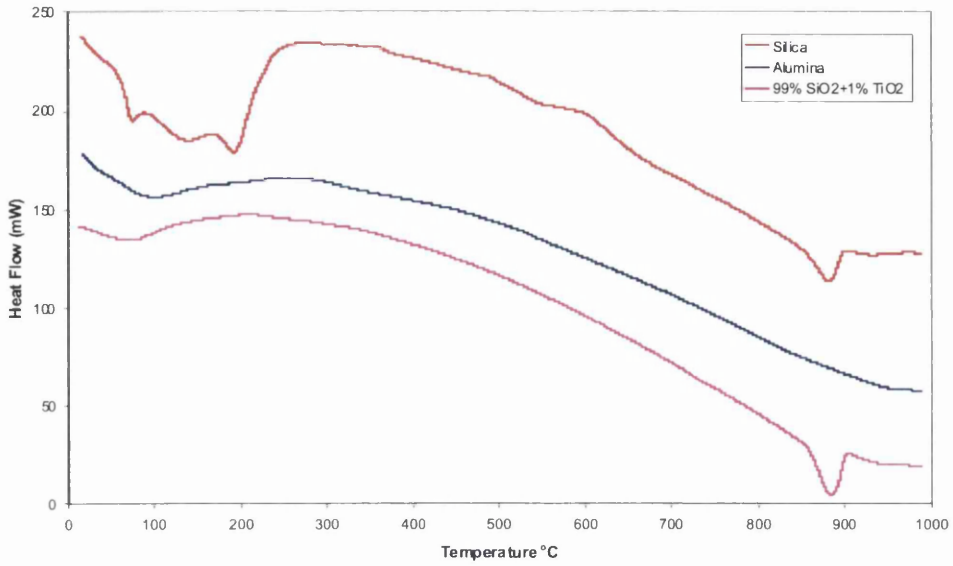

Like the derivative weight loss profile, the heat flow profile shown in figure 4.9 exhibits several inflections before 400°C. An endothermic event can clearly be seen in each trace for each of the catalysts before 100°C indicating the desorption of hydrate water molecules. With the CoNS there are three distinctive endothermic events before 250°C. These are seen with a clarity that is not seen with the derivative weight curves. The weight loss seen around 880°C, for CoNS and CoNST1 catalsysts, is accompanied by an endothermic event on the heat flow curve.

4.3.1.2.3 Mass Spectrometric analysis

Figure 4.10: Mass spectrometric data of NO (m/z=30) for silica, alumina and 99% silica + 1% titania supported cobalt catalysts in oxygen.

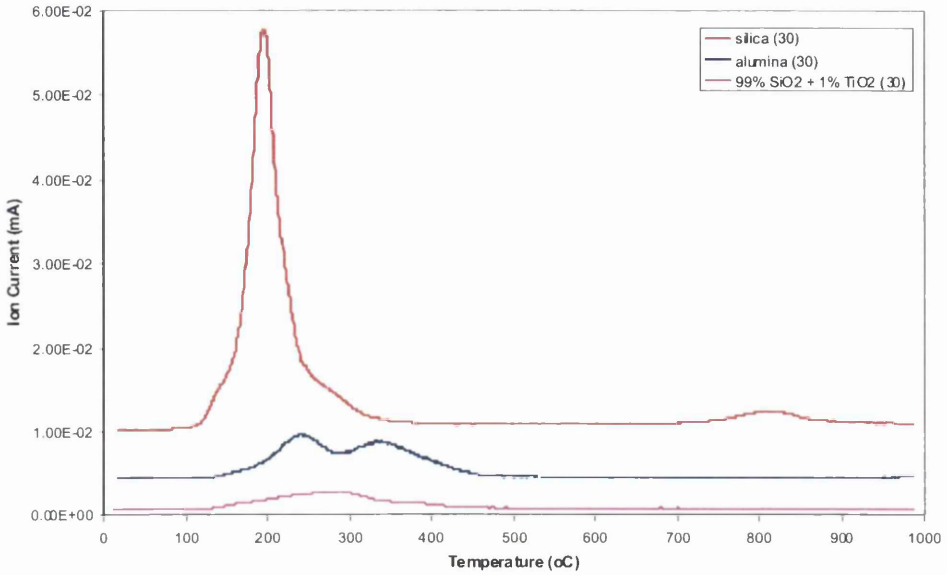

From the graph below of the evolved nitrate gas, we can see the temperatures of decomposition in oxygen of the cobalt nitrate precursors. It can clearly be seen that although being prepared via the same precursor, the decomposition of the nitrate in oxygen is different for each catalyst. CoNS decomposition occurs a single major event at 195°C. However, there is a small shoulder present before and after this event therefore suggesting there may be three evolutions of NO. There is also a small amount of NO_2 associated with the decomposition at 195°C.

For the CoNA catalysts, decomposition of the nitrate precursor in oxygen occurs as two distinct events, occurring at 245°C and 340°C. CoNST1 decomposition occurs as a single broad evolution of NO suggesting that this could be made up of more than one component. In contrast to the CoNS, there was no NO_2 gas detected during the decomposition of CoNA or CoNST1. From the mass spectrometric data of evolved O_2 (m/z =32), a small peak is seen at 880°C on CoNS and CoNST1, corresponding with the event on the TGA-DSC curves.

4.3.1.2.4 Hot-stage X-ray Diffraction (XRD)

The structure of the cobalt species in the catalysts prepared from nitrate were characterised by hot-stage x-ray diffraction as described in section 2.2.1.

Figure 4.11: Hot-stage XRD patterns of cobalt nitrate on alumina in oxygen.
Phases denoted are (¤) Co_3O_4 and (+) Al_2O_3. The XRD patterns are offset for clarity.

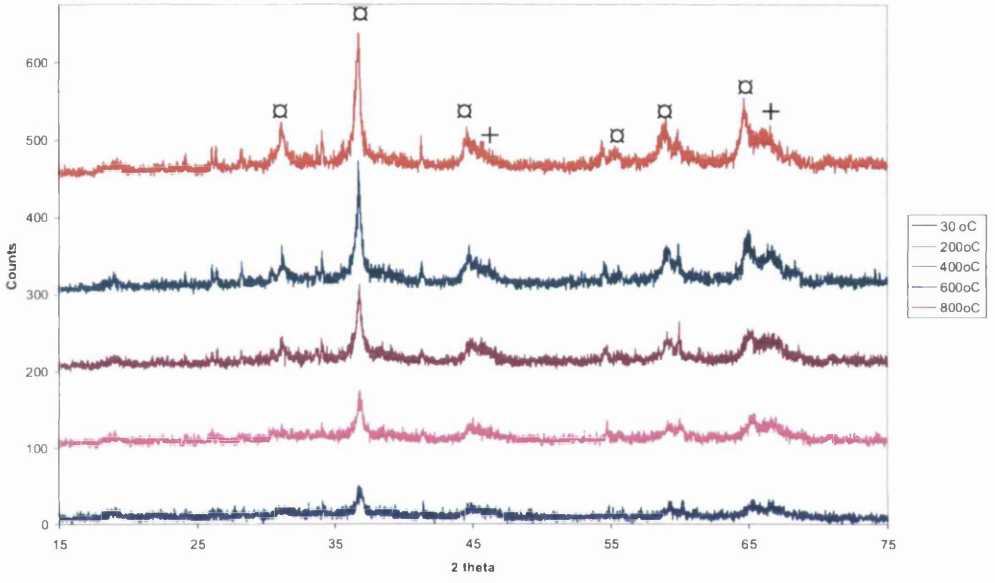

Figure 4.11 shows the hot-stage XRD pattern for the cobalt nitrate on alumina. The location of the peaks confirm that Co_3O_4 was the only crystalline phase of Co present. Except for Co_3O_4, only peaks for amorphous alumina were detected. As stated earlier in section 3.2.1, the width at half maximum of the most intense Co_3O_4 peak, in this case at $2\theta = 36.9^{o}$ was used to calculate the Co_3O_4 particle sizes. The average particle size calculated for all the temperatures from the Scherrer equation is given in table 4.2. There is little variation in the Co_3O_4 particle sizes, with the exception of the value at 600°C which appears slightly larger.

Table 4.2: Co_3O_4 crystallite size as determined by hot-stage XRD of cobalt nitrate on alumina in oxygen.

Temperature (°C)	Co_3O_4 crystallite size (nm)
30	16
100	
200	20
300	16
400	20
500	18
600	26
700	20
800	20

Figure 4.12: Hot-stage XRD patterns of cobalt nitrate on 99% silica + 1% titania in oxygen.
Phases denoted are (¤) Co_3O_4. The XRD patterns are offset for clarity.

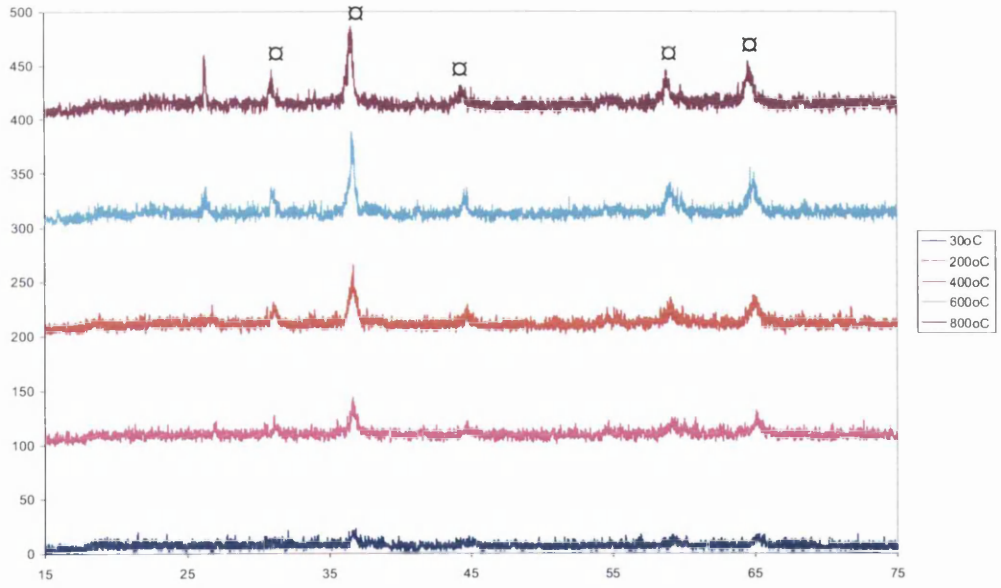

Treatment of cobalt nitrate on 99% silica + 1% titania supports in oxygen leads to characterisation data that is similar to that of the alumina. Again signals confirm that only Co_3O_4 is present as crystalline phase. In contrast to CoNA, there is less evidence of amorphous support present. Diameters of the Co_3O_4 crystallites were calculated, as explained previously, from the width of the diffraction peaks at different temperatures are

shown in table 4.3. The crystallite size changes slightly with temperature with again the largest being produced at 600°C.

Table 4.3: Co_3O_4 crystallite size as determined by hot-stage XRD of cobalt nitrate on 99% silica + 1% titania in oxygen.

Temperature (°C)	Co_3O_4 Crystallite size (nm)
30	20
100	20
200	20
300	13
400	14
500	26
600	32
700	20
800	18

When evaluating the hot-stage XRD of CoNST1 at 900°C a much more complex diffraction pattern is produced. Due to overlapping of other peaks, the size of the Co_3O_4 crystalline were difficult to measure at this temperature. An exact assignment of the peaks was not possible but revealed the presence of cobalt silicate.

4.3.2 Hydrogen after calcination in oxygen (treatment 2)

4.3.2.1 Cobalt nitrate supported catalysts

For this treatment, the catalysts have been pre-calcined in oxygen heating to 500°C at 10°C min^{-1} prior to the treatment in hydrogen. The results in this section relate to the treatment in hydrogen.

4.3.2.1.1 Thermogravinometric analysis (TGA)

Figure 4.13: TGA weight profiles curves of the silica, alumina and 99% silica +1% titania supported cobalt catalysts in hydrogen after calcination in oxygen.

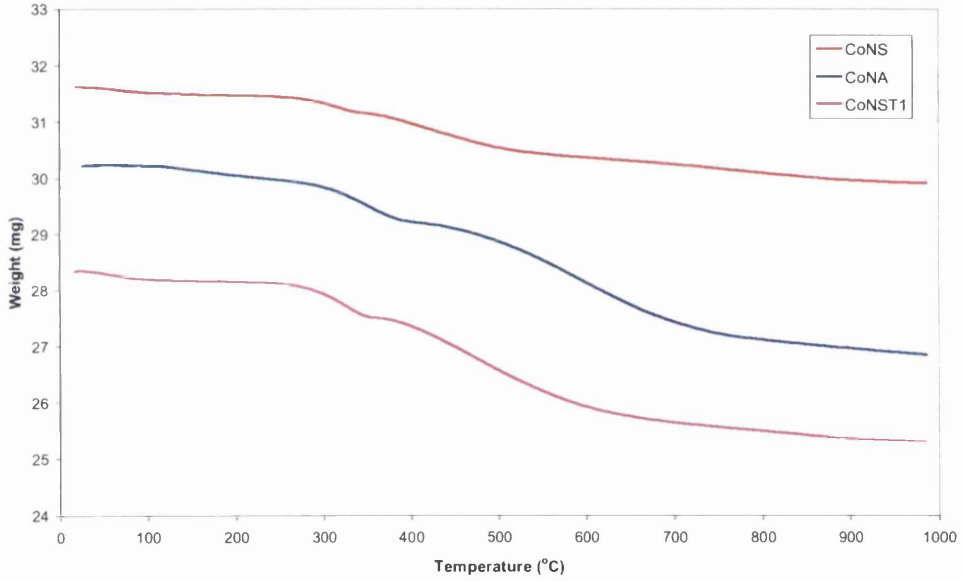

Figure 4.14: TGA derivative weight profiles of the silica, alumina and 99% silica +1% titania supported cobalt catalysts in hydrogen after calcination in oxygen.

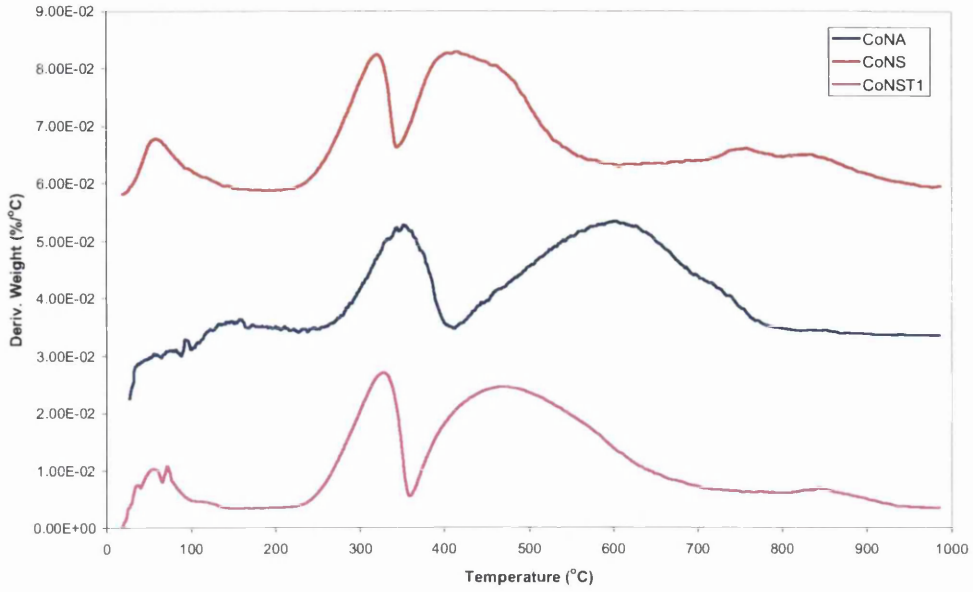

Figures 4.13 and 4.14 present the TGA curves for the supported cobalt nitrate catalysts in hydrogen (after oxygen). The derivative weight profile exhibits similar peaks for all the catalysts. The first small peak before 100°C is again due to the desorption of water molecules. With CoNA, an additional peak is seen overlapping at ~160°C, which might be assigned to the decomposition in the presence of hydrogen of residual nitrate species. Two main peaks are apparent in all the catalysts between 250-800°C and are probably due to the reduction of the supported cobalt oxide species. In CoNS and CoNST1 several more peaks are seen at temperatures above 750°C.

4.3.2.1.2 Differential Scanning Calorimetry (DSC)

Figure 4.15: DSC heat flow profile of silica, alumina and 99% silica + 1% titania supported cobalt catalysts in hydrogen after calcination in oxygen.

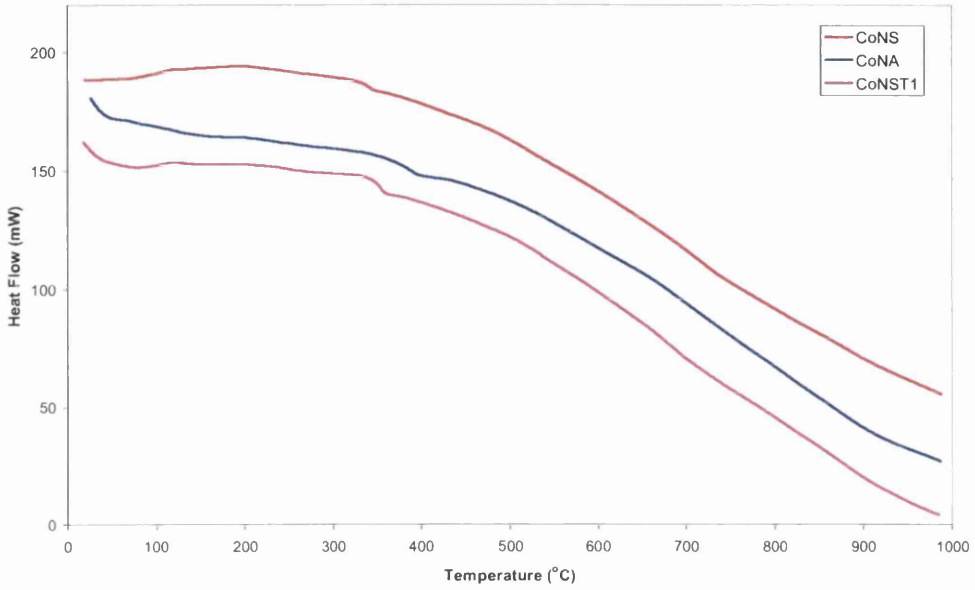

Apart from the initial endothermic desorption of water, the heat flow curves for the supported catalysts in hydrogen are relatively featureless. However, in all three curves for each of the catalysts there is clear exotherm spread over 200°C, ending around 350°C. There is also a possibly a subsequent exotherm after this temperature.

4.3.2.2 Mass spectrometric analysis

Figure 4.16: Mass spectrometric data of H_2 (m/z=2) and H_2O (m/z=18) for silica supported cobalt catalyst in hydrogen after calcination in oxygen.

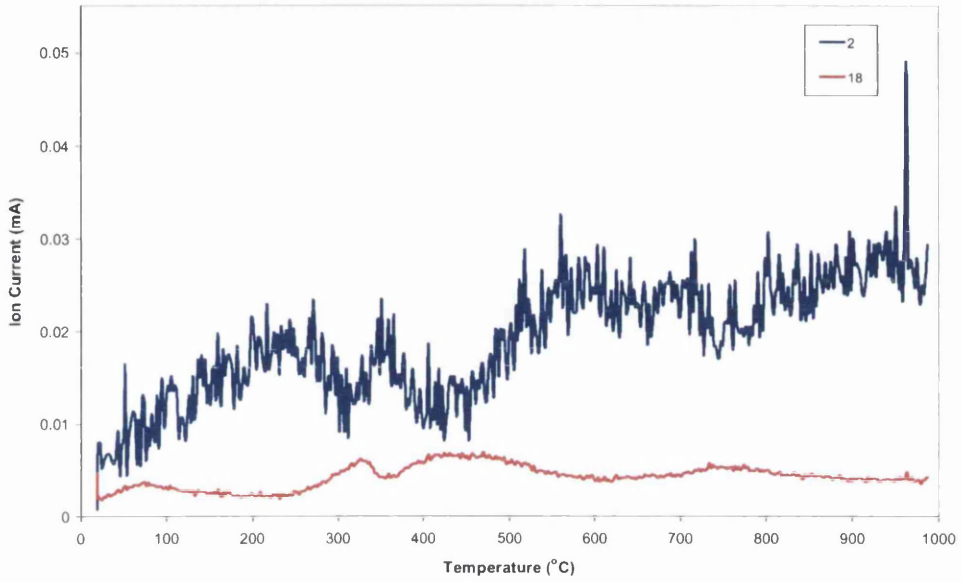

Figure 4.17: Mass spectrometric data of H_2 (m/z=2) and H_2O (m/z=18) for alumina supported cobalt catalyst in hydrogen after calcination in oxygen.

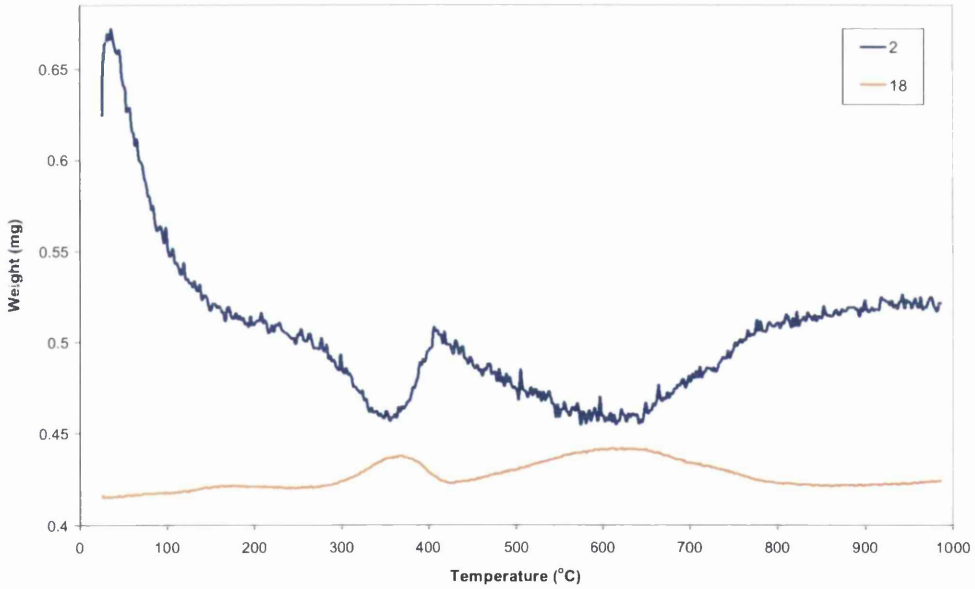

Figure 4.18 Mass spectrometric data of H_2 (m/z=2) and H_2O (m/z=18) for 99% silica + 1% titania supported cobalt catalyst in hydrogen after calcination in oxygen.

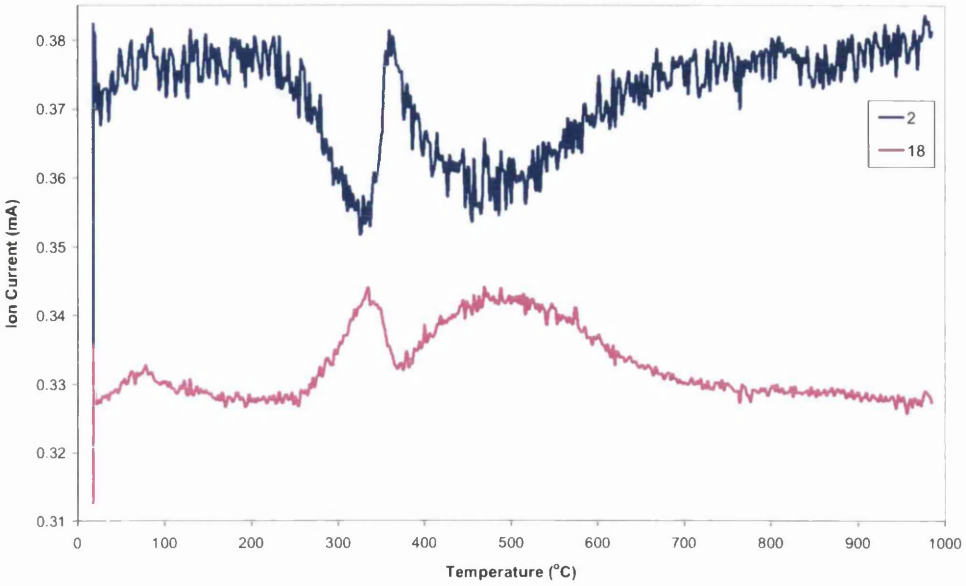

Figures 4.16, 4.17 and 4.18 show the uptake of hydrogen gas and the corresponding production of water for each of the supported cobalt catalysts. The uptake of hydrogen is seen clearly to occur as two distinct events, with the relative intensities of these two peaks consistent for each support.

4.3.2.4 Hot-stage X-ray Diffraction (XRD)

Reduction of cobalt oxide species in supported cobalt nitrate catalysts were followed by hot-stage XRD.

Figure 4.19: Hot-stage XRD patterns of cobalt nitrate on alumina support in hydrogen after calcination in oxygen.
Phases denoted are (¤) Co_3O_4, (+) CoO and (*) metallic Co. The XRD pattern is offset for clarity.

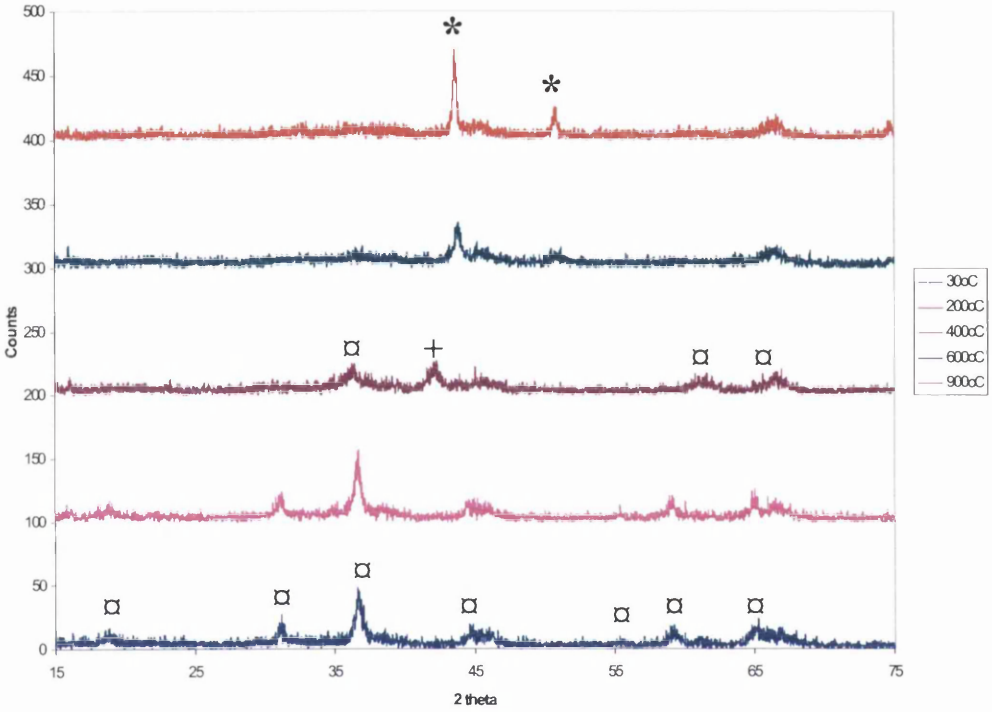

The *in-situ* hot-stage XRD patterns in figure 4.19 show the reduction of Co_3O_4 and the appearance of Co metal. During the reduction, the Co_3O_4 crystallite size decreases until 400°C, at which point the XRD lines were so broad that accurate estimations of size were not possible. Signals confirm the presence of CoO species between 300°C and 400°C, with metallic Co appearing at 500°C. The cobalt crystallite size after reduction was calculated at each temperature and is shown in table 4.4. The smallest Co crystallite size was 20 nm occurring at 600°C.

It should be noted that the hot-stage XRD results are consistent with the peaks in the mass spectrometric data attributed to the reduction of Co_3O_4 to CoO, which then reduces at higher temperatures to metallic Co.

Table 4.4: Co metal crystallite size as determined by hot-stage XRD of cobalt nitrate on alumina in hydrogen after calcination in oxygen

Temperature (°C)	Co metal crystallie size (nm)
500	27
600	20
700	32
800	23
900	32

Figure 4.20: Hot-stage XRD patterns of cobalt nitrate on 99% silica + 1% titania in hydrogen after calcination in oxygen.
Phases denoted are (¤) Co_3O_4, (+) CoO and (*) metallic Co. The XRD pattern is offset for clarity.

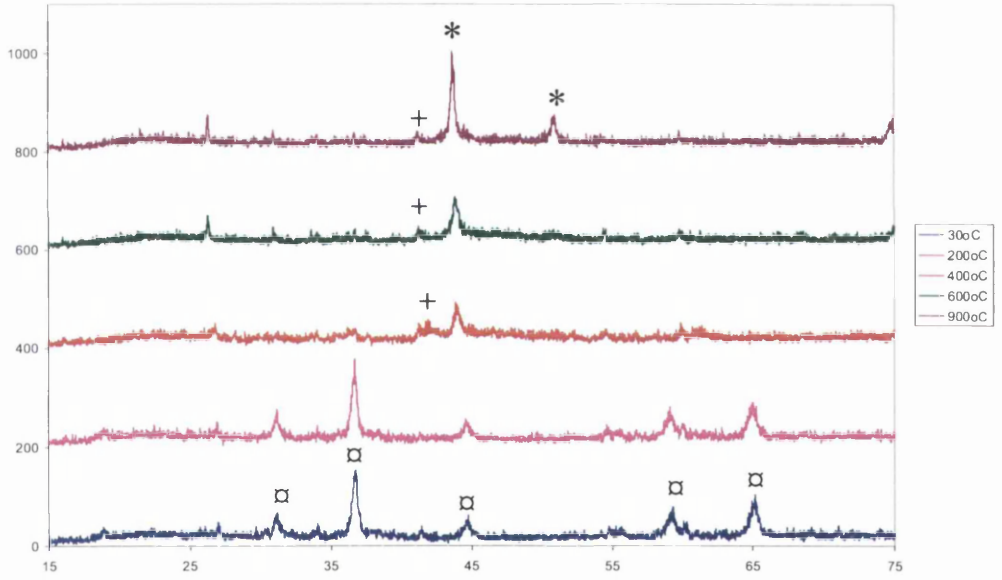

The hot-stage XRD data from cobalt on 99% silica + 1% titania catalyst shows the rapid reduction of the Co_3O_4 and the simultaneous appearance of metallic Co, which appears at 400°C .The Co crystallite sizes generally increase with temperature during reduction are shown in table 4.5. In this case the smallest Co particle size is 13 nm and occurs at 400°C.

Table 4.5: Co metal crystallite size as determined by hot-stage XRD of cobalt nitrate on 99% silica + 1% titania in hydrogen after calcination in oxygen.

Temperature (°C)	Co metal crystallite size (nm)
400	13
500	18
600	18
700	16
800	20
900	27

4.3.3 Hydrogen (treatment 3)

The results show in this section are of the 'as prepared' catalysts in hydrogen with no pre-treatment.

4.3.3.1 Cobalt nitrate

4.3.3.1.1 Thermogravimetric analysis-Differential Scanning Calorimetry (TGA-DSC)

Figure 4.21: TGA weight and derivative weight profiles of cobalt nitrate in hydrogen.

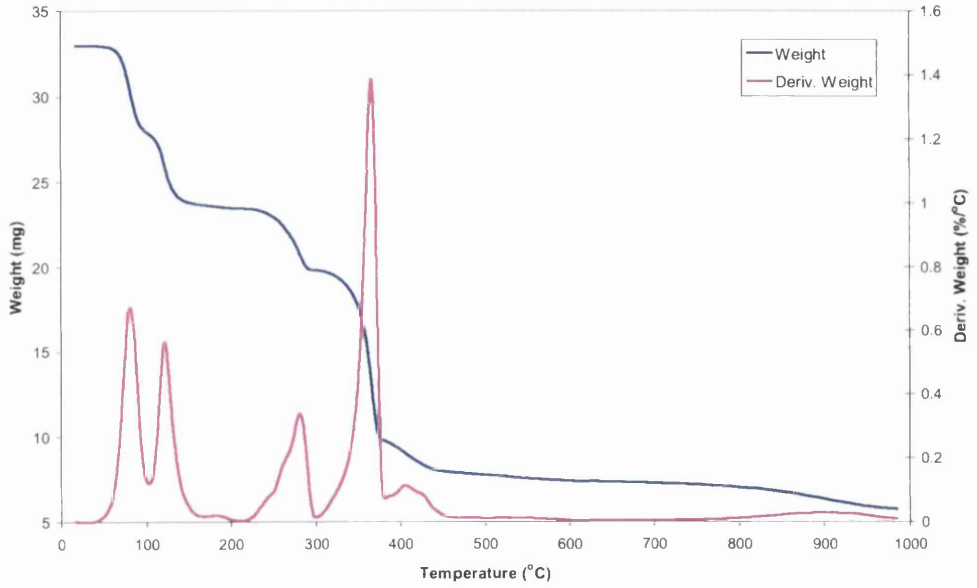

Figure 4.22: TGA-DSC derivative weight and heat flow profile of cobalt nitrate in hydrogen.

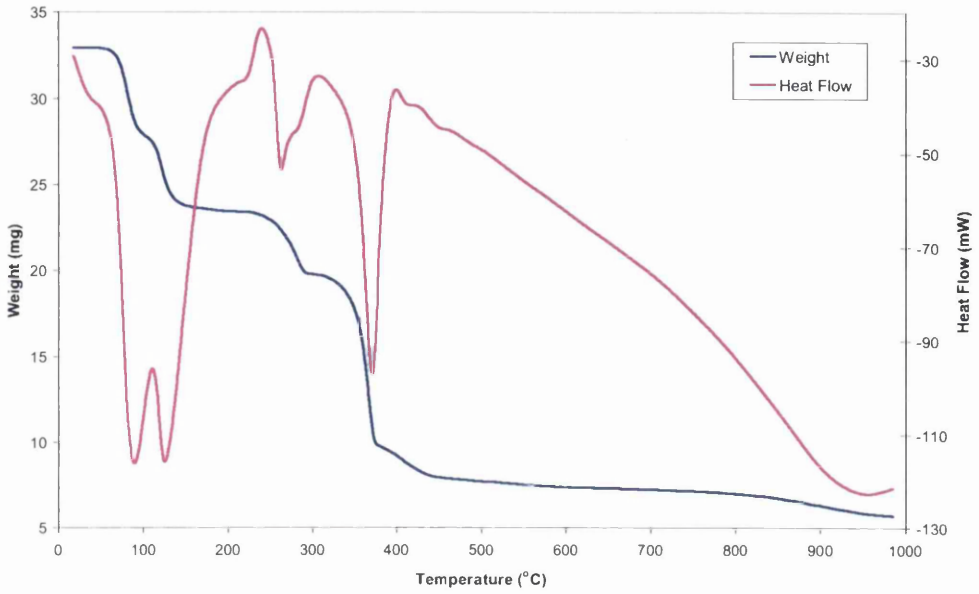

From the weight and derivative weight profiles in figure 4.21 the reduction of cobalt nitrate occur appears complex with around seven weight loss events. From the heat flow profile in figure 4.22 it is clear that weight losses up until 383°C are endothermic events. The weight loss events above this temperature are shown to be relatively featureless on the heat flow profile. Mass spectrometric data in figure 4.23 and 4.24 confirm that weight loss events below 383°C are accompanied by the evolution of water, oxygen, nitrogen monoxide and nitrogen dioxide. The weight loss events above this temperature involve the uptake of hydrogen coinciding with the evolution of water.

4.3.3.1.2 Mass Spectrometric analysis

Figure 4.23: Mass spectrometric analysis for H_2 (m/z=2), H_2O (m/z=18) and O_2 (m/z=32) for cobalt nitrate in hydrogen.

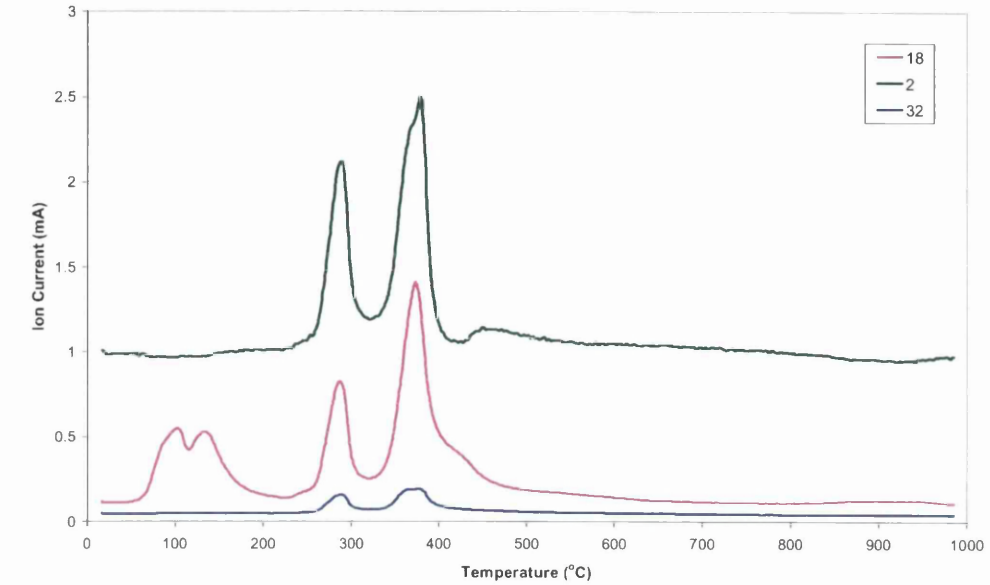

Figure 4.24 Mass spectrometric analysis for NO (m/z=30) and NO_2 (m/z=46) for cobalt nitrate in hydrogen.

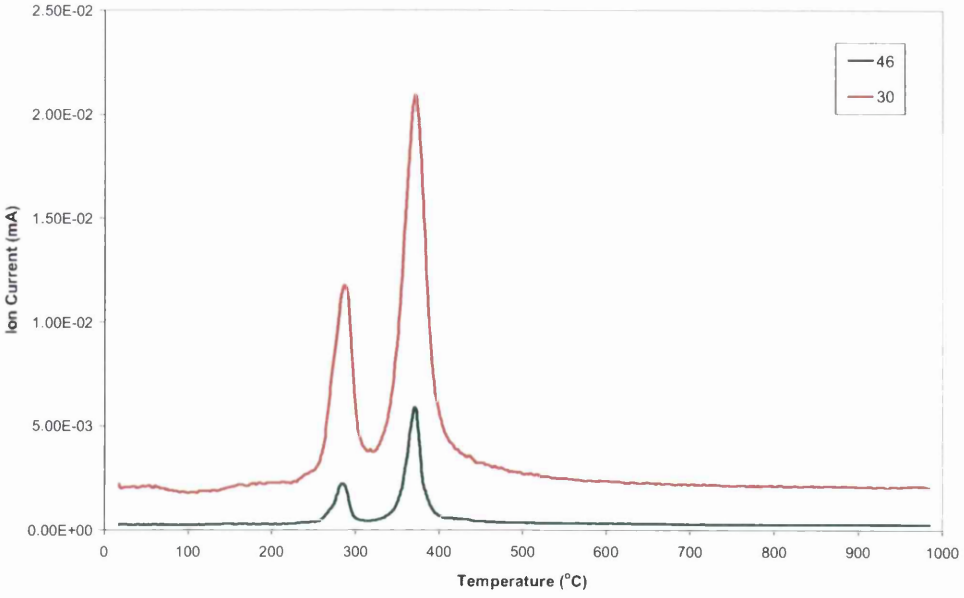

4.3.3.2 Cobalt nitrate supported catalysts

4.3.3.2.1 Thermogravinometric analysis (TGA)

Figure 4.25: TGA weight profiles of silica, alumina and 99% silica +1% titania supported cobalt catalysts in hydrogen.

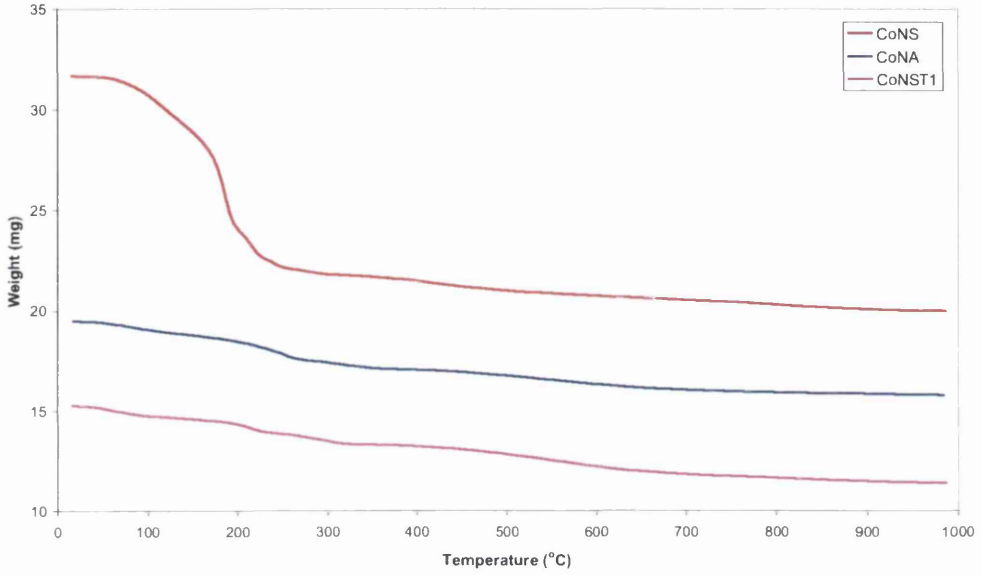

The weight loss profiles for all three catalysts are deceptively simple, however after looking at their derivative weight profiles shown in figure 4.26, the complexity can be seen. The derivative weight curves comprise of several overlapping peaks, which are probably due to the decomposition of nitrate precursor and the reduction of the supported cobalt oxide species. The derivative weight profile of CoNS exhibits a broad peak with several shoulders with the overall maximum at 186°C. The curves for CoNA and CoNST1 appear similar, exhibiting 4 peaks, with CoNA proceeding at a slightly higher temperature. The complexity of the derivative weight profiles however, makes it difficult to draw any conclusions in regards to the attribution of peaks.

Figure 4.26: TGA derivative weight profiles of silica, alumina and 99% silica +1% titania supported cobalt catalysts in hydrogen.

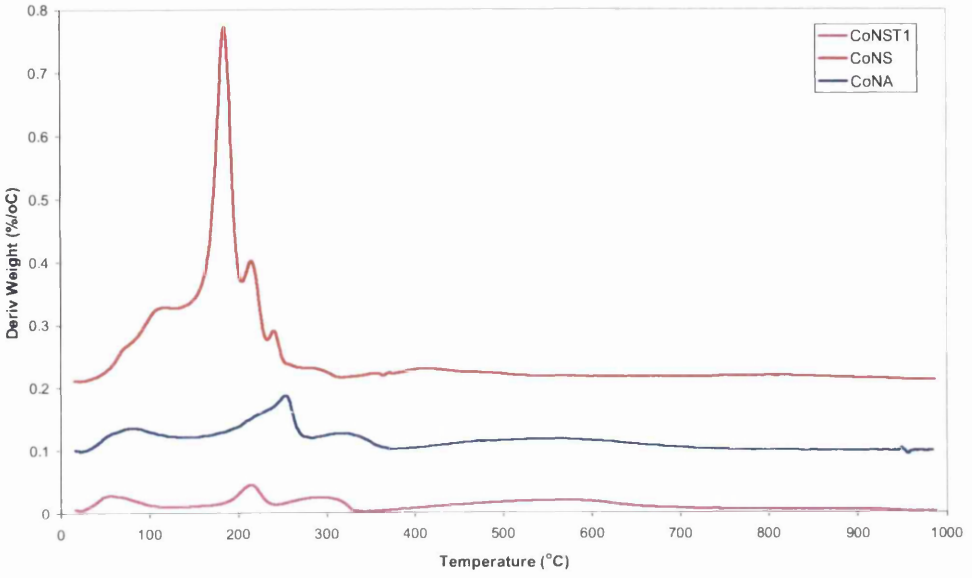

4.3.3.2.2 Differential Scanning Calorimetry (DSC)

Figure4.27: DSC heat flow profiles of silica, alumina and 99% silica + 1% titania supported cobalt catalysts in hydrogen.

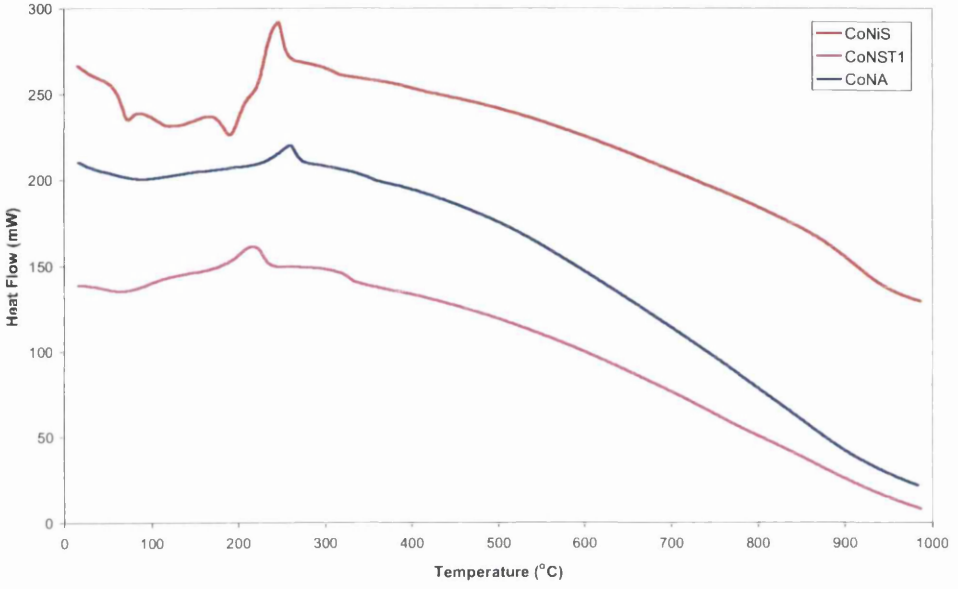

The heat flow curves for each of the catalsysts is quite different. With the CoNS again we see three clear endothermic events that were present when DSC was performed in oxygen, in addition to this is an exotherm at 248°C. The CoNA and CoNST1 also exhibits several exotherms at a temperature of 262°C for the CoNA and 221°C and 307°C for CoNST1.

4.3.3.2.3 Mass Spectrometric analysis

Figure 4.28: Mass spectrometric data of H_2 (m/z=2), H_2O (m/z=18) and NO (m/z=30) for silica supported cobalt catalysts in hydrogen.

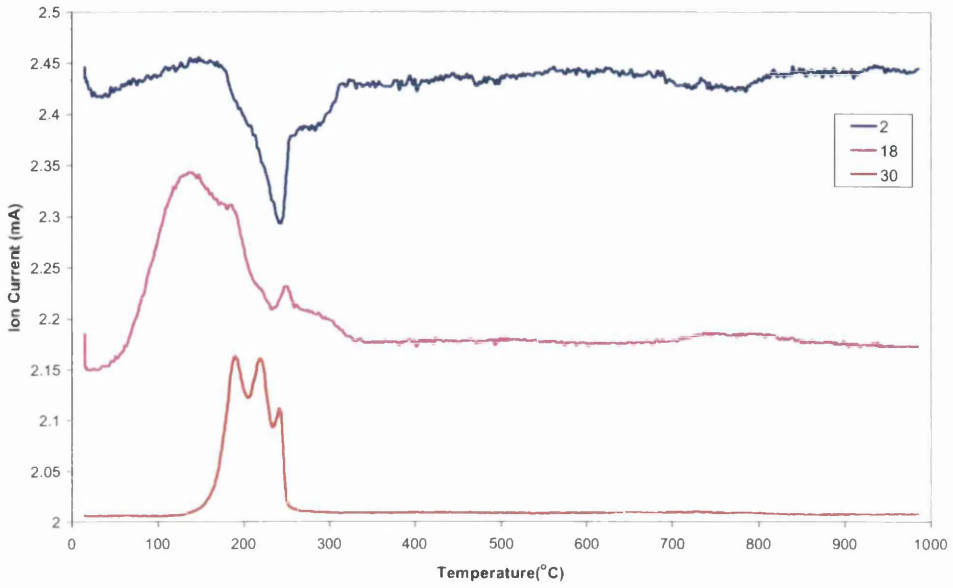

The complex nature of the mass spectrometric profiles make it still difficult to evaluate the extent of reduction from hydrogen consumption data. It can be seen clearly that the nitrate precursor decomposes in hydrogen as three evolutions of NO between 110-280°C. Large hydrogen uptake peak with several shoulders is seen around 150-330°C, where evolution of water is detected at the same time. The overall maximum of the hydrogen uptake peak at 250°C corresponds to the exothermic peak on the heat flow curve. Another broad hydrogen uptake coupled with the release of water can also be seen at around 770°C. Unfortunately, due to insufficient material to allow XRD to be performed, there is no *in-situ* hot-stage XRD data to help quantify information about the extent of cobalt reduction.

Figure 4.29: Mass spectrometric data of H_2 (m/z=2), H_2O (m/z=18) and NO (m/z=30) for cobalt supported on alumina catalysts in hydrogen.

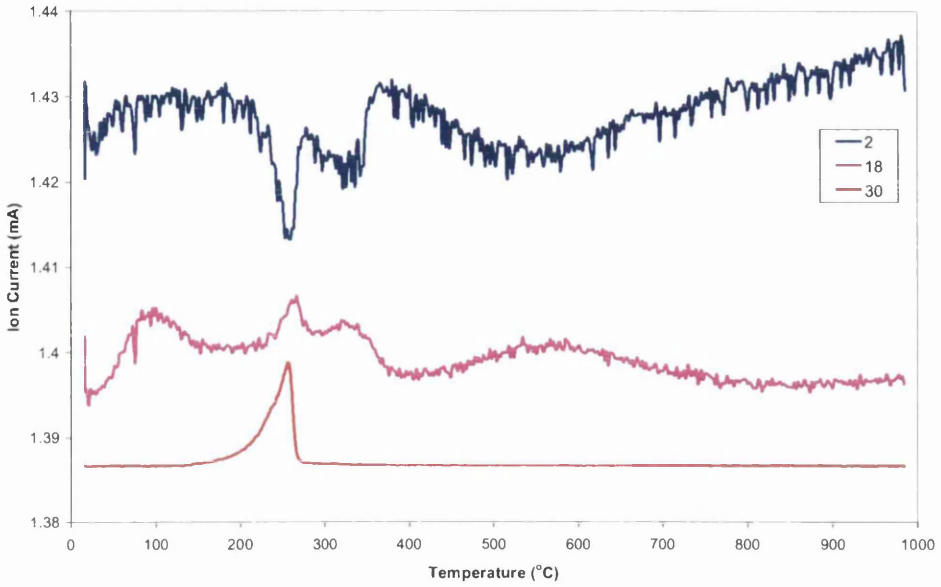

Despite the unclear attribution of TGA-DSC peaks, the evaluation of the CoNA reduction is made clear by the mass spectrometric data. The first region corresponds to the desorption of water before 100°C. The second region is the decomposition of the nitrate precursor in hydrogen which happens as a single evolution and coincides with an exotherm on the heat flow curve. Last two peaks (the first overlapping with the nitrate decomposition peak) around 325°C and 560°C see the simultaneous detection of hydrogen consumption and evolution of water.

Figure 4.30: Mass spectrometric data of H_2 (m/z=2), H_2O (m/z=18) and NO (m/z=30) for 99% silica + 1% titania supported cobalt catalysts in hydrogen.

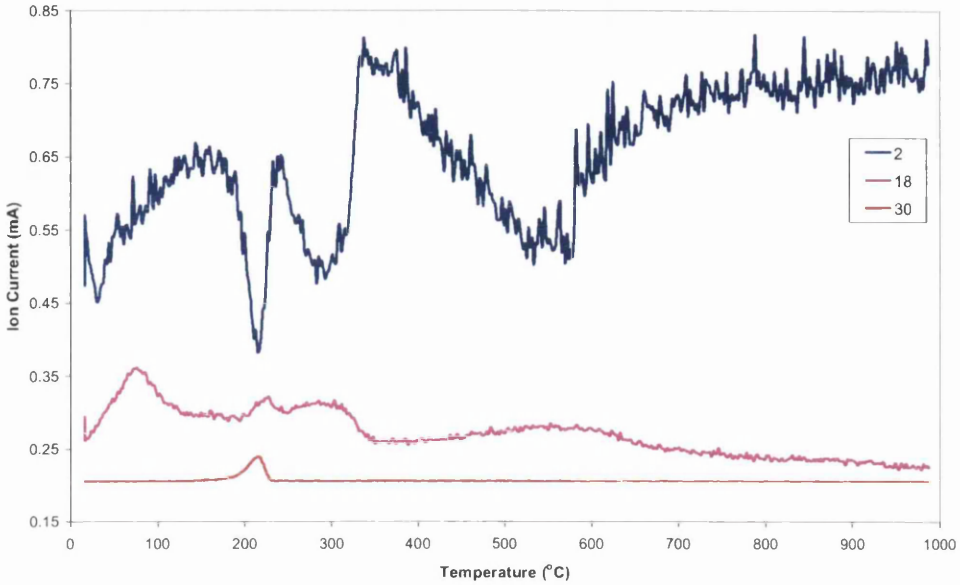

The reduction of CoNST1 is very similar to that of CoNA, although proceeding at a slightly lower temperature. The desorption of water can be seen before 100°C, followed by the decomposition of the nitrate anion at 219°C again coinciding with a slight exotherm on the heat flow curve. The two peaks in the 240-900°C region are again attributed to the reduction of Co_3O_4.

4.3.3.2.4 Hot-stage X-ray diffraction (XRD)

Figure 4.31: Hot-stage XRD patterns of cobalt nitrate on alumina in hydrogen.
Phases denoted are (¤) Co_3O_4 and (*) metallic Co. The XRD pattern is offset for clarity.

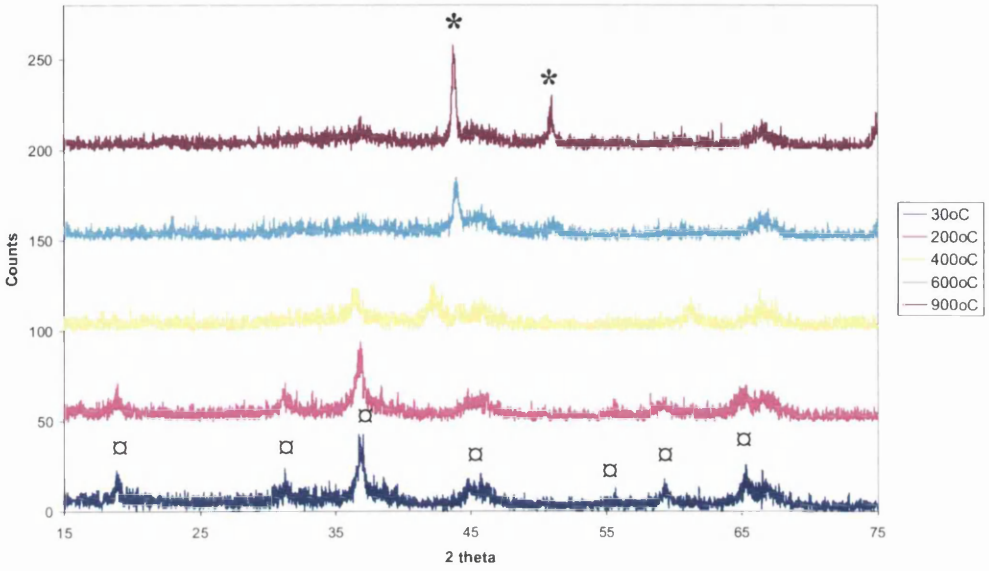

From the CoNA hot-stage XRD pattern, the presence of Co_3O_4 was recognised at 30°C, which disappeared with an increase in temperature. At 300°C and 400°C peaks are present corresponding to the presence of CoO. By 500°C these CoO peaks disappear and sharp peaks appear indicating metallic cobalt are present. Calculations of the size of the cobalt particle size with temperature are shown in table 4.6. The presence of amorphous alumina is also seen throughout. These results again confirm that the reduction of the cobalt oxide spinel Co_3O_4 to metallic Co happens in two steps via CoO.

Table 4.6: Co metal crystallite size as determined by hot-stage XRD of cobalt nitrate on alumina in hydrogen.

Temperature (°C)	Co metal crystallite size (nm)
500	16
600	16
700	18
800	23
900	27

Figure 4.32: Hot-stage XRD patterns of cobalt nitrate on 99% silica + 1% titania in hydrogen.
Phases denoted are (¤) Co_3O_4, (+) CoO and (*) metallic Co. The XRD pattern is offset for clarity.

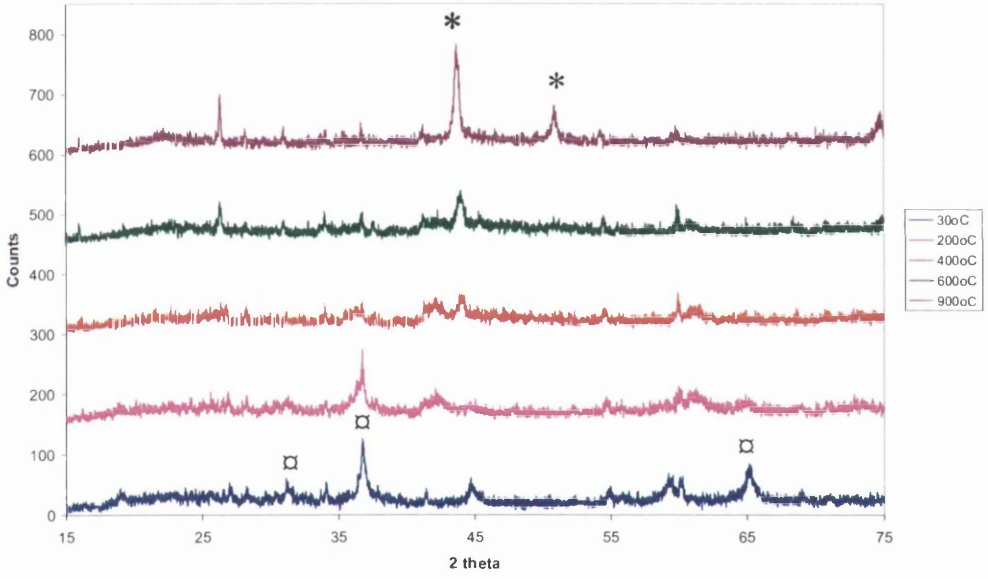

With the hot-stage XRD pattern of CoNST1 again the characteristic peaks of the spinel Co_3O_4 are prominent at 30°C. CoO was detected at 400-600°C, with peaks corresponding to the Co metal appearing at 400°C. Calculation of the Co metal size is shown below from 500°C in table 4.7, showing that the smallest Co particle size occurs at a temperature of 700°C.

Table 4.7: Co metal crystallite size as determined by hot-stage XRD of cobalt nitrate on 99% silica + 1% titania in hydrogen.

Temperature (^{o}C)	Co metal crystallite size (nm)
500	23
600	20
700	13
800	16
900	16

4.3.4 Argon (treatment 4)

4.3.4.1 Cobalt nitrate

4.3.4.1.1 Thermogravimetric analysis-Differential Scanning Calorimetry (TGA-DSC)

Figure 4.33: TGA weight and derivative weight profiles of cobalt nitrate in argon.

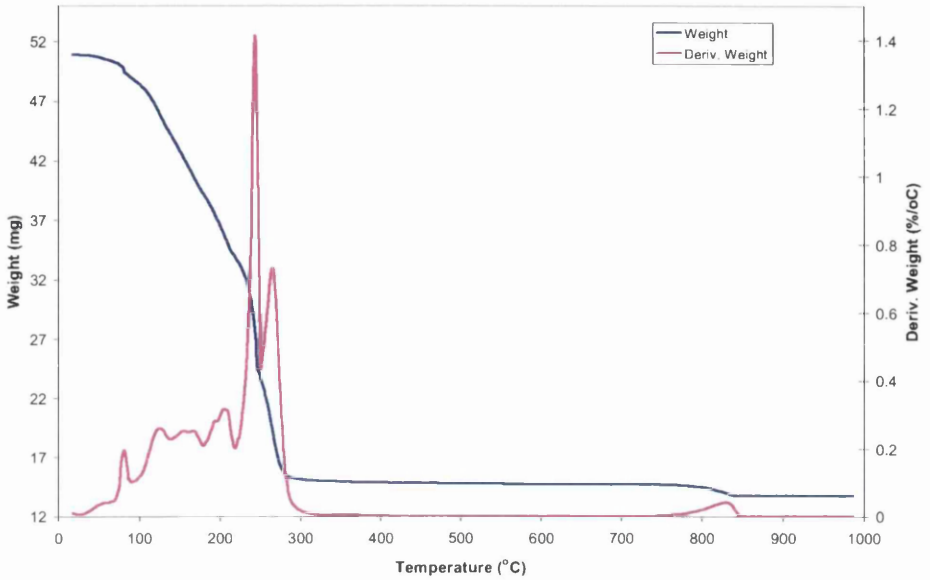

Figure 4.34: TGA-DSC weight and heat flow profiles of cobalt nitrate in argon.

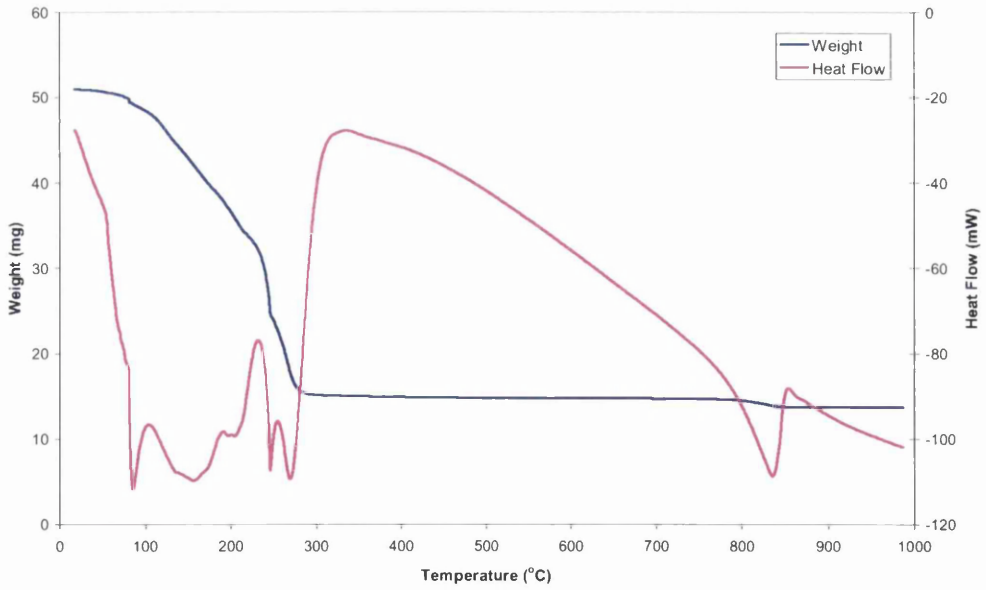

From the weight loss and derivative weight profiles shown in figure 4.33 is it clear that main part of decomposition occurs as several overlapping events before 400°C. There is also an addition weight loss event around 835°C. From the heat flow data in figure 4.34 it

can be seen that all the weight loss are endothermic events. The mass spectrometric data shows that the decomposition occurs via the evolution of water, oxygen, nitrogen monoxide and a small amount of nitrogen dioxide. It can also been seen that the high temperature weight loss around 835°C is accompanied by the evolution of oxygen.

4.3.4.1.2 Mass Spectrometric analysis

Figure 4.35: Mass spectrometric data of H_2O (m/z=18) and O_2 (m/z=32) for cobalt nitrate in argon.

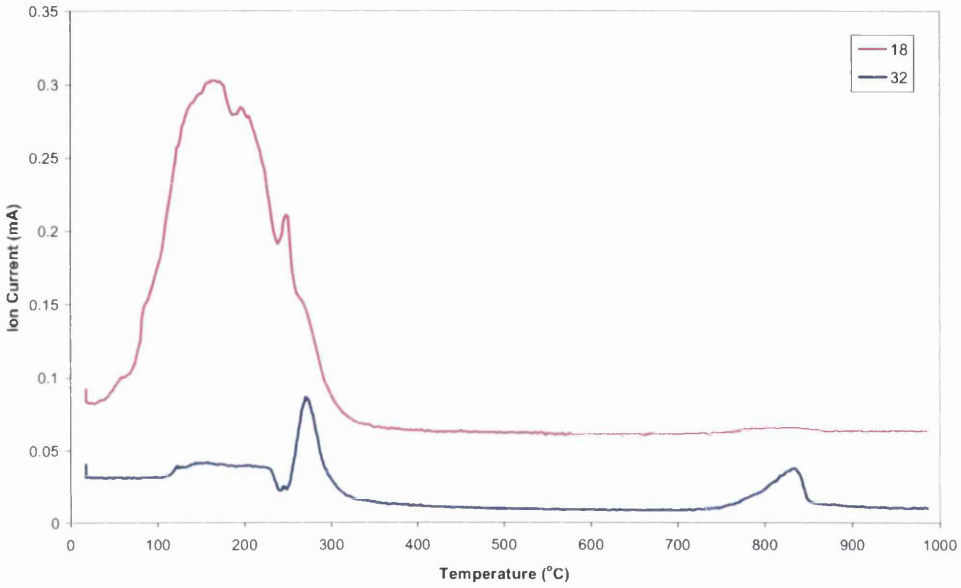

Figure 4.36: Mass spectrometric data of NO (m/z=30) and NO_2 (m/z=46) for cobalt nitrate in argon.

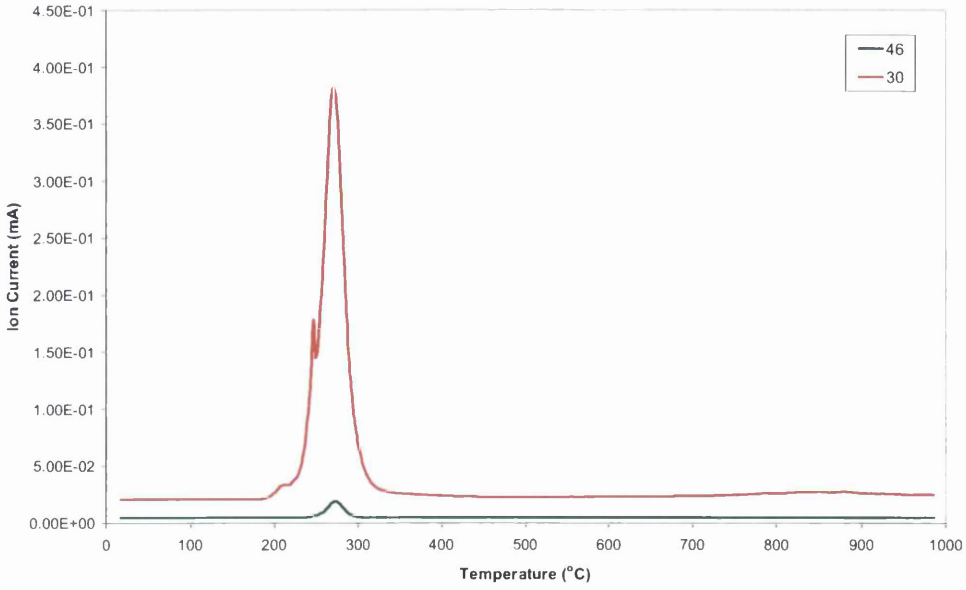

4.3.3.3 Cobalt nitrate supported catalysts

4.3.4.2.1 Thermogravinometric analysis (TGA)

Figure 4.37: TGA weight profiles for cobalt supported on silica, alumina and 99% silica + 1% titania catalysts in argon.

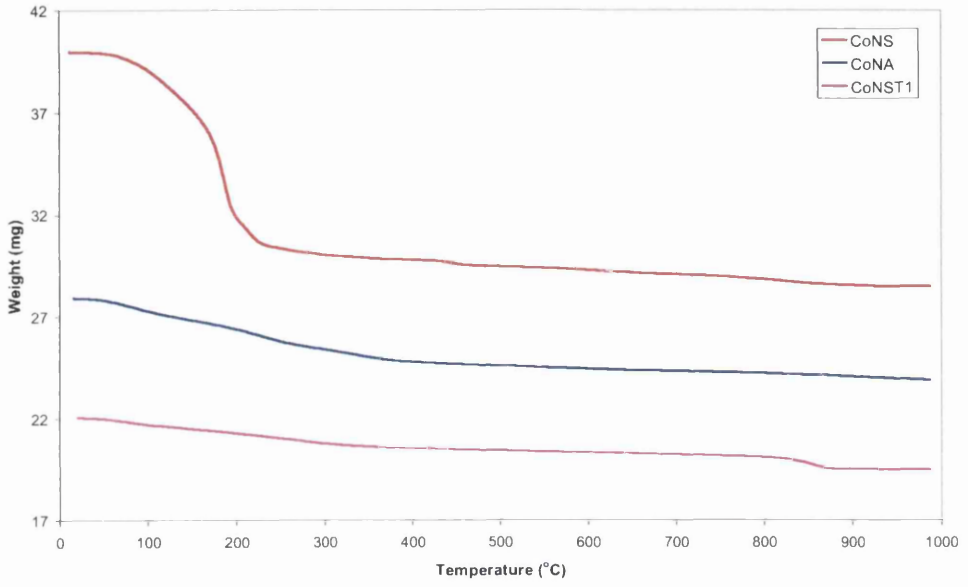

Figure 4.38: TGA derivative weight profiles for silica, alumina and 99% silica + 1% titania supported cobalt catalysts in argon.

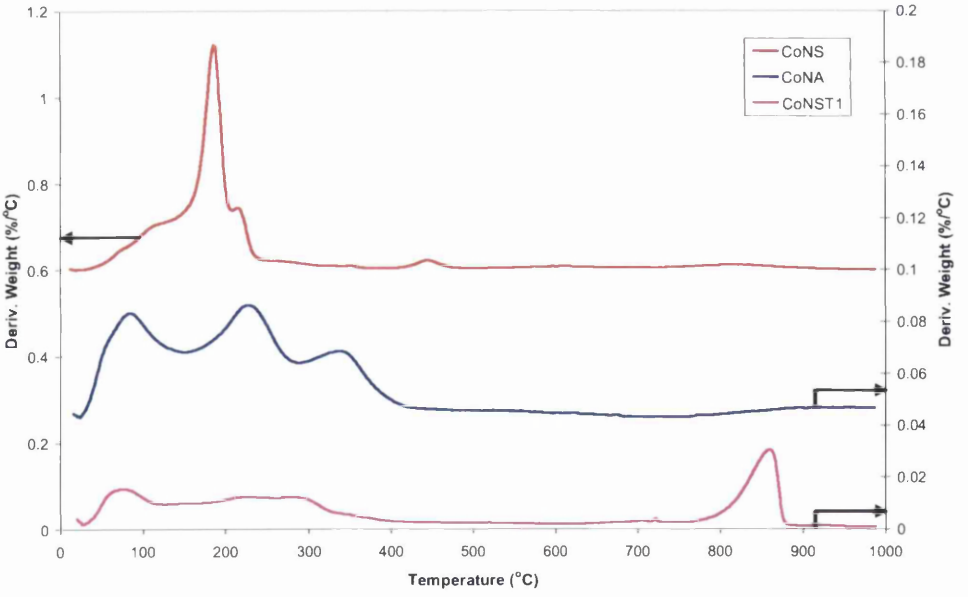

Each of the traces for each of the catalysts shown in figure 4.37 and 4.38 show major weight losses before 500°C. This weight loss is thought to be associated with the desorption of water and decomposition of the nitrate precursor. The CoNS curve is complex, consisting of a single peak with several shoulders with an overall maximum at 187°C. Another small peak is seen at 450°C and two broad higher temperature peaks around 613°C and 824°C. CoNA consists of three main weight loss, with a fourth continuous weight loss region see at temperature higher than 750°C. The TGA curve for CoNST1 shows again three main weight loss events, the first weight loss due to desorption of water before 100°C. The second weight loss region with onset temperatures around 180-400°C are considered to be due to the decomposition of the nitrate anion, with the third weight loss region at much higher temperature of 860°C.

4.3.4.2.2 Differential Scanning Calorimetry (DSC)

Figure 4.39: DSC heat flow profiles of silica, alumina and 99% silica + 1% titania supported cobalt catalysts in argon.

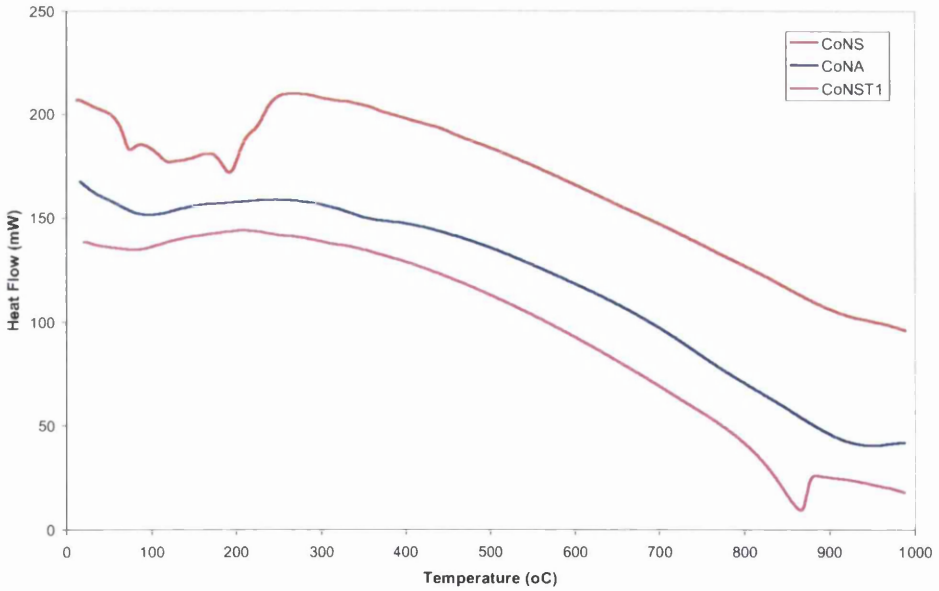

The DSC pattern for each of the catalysts exhibits an endothermic event around 100°C attributed to the removal of physically adsorbed water. The CoNS curve shows a further two endotherms at 125°C and 195°C, which are thought to be due to the decomposition of

nitrate precursor. These events are seen on the CoNS DSC curve with a clarity that is not seen with the derivative weight curve. In the DSC trace of CoNA, as well as the endotherm before 100°C, a possible exotherm is observed around 100-370°C. The DSC pattern for CoNST1 exhibits a small peak at 870°C which is consistent with the weight loss seen in the TGA at that temperature.

4.3.4.2.3 Mass spectrometric analysis

Figure 4.40: Mass spectrometric data of NO (m/z=30) for silica, alumina and 99% silica + 1% titania supported cobalt catalysts in argon.

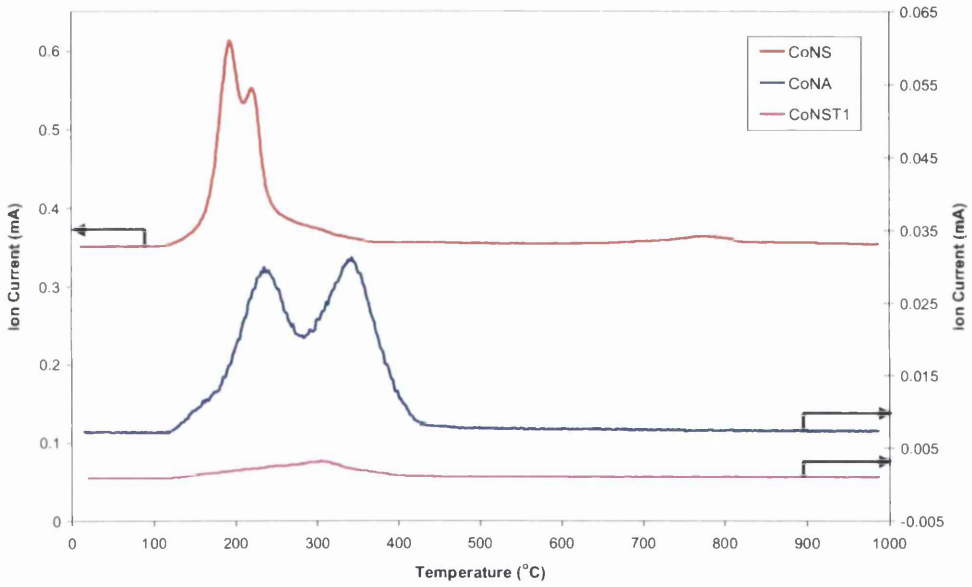

From the graph above of the evolved nitrogen monoxide gas, we can see the temperatures of decomposition of the cobalt nitrate precursors. CoNS curve exhibits three evolutions of NO, two overlapping at 193°C and 220°C and a much higher temperature peak at around 780°C. The nitrate precursors for CoNA decomposes in two steps leading to distinct evolutions of NO at 240°C and 345°C. In contrast, CoNST1 appears to decompose in a single step, with NO evolving as a broad peak between 125-425°C. Although due to the wide breadth of the peak, this could be made up of more than one component.

4.3.4.2.4 Hot-stage X-ray Diffraction (XRD)

Figure 4.41: Hot-stage XRD patterns of cobalt supported on alumina in argon. Phases denoted are (¤) Co_3O_4, (+) CoO and (*) metallic Co. The XRD pattern is offset for clarity.

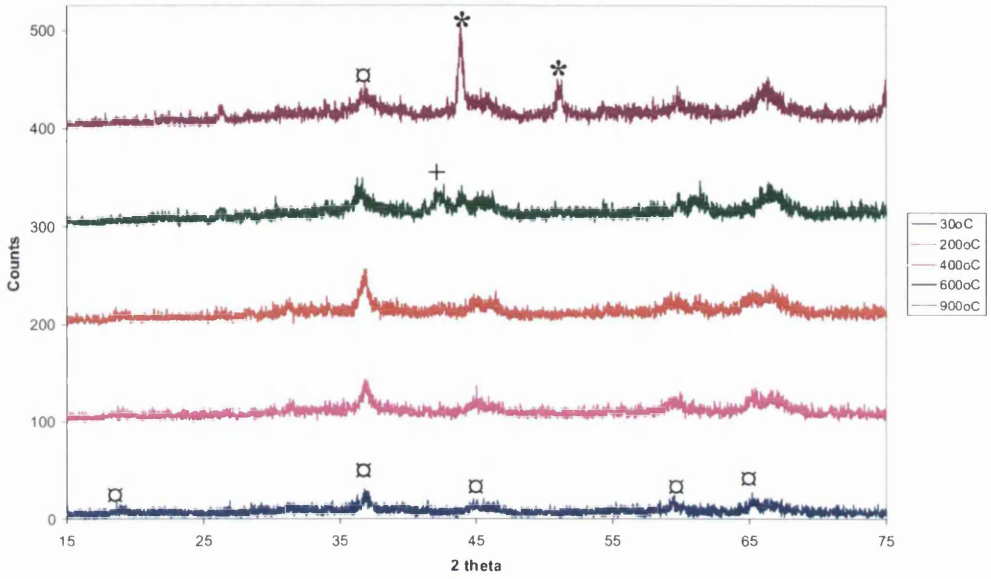

From the hot-stage XRD pattern shown in figure 4.41 it can be seen that Co_3O_4 is clearly present throughout the temperature increase. Calculation of Co_3O4 crystallite size with temperature is shown in table 4.8 below. Crystalline CoO was detected at 600°C which then disappears. However the most interesting feature of the hot-stage XRD is the presence of metallic cobalt appearing at 600-800°C. By means of X-ray line broadening analysis the size of the cobalt metal particles was found to be 13nm and 20 nm, at 700 and 800°C respectively.

Table 4.8: Co_3O_4 crystallite size as determined by hot-stage XRD of cobalt nitrate on alumina in argon.

Temperature (°C)	Co_3O_4 crystallite size (nm)
30	16
100	13
200	10
300	11
400	10
500	10
600	13
700	13

4.4 Cobalt Acetate

4.4.1 Oxygen (treatment 1)

4.4.1.1 Cobalt acetate

4.4.1.1.1 Thermogravimetric analysis-Differential Scanning Calorimetry (TGA-DSC)

Figure 4.42: TGA weight and derivative weight profiles for cobalt acetate in oxygen.

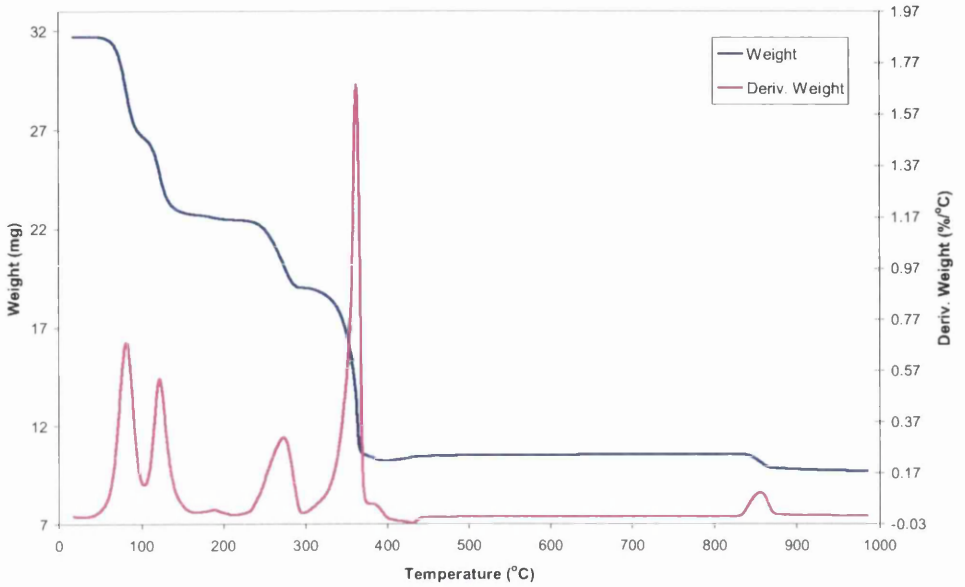

Figure 4.43: TGA-DSC weight and heat flow profiles for cobalt acetate in oxygen.

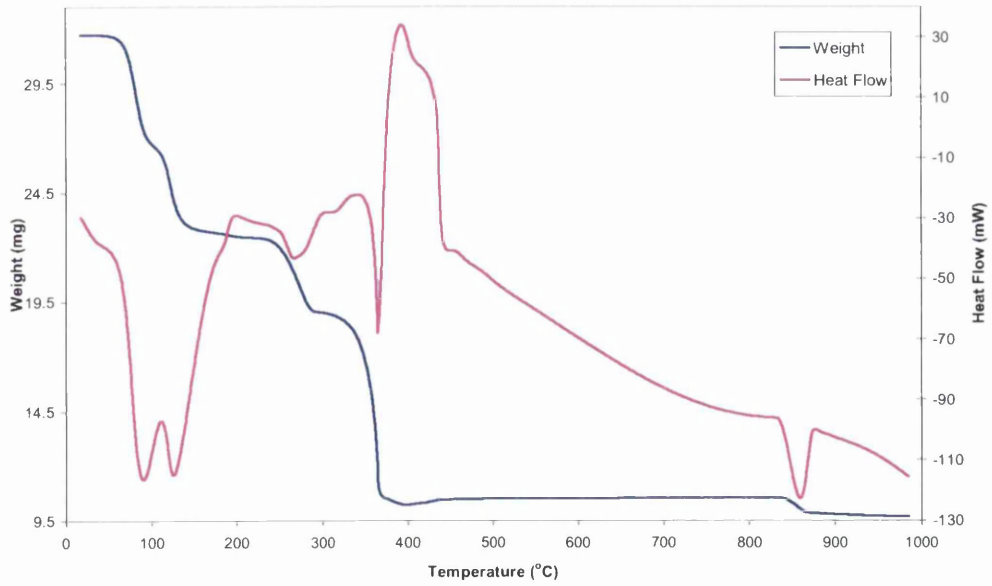

From the weight loss and derivative weight profiles in figure 4.42 it can be seen that there are four main weight loss events before 385°C. Between 388-447°C, weight loss and derivative weight profiles suggest a weight gain. There is an additional weight loss event at higher temperatures around 860°C. The heat flow profile in figure 4.43 shows that all the weight losses correspond to an endothermic event. In contrast to this, from the heat flow profile, it can be seen that the weight gain that is observed is highly exothermic. Mass spectrometric data confirms that the cobalt oxide decomposition in oxygen occurs via the evolution of water, oxygen, hydrogen, carbon monoxide and carbon dioxide.

4.4.1.1.2 Mass Spectrometric analysis

Figure 4.44: Mass spectrometric data of CO (m/z=28), O_2 (m/z=32) and CO_2 (m/z=44) for cobalt acetate in oxygen.

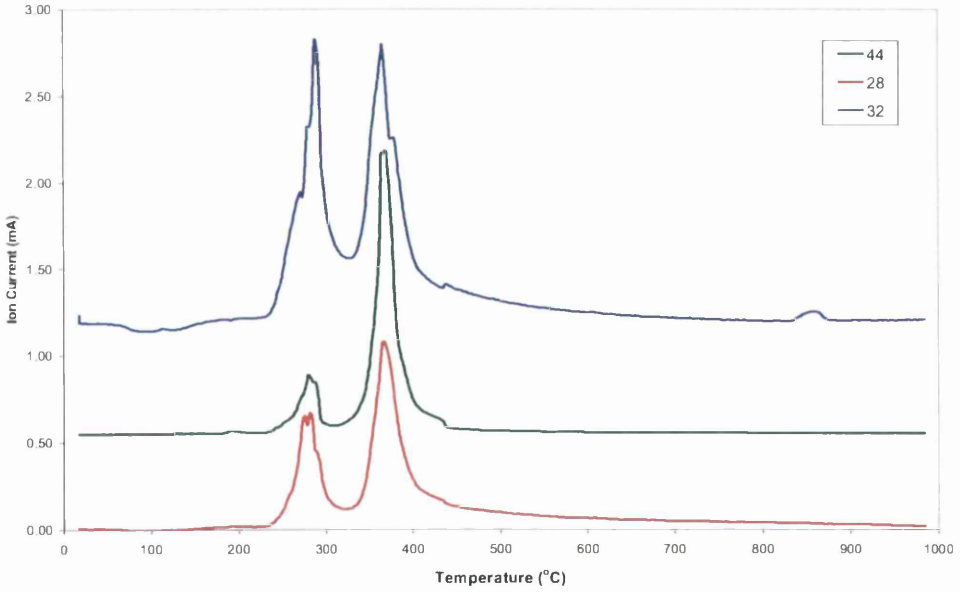

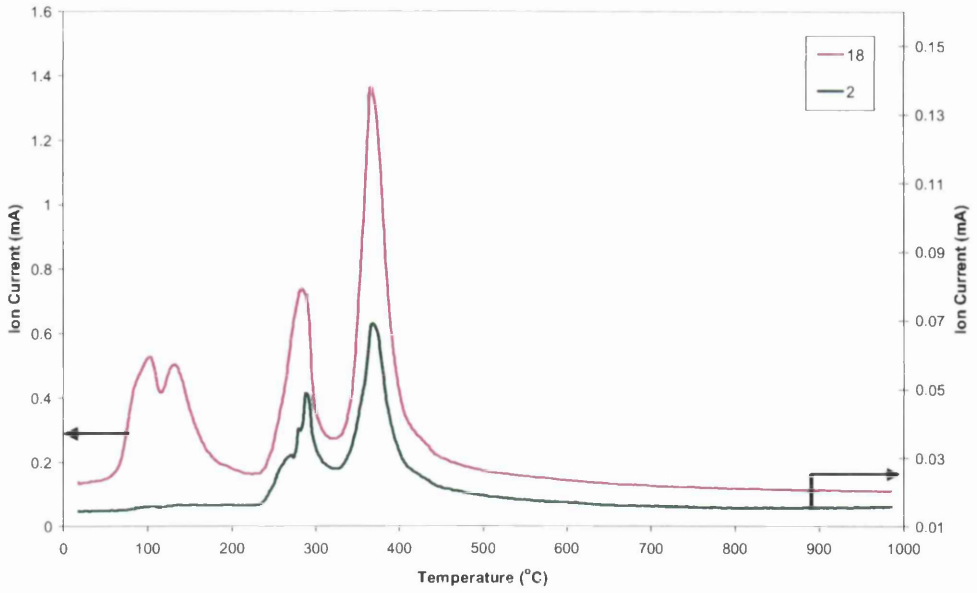

Figure 4.45: Mass spectrometric data of H_2 (m/z=2), H_2O (m/z=18) for cobalt acetate in oxygen.

4.4.1.2 Cobalt acetate supported catalysts

4.4.1.2.1 Thermogravimetric analysis (TGA)

Figure 4.46: TGA weight profiles of silica, alumina and 99% silica + 1% titania supported cobalt catalysts in oxygen.

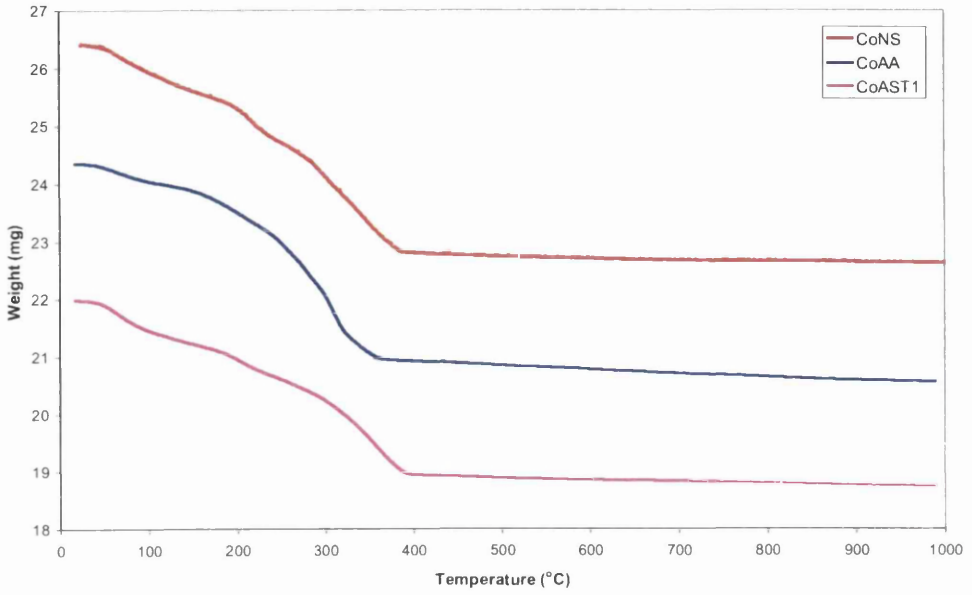

The TGA curves in figure 4.46 shows significant weight loss for each the catalysts upon heating to 400°C. Above this temperature there is very little weight loss. From the derivative weight profiles shown in figure 4.47 it can been see that the curves for the CoAS and CoNST1 catalysts are similar, and show three main weight loss events. In contrast to this the CoAA catalyst is more complex showing a first peak before 100°C followed by a broad main peak with several shoulders and a maximum at 310°C.

Figure 4.47: TGA derivative weight profiles of silica, alumina and 99% silica + 1% titania supported cobalt catalysts in oxygen.

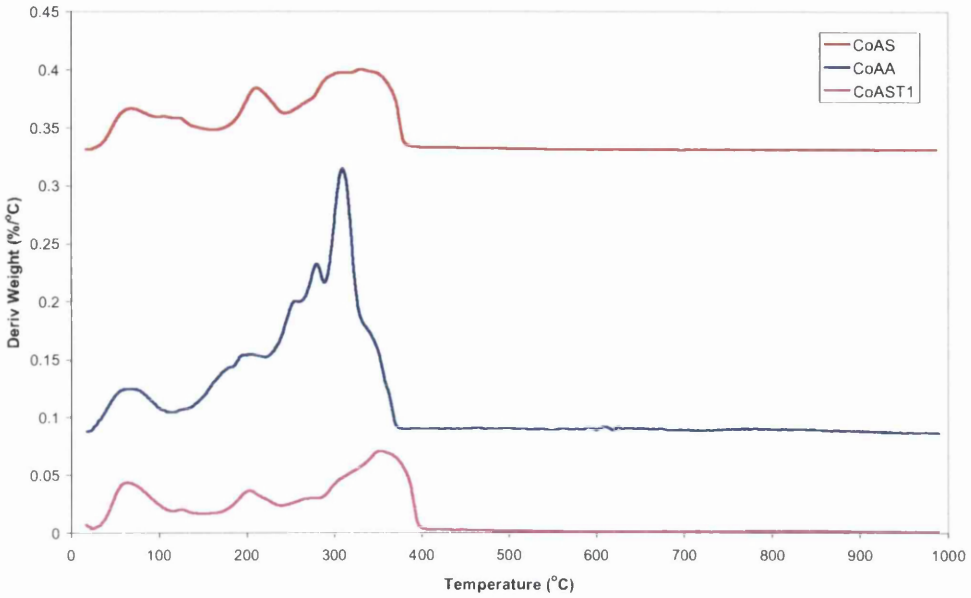

4.4.1.2.2 Differential Scanning Calorimetry (DSC)

Figure 4.48: DSC heat flow profiles of silica, alumina and 99% silica + 1% titania supported cobalt catalysts in oxygen.

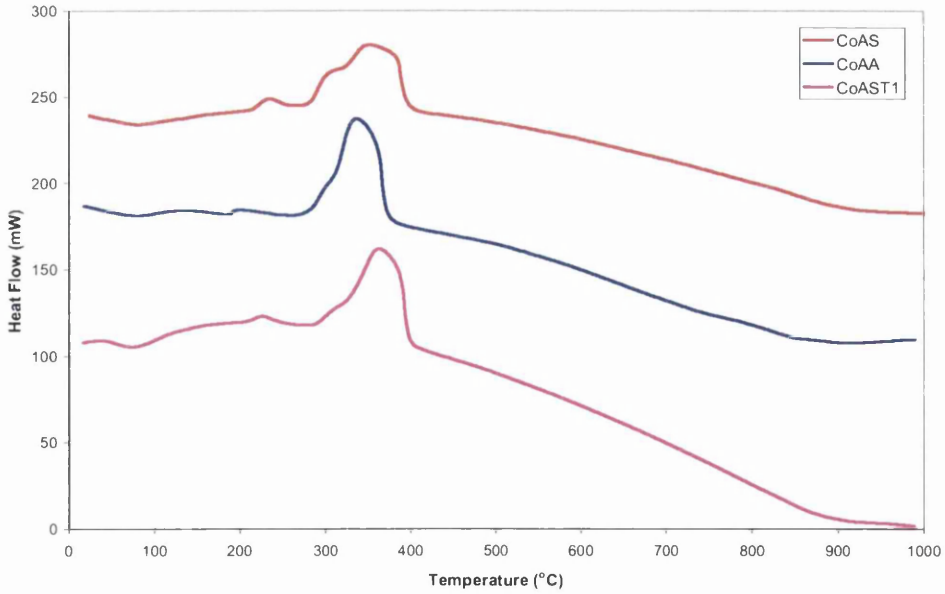

The DSC curves shown in figure 4.48 for each of the catalysts all indicate an endothermic event before 100°C which can be attributed to the desorption of water. CoAS and CoAST1 catalysts are similar again in that further to this endothermic loss of water, their DSC curves exhibit two exotherms at higher temperatures. The second of these peaks is highly exothermic but also broad with a small shoulder seen suggesting perhaps two separate thermal events .The maximum for these highly exothermic events second peak, occur at 353°C for CoAS and 366°C for CoAST1. In addition to the endotherm before 100°C, the DSC curve for CoAA catalysts also exhibits three exothermic events at 141°C, 204°C and a main peak at 340°C. Again this highly exothermic last peak is seen to have a slight shoulder suggesting more than one thermal event.

4.4.1.2.3 Mass Spectrometric analysis

Figure 4.49: Mass spectrometric data of H2 (m/z=2), H2O (m/z=18), CO (m/z=28), O2 (m/z=32) and CO2 (m/z=44) for silica supported cobalt catalyst in oxygen.

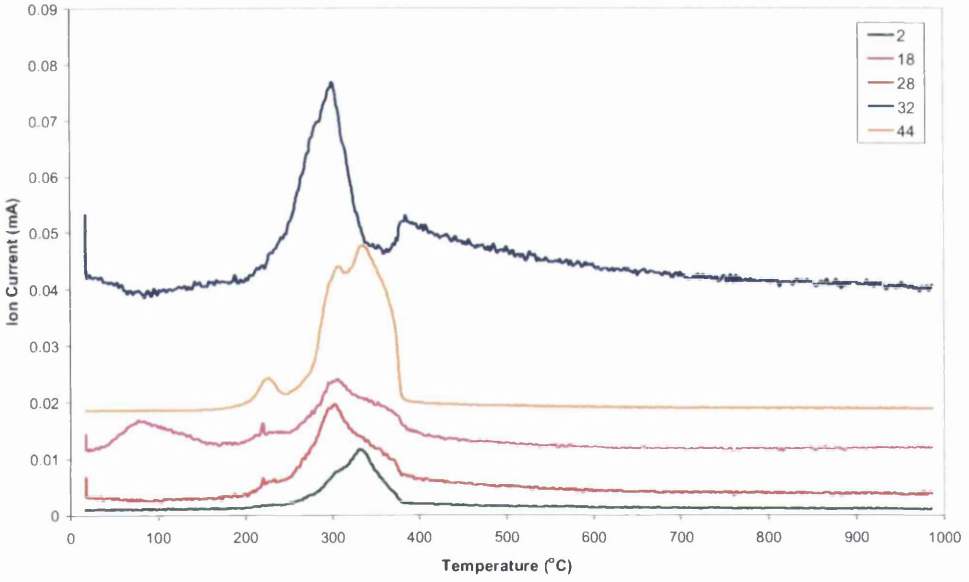

The products from the decomposition in oxygen of the CoAS catalyst, reported by the mass spectrometric analysis, are shown above in figure 4.49. Apart from the evolution of water before 100°C, all the products detected evolve around the same temperature between 200-400°C. The MS data for the decomposition of CoAS in oxygen show the release of CO and CO_2, as well as hydrogen and water. The most interesting feature however is the evolution of oxygen, since uptake of oxygen was expected.

Figure 4.50: Mass spectrometric data of H2 (m/z=2), H_2O (m/z=18), CO (m/z=28), O_2 (m/z=32) and CO_2 (m/z=44) for alumina supported cobalt catalyst in oxygen

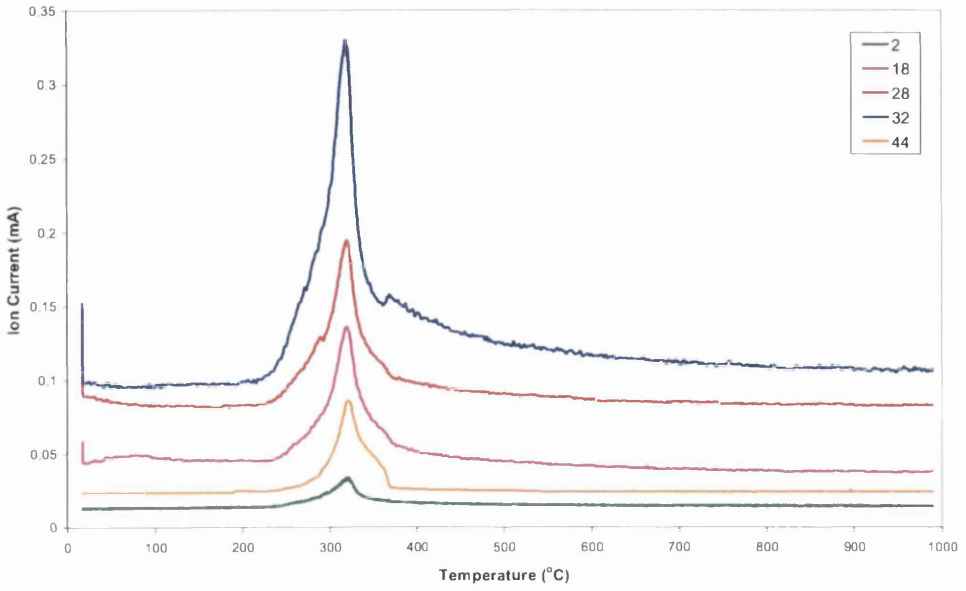

For CoAA, with the exception of desorption of water around 100°C, the products detected with MS all evolve at 320°C. A shoulder is present on some of the evolved gas peaks suggesting perhaps more than one evolution. Again the CoAA catalyst decomposes in oxygen via the release of carbon monoxide, carbon dioxide, hydrogen, water and oxygen.

Figure 4.51: Mass spectrometric data of H_2 (m/z=2), H_2O (m/z=18), CO (m/z=28), O_2 (m/z=32) and CO_2 (m/z=44) for 99% silica + 1% titania supported cobalt catalyst in oxygen

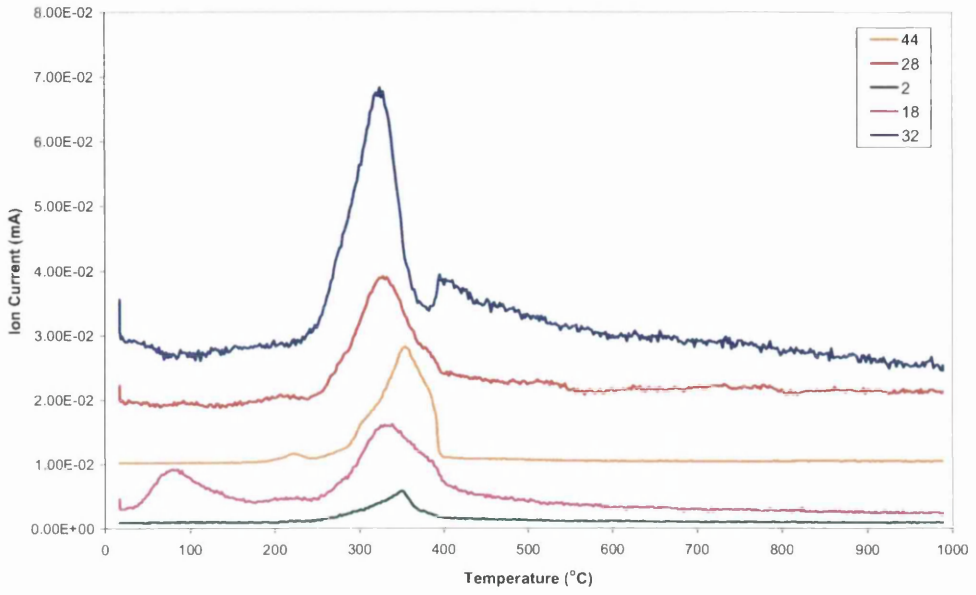

The MS data for CoAST1 is similar to that of CoAS, although the evolution of products occur at a slightly higher temperature, between 250-450°C.

4.4.1.2.4 Hot-stage X-ray Diffraction (XRD)

CoAA catalyst was analysed by *in-situ* hot-stage XRD. From its pattern, shown in figure 4.52, the appearance of the spinel oxide Co_3O_4 was recognised. Using line broadening analysis, the peak at 36.5° was used to determine the average Co_3O_4 particle size with temperature. The results shown in table 4.9 range from 500-900°C. Unfortunately, below this temperature the XRD lines were so broad that accurate estimations of size were not possible.

Figure 4.52: Hot-stage XRD pattern of cobalt acetate on alumina in oxygen. Phases denoted are (¤) Co_3O_4. The XRD patterns are offset for clarity.

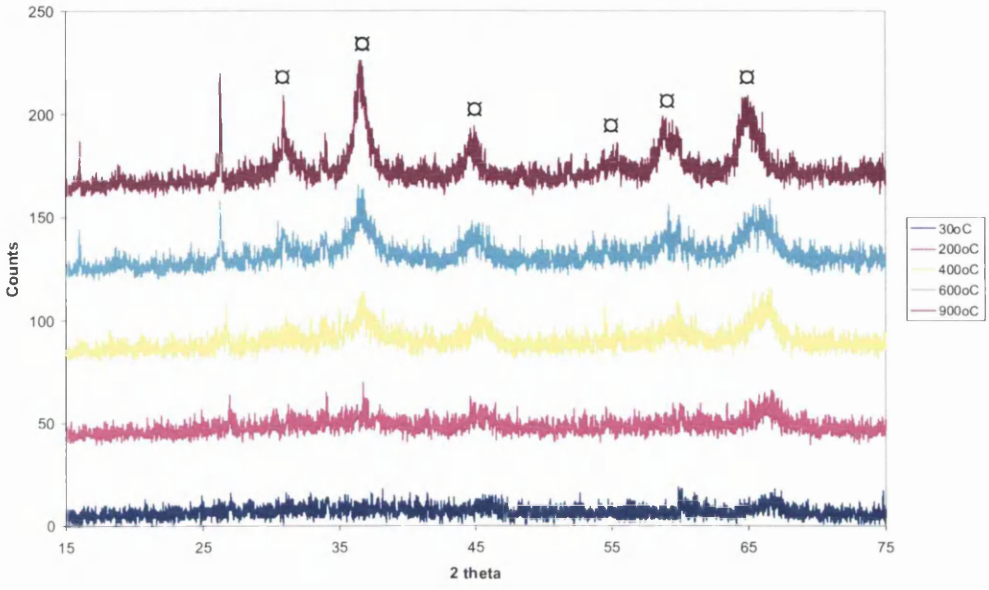

Table 4.9: Co_3O_4 crystallite size as determined by hot-stage XRD of cobalt acetate on alumina in oxygen.

Temperature (°C)	Co_3O_4 crystallite size (nm)
500	10
600	9
700	9
800	13
900	9

4.4.2 Hydrogen after calcination in oxygen (treatment 2)

4.4.2.1 Cobalt acetate supported catalysts

4.4.2.1.1 Thermogravimetric analysis (TGA)

Figure 4.53: TGA weight profiles of silica, alumina and 99% silica + 1% titania supported cobalt catalysts in hydrogen after calcination in oxygen.

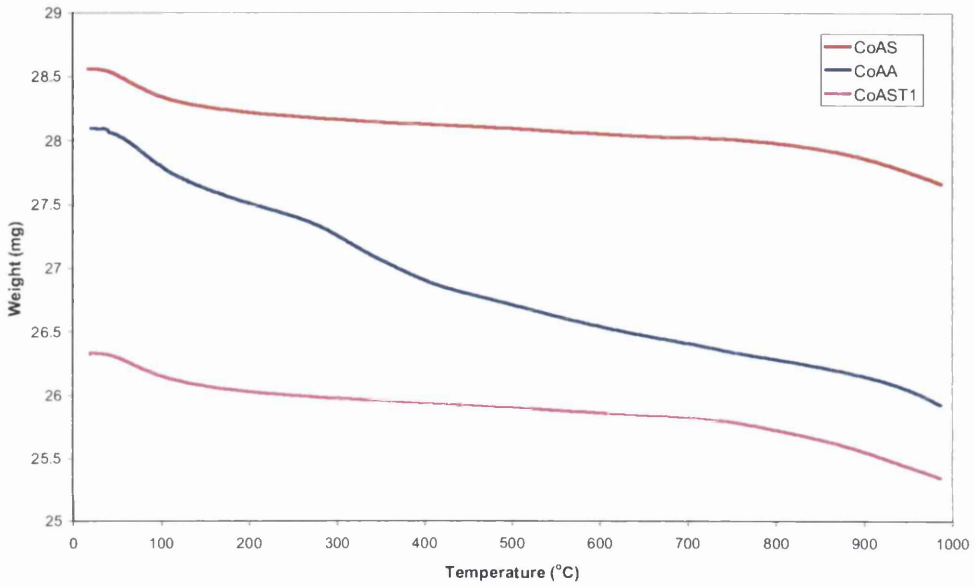

The weight loss and derivative weight curves obtained from the TGA analysis in a hydrogen atmosphere for all the catalysts are depicted in figures 4.53 and 4.54, respectively. The derivative weight curves are similar for CoAS and CoAST1 catalysts, with two main regions of weight loss observed. The derivative weight curve for CoAA shows one peak around 70°C, with a broad peak which appears to be two separate weight loss events at 318°C and 377°C. Another smaller peak is seen at 735°C with again a continuous weight loss region seen at temperature higher than 800°C.

Figure 4.54: TGA derivative weight profiles of silica, alumina and 99% silica + 1% titania supported cobalt catalysts in hydrogen after calcination in oxygen.

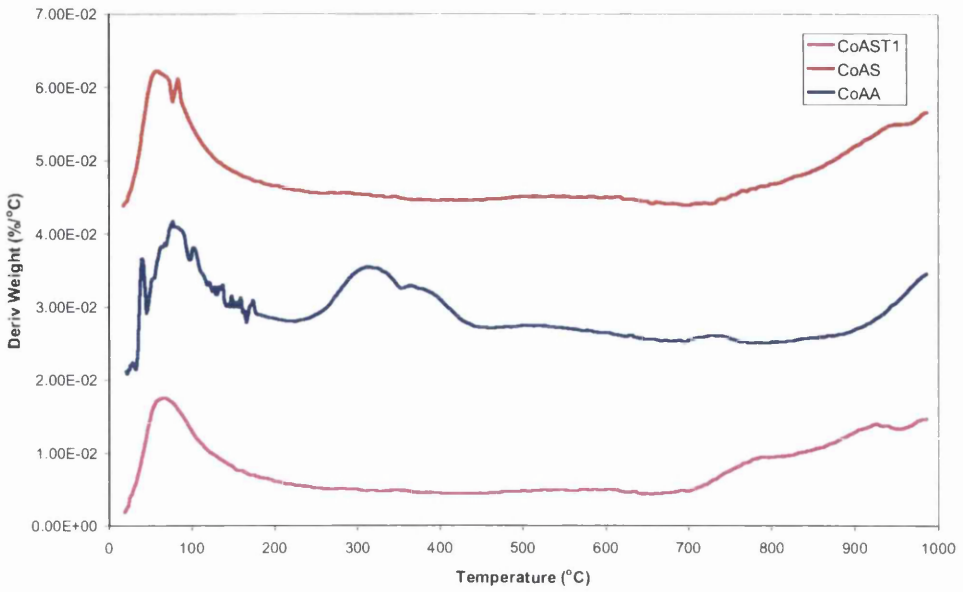

4.4.2.1.2 Differential Scanning Calorimetry (DSC)

Figure 4.55: DSC heat flow profiles of silica, alumina and 99% silica + 1% titania supported cobalt catalysts in hydrogen after calcination in oxygen.

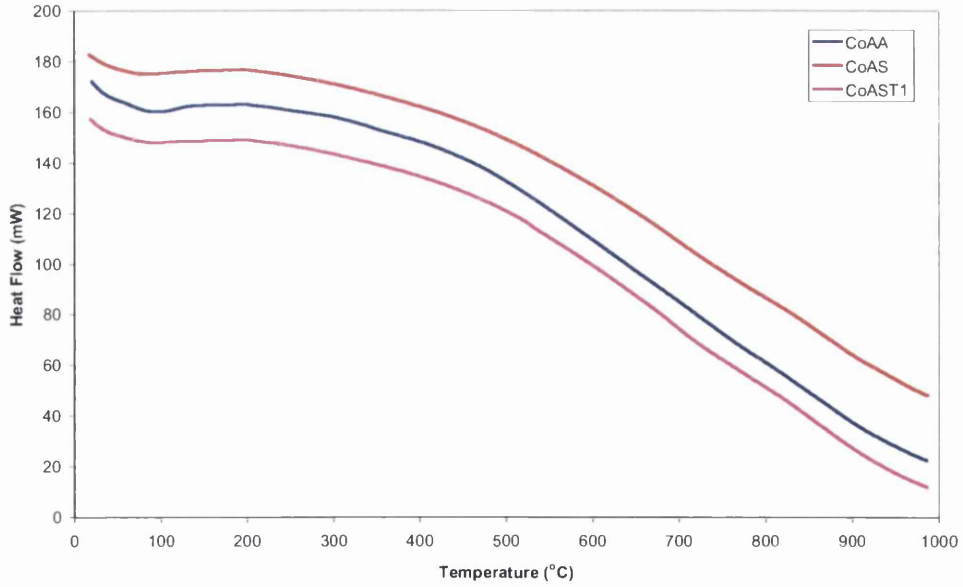

The DSC curves for each of the catalysts are shown in figure 5.55. Apart from the characteristic endothermic peak typically associated with the desorption of water before 100°C, the DSC curves for all of the catalysts appear relatively featureless.

4.4.2.1.3 Mass Spectrometric analysis

Figure 4.56: Mass spectrometric data of H_2 (m/z=2), H_2O (m/z=18) for silica supported cobalt catalyst in hydrogen after calcination in oxygen.

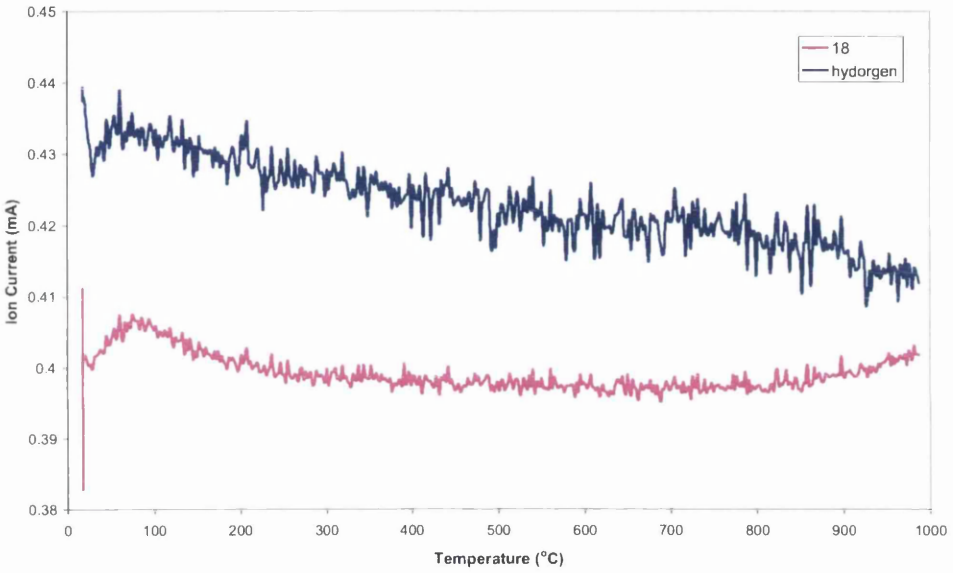

The curves for hydrogen uptake and water formed are shown in figure 4.56. As well as the evolution of water just before 100°C, the uptake of hydrogen coinciding with the evolution of water can be seen beyond 750°C.

Figure 4.57: Mass spectrometric data of H_2 (m/z=2), H_2O (m/z=18) for alumina supported cobalt catalyst in hydrogen after calcination in oxygen.

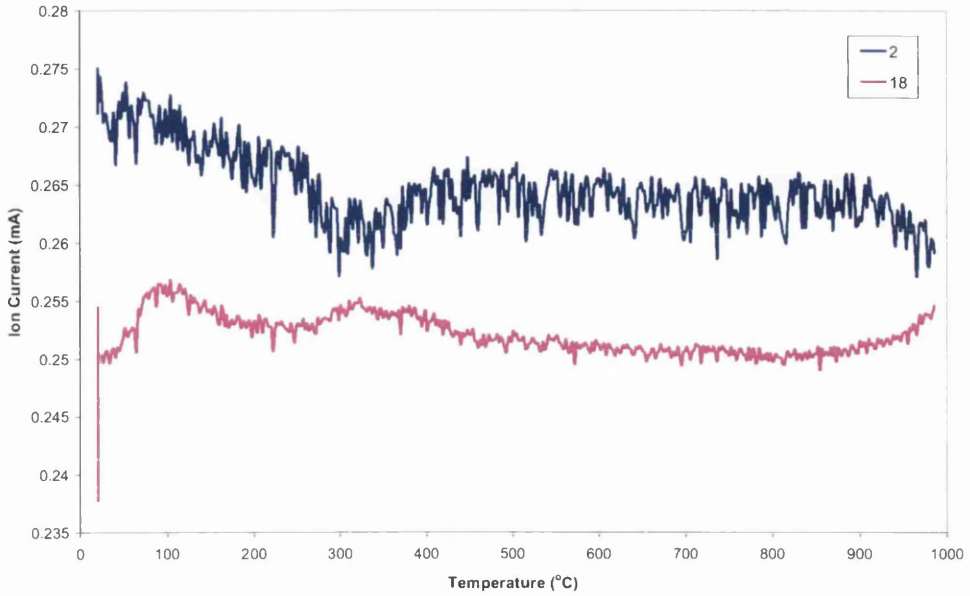

For CoAA catalyst, water is evolved and observed on three separate occasions corresponding to the uptake of hydrogen. These occur around 100°C, 350°C and a continuous increase in hydrogen consumption at temperatures higher than 850°C. The breadth of the peak at 350°C suggests perhaps two evolutions of water occur.

Figure 4.58: Mass spectrometric data of H_2 (m/z=2), H_2O (m/z=18) for 99% silica + 1% titania supported cobalt catalyst in hydrogen after calcination in oxygen.

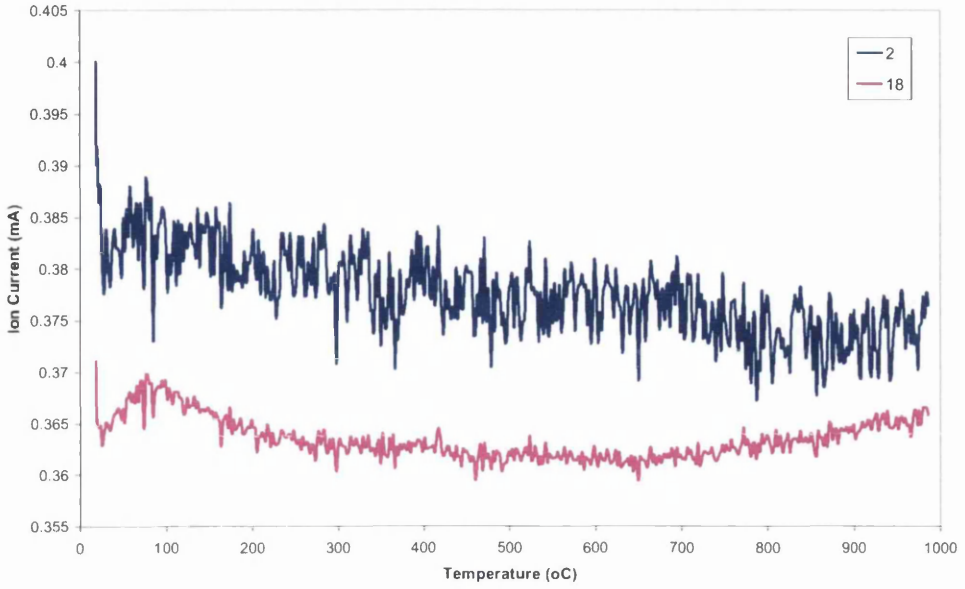

Again the mass spectrometric data for CoAST1 is similar to that of the CoAS. It shows the evolution of water around 100°C followed by continuous uptake of hydrogen with further evolution of water above 650°C.

4.4.2.1.4 Hot-stage X-ray Diffraction (XRD)

The hot-stage XRD patterns for CoAA are presented in figure 4.59. At 30°C the pattern clearly exhibits crystalline Co_3O_4 and CoO, by 500°C cobalt metal can be detected. From the broadening of lines the crystallite size of Co metal can be estimated, and shows at 800°C and 900°C the particles were 12nm and 13nm, respectively.

Figure 4.59: Hot-stage XRD patterns of cobalt acetate on alumina hydrogen after calcination in oxygen.
Phases denoted are (¤) Co_3O_4, (+) CoO and (*) metallic Co. The XRD pattern is offset for clarity.

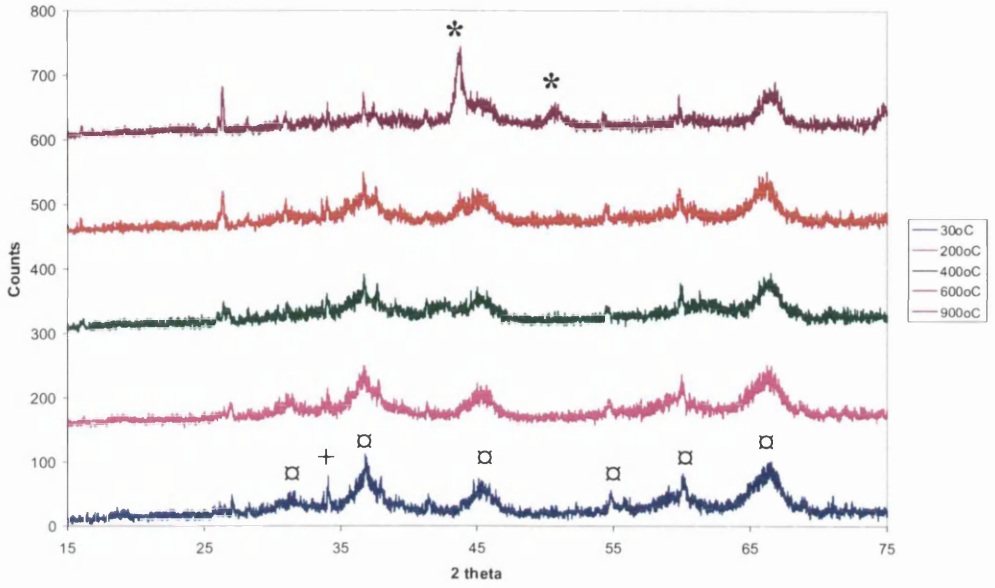

Figure 4.60: Hot-stage XRD patterns of cobalt acetate on 99% silica + 1% titania in hydrogen after calcination in oxygen.
Phases denoted are (¤) Co_3O_4, and (*) metallic Co. The XRD pattern is offset for clarity.

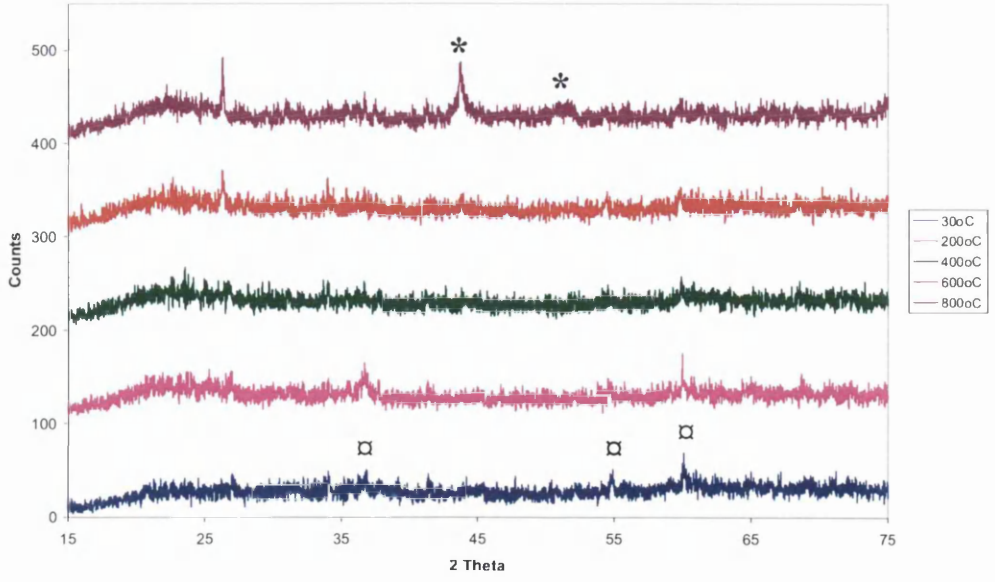

In figure 4.60 the hot-stage XRD patterns for CoAST1 catalyst in hydrogen are shown. From its pattern at 30°C, the presence of Co_3O_4 was recognised. The relatively featureless XRD patterns suggests the presence of much non-crystalline material. A sharp peak at 43.7° indicating the presence of metallic cobalt is seen from 700°C. Again using line-broadening analysis, the crystallite size of the cobalt metal was calculated and found to be 20nm at both 700°C and 800°C.

4.4.3 Hydrogen (treatment 3)

4.4.3.1 Cobalt acetate

4.4.3.1.1 Thermogravimetric analysis-Differential Scanning Calorimetry (TGA-DSC)

The results show in this section are of the 'as prepared' catalysts in hydrogen with no pre-treatment.

Figure 4.61: TGA weight and derivative weight profiles of cobalt acetate in hydrogen.

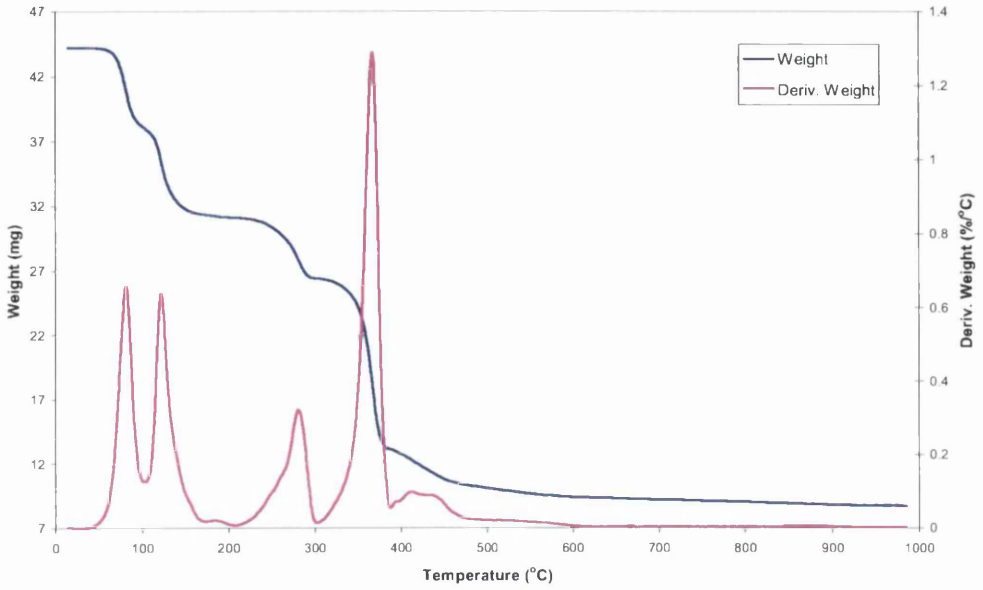

Figure 4.62: TGA-DSC derivative weight and heat flow profiles of cobalt acetate in hydrogen.

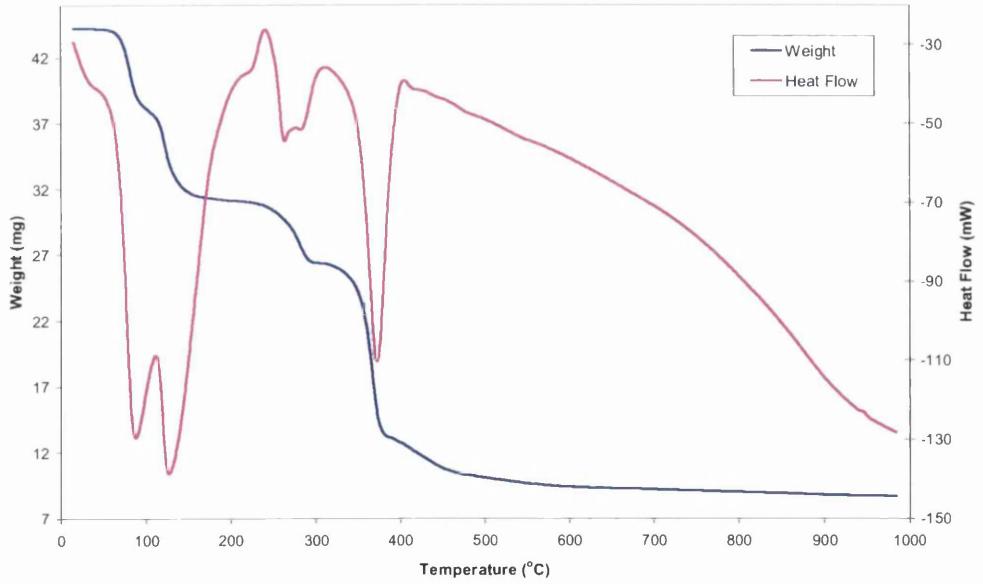

The weight and derivative weight profiles in figure 4.61 show that the reduction of cobalt acetate occurs as about six events. From the heat flow profile in figure 4.62 it is clear that the four events before 390°C are endothermic, with the weight loss events after this temperature appearing relatively featureless on the heat flow profile. From the mass spectrometric data it can be seen that the endothermic weight loss events occur via the evolution of water, oxygen, carbon monoxide and carbon dioxide. The events after 390°C correspond to the uptake of hydrogen and simultaneous evolution of water.

4.4.3.1.2 Mass Spectrometric analysis

Figure 4.63: Mass spectrometric data of H_2 (m/z=2) and H_2O (m/z=18) for cobalt acetate in hydrogen.

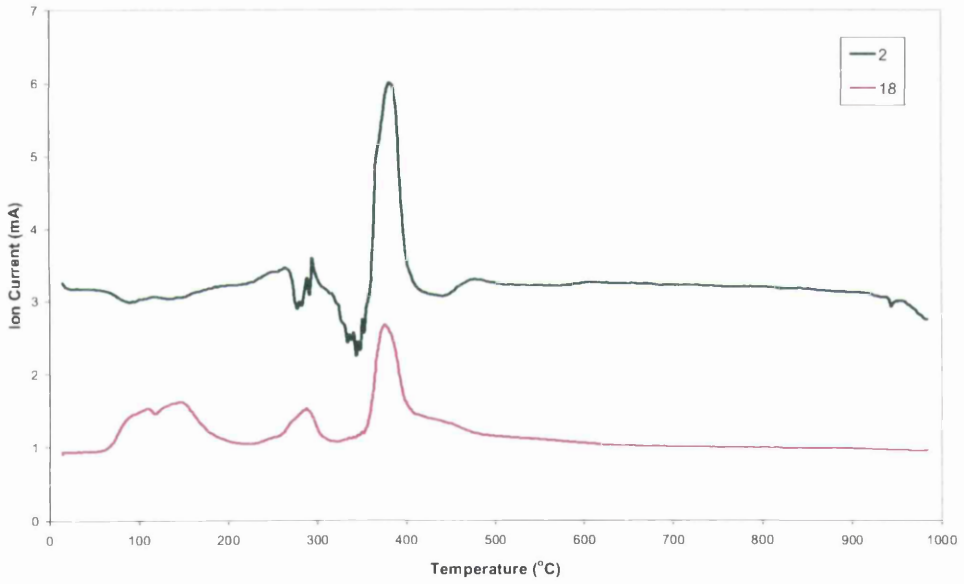

Figure 4.64: Mass spectrometric data of H_2 (m/z=2) and H_2O (m/z=18) for cobalt acetate in hydrogen.

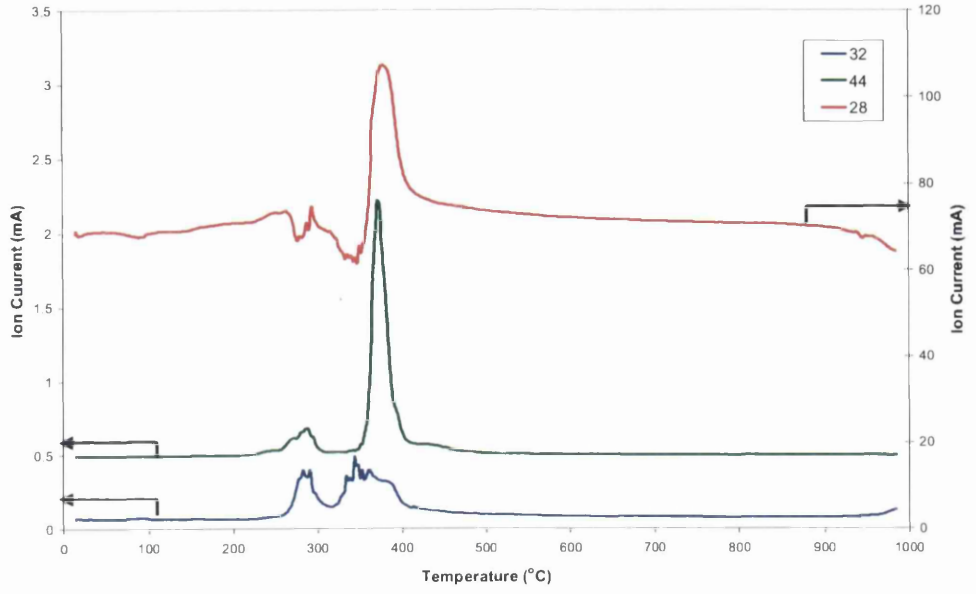

4.4.2.2 Cobalt acetate supported catalysts

4.4.3.2.1 Thermogravimetric analysis (TGA)

Figure 4.65: TGA weight profiles silica, alumina and 99% silica +1% titania supported cobalt catalysts in hydrogen.

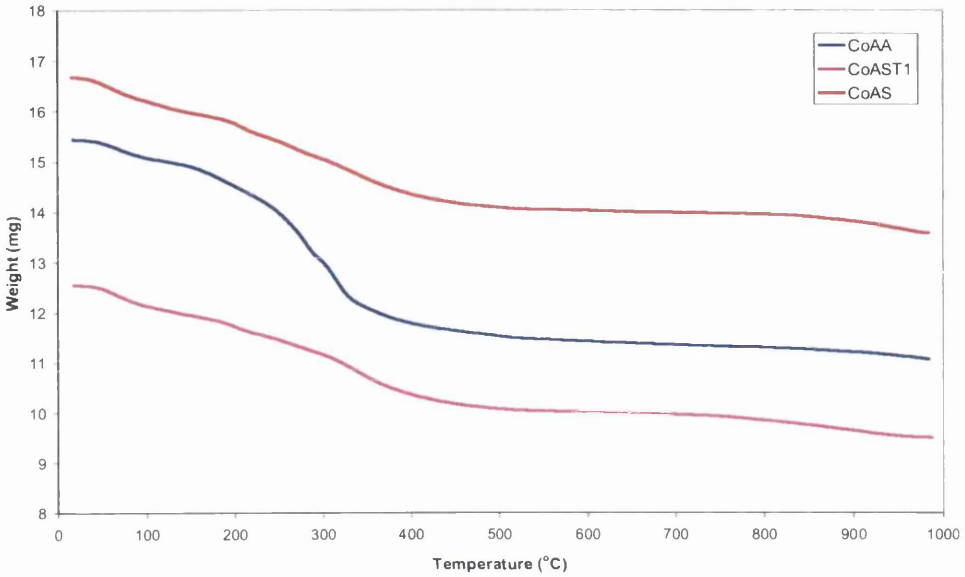

Weight loss and derivative weight profiles of cobalt catalysts on various oxide supports are shown in figures 4.65 and 4.66, respectively. The derivative weight curves for each of the catalysts is complex, consisting of a series of overlapping peaks up to 550°C, with several broader peaks at higher temperatures. These weight losses are thought to be due to the desorption of water, decomposition of the acetate precursor and reduction of cobalt oxide. For each of the catalysts the weight loss profile, shows that the majority of weight is lost before 550°C.

Figure 4.66: TGA derivative weight profiles of silica, alumina and 99% silica +1% titania supported cobalt catalysts in hydrogen.

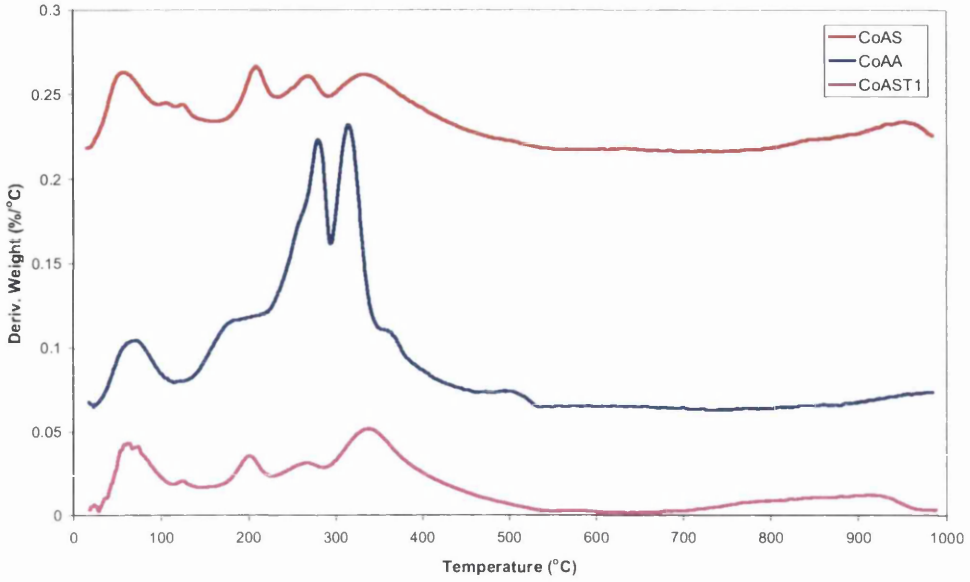

4.4.3.2.2 Differential Scanning Calorimetry (DSC)

Figure 4.67: DSC heat flow profiles of silica, alumina and 99% silica + 1% titania supported cobalt catalysts in hydrogen.

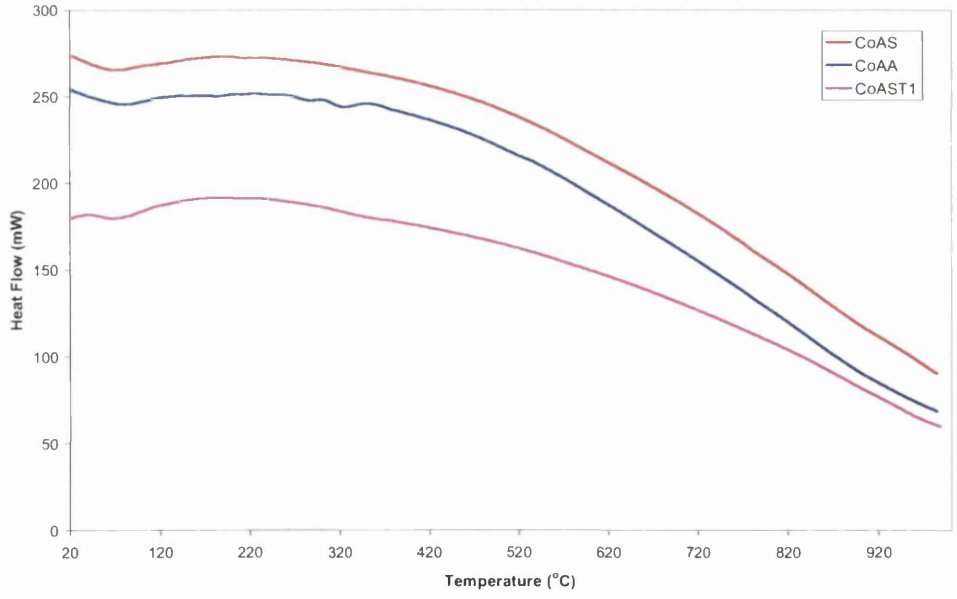

Comparison of the DSC profiles in figure 4.67 show very little variation. An endotherm around 80°C is seen in the DSC profile for each of the catalysts, and can be ascribed to the desorption of water. The CoAA catalyst shows a subtle difference from the other catalysts in that two small endothermic inflections are observed at 290°C and 330°C.

4.4.3.2.3 Mass Spectrometric analysis

Figure 4.68 : Mass spectrometric data of H_2 (m/z=2), H_2O (m/z=18) and CO (m/z=28) for silica supported cobalt catalysts in hydrogen.

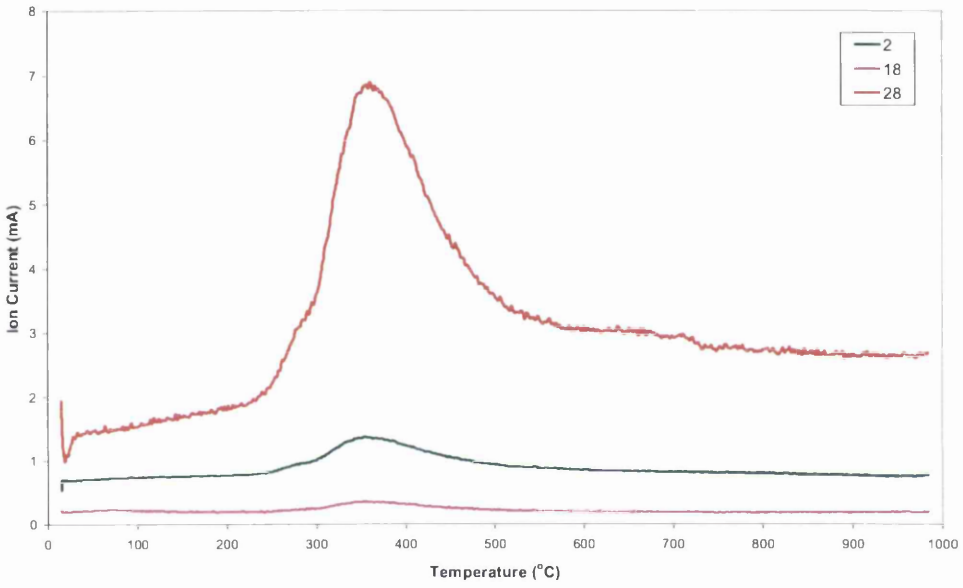

Mass spectrometric analysis of the effluent gas during this treatment is shown in figure 4.68. It shows that the decomposition of the cobalt precursor is accompanied by the evolution of hydrogen, water, carbon monoxide as well as small amounts of oxygen and carbon dioxide. These all evolve over a wide temperature range with a maximum at 360°C.

Figure 4.69 : Mass spectrometric data of H_2 (m/z=2), H_2O (m/z=18) and CO (m/z=28) for alumina supported cobalt catalysts in hydrogen.

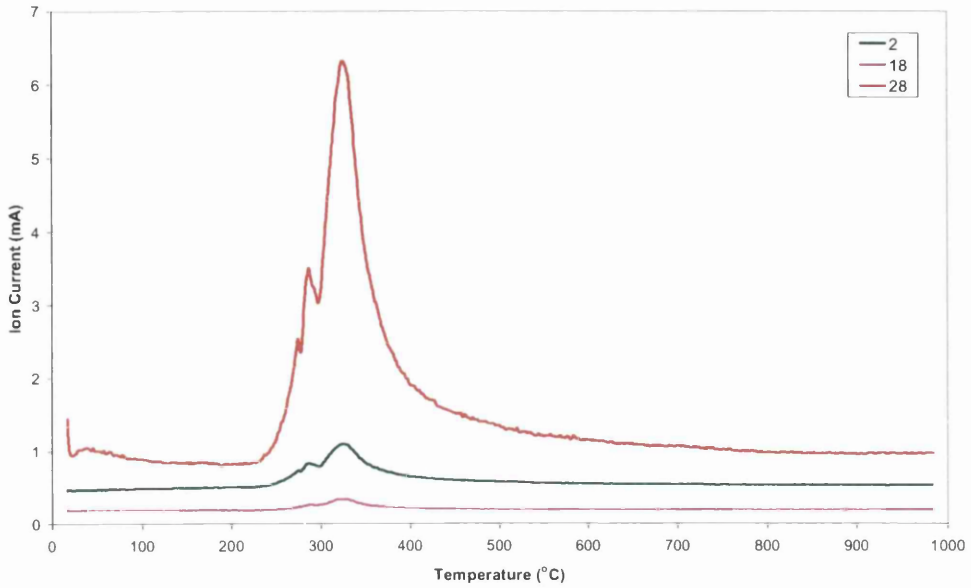

Again from the mass spectrometric data we can see that the decomposition of the cobalt precursor occurs via the evolution of hydrogen, water and carbon monoxide with small amounts of oxygen and carbon dioxide are also observed. These gases evolve over a wide temperature range and their peaks show several shoulders, suggesting more than one evolution.

Figure 4.70: Mass spectrometric data of H_2 (m/z=2), H_2O (m/z=18) and CO (m/z=28) for 99% silica + 1% titania supported cobalt catalysts in hydrogen.

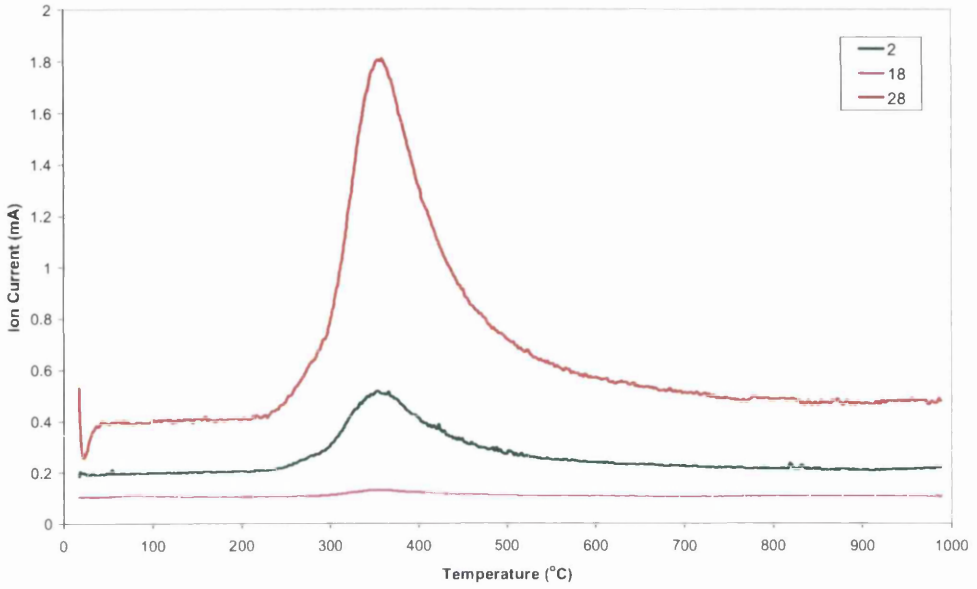

The mass spectrometric data for CoAST1 catalyst is similar to that of the CoAS. The gases all evolve over a broad temperature range with a maximum at 360°C. Again as well as hydrogen, water and carbon monoxide, small amounts of evolved oxygen and carbon dioxide were seen.

4.4.3.2.4 Hot-stage X-ray Diffraction (XRD)

Figure 4.71 : Hot-stage XRD patterns of cobalt acetate supported on silica in hydrogen.
Phases denoted are (¤) Co_3O_4 and (*) metallic Co The XRD pattern is offset for clarity.

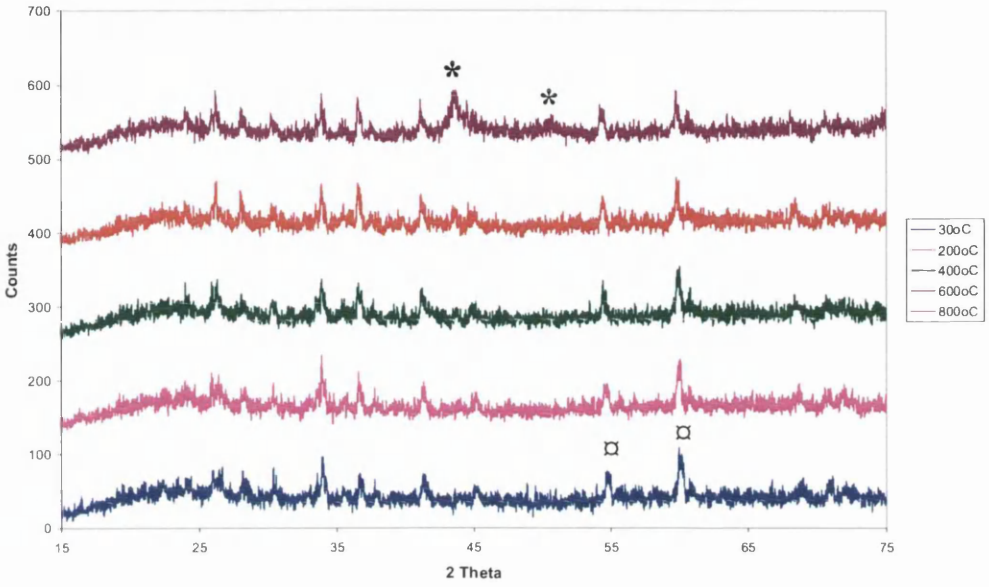

Figure 4.71 depicts the CoAS catalysts analysis by hot-stage XRD. From its pattern the presence of the spinel oxide at 30°C is recognised, and at 700°C and 800°C, metallic cobalt is detected. Using the Debye-Scherrer equation the crystallite size of these was found to be 20nm at 700°C and and 12 nm at 800°C.

Figure 4.72: Hot-stage XRD patterns of cobalt acetate supported on alumina in hydrogen.
Phases denoted are (¤) Co_3O_4 and (*) metallic Co. The XRD pattern is offset for clarity.

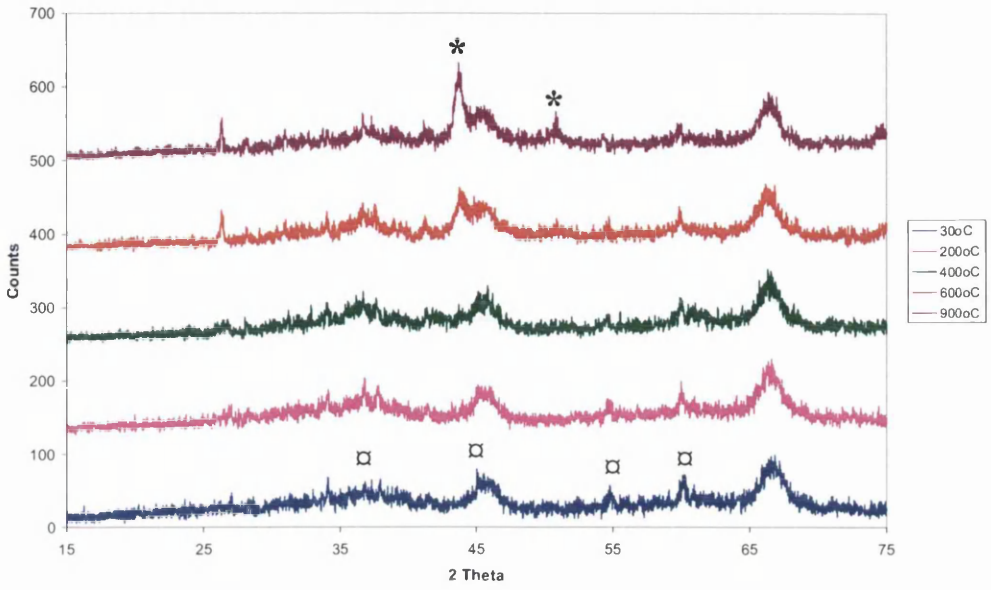

The hot-stage XRD patterns for CoAA catalysts are shown in figure 4.72. The pattern at 30°C shows the reflections characteristic of the Co_3O_4 spinel. Peaks appearing at 500°C indicate the presence of metallic cobalt. The cobalt metal crystallite size calculated by using the Scherrer equation are presented in table 4.10.

Table 4.10: Co metal crystallite size as determined by hot-stage XRD of cobalt acetate on alumina in hydrogen.

Temperature (°C)	Co metal crystallite size (nm)
600	10
700	13
800	13
900	12

Figure 4.73 **Hot-stage XRD patterns of cobalt acetate supported on 99% silica + 1% titania in hydrogen.**

Phases denoted are (¤) Co_3O_4, (+) CoO and (*) metallic Co. The XRD pattern is offset for clarity.

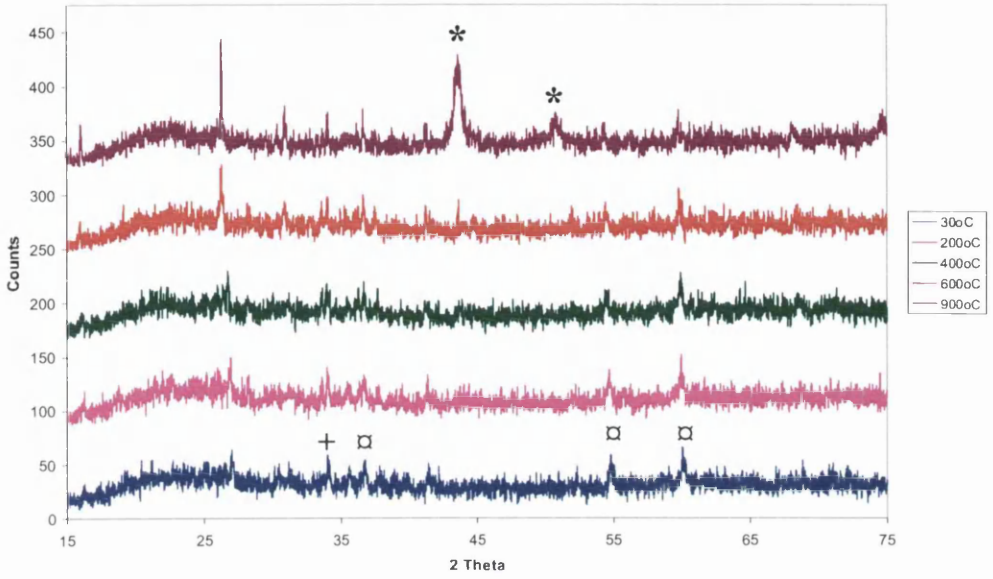

The hot-stage XRD pattern of CoAST1 is presented in figure 4.73. At 30°C as well as Co_3O_4 spinel phase, CoO appeared to be present. In this series of patterns, Co metal peaks are detected from 800°C. Using line broadening analysis, the cobalt metal crystallite size at 800°C and 900°C was found to be 12nm and 15 nm, respectively.

4.4.4 Argon (treatment 4)

4.4.4.1 Cobalt acetate

4.4.4.1.1 Thermogravimetric analysis-Differential Scanning Calorimetry (TGA-DSC)

Figure 4.74: TGA weight and derivative weight of cobalt acetate in argon.

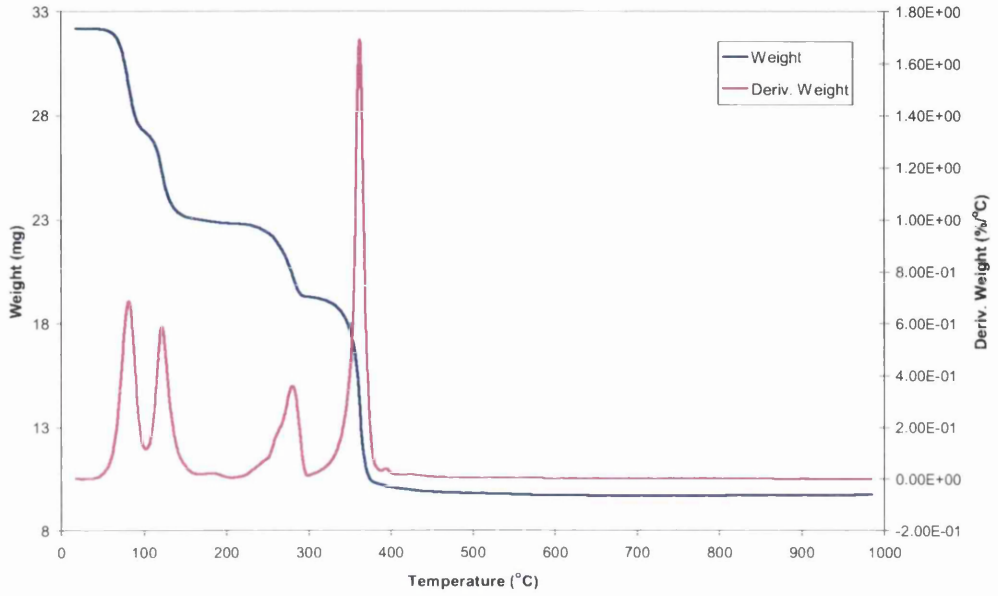

Figure 4.75: TGA-DSC weight and heat flow of cobalt acetate in argon.

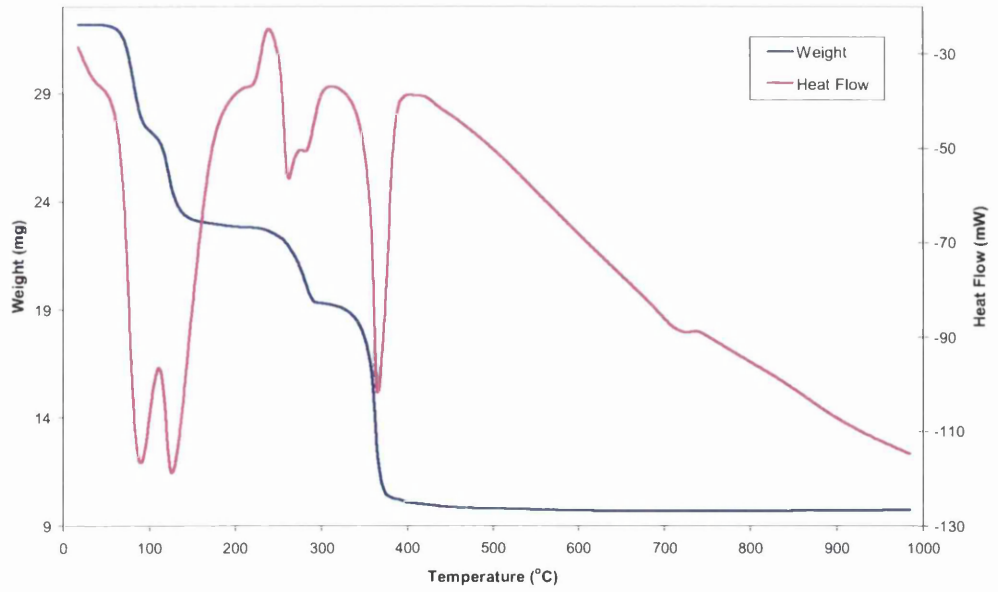

From the weight and derivative weight profiles in figure 4.74 it is clear that the majority of weight lost occurs below 400°C. The cobalt acetate decomposition occurs as four main weight loss events which can be seen from figure 4.75 to all be endothermic. From the mass spectrometric data, it can be seen that the decomposition occurs via the evolution of water, oxygen, carbon monoxide, carbon dioxide and hydrogen.

4.4.4.1.2 Mass Spectrometric analysis

Figure 4.76: Mass spectrometric data of H_2 (m/z=2), CO (m/z=28) and CO_2 (m/z=44) for cobalt acetate in argon.

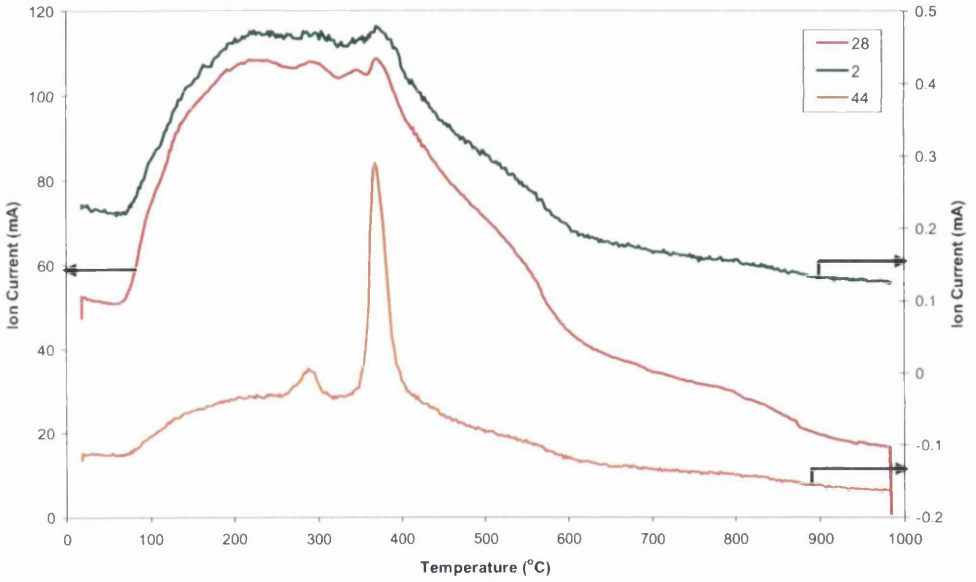

Figure 4.77: Mass spectrometric data of H_2O (m/z=18), and O_2 (m/z=32) for cobalt acetate in argon.

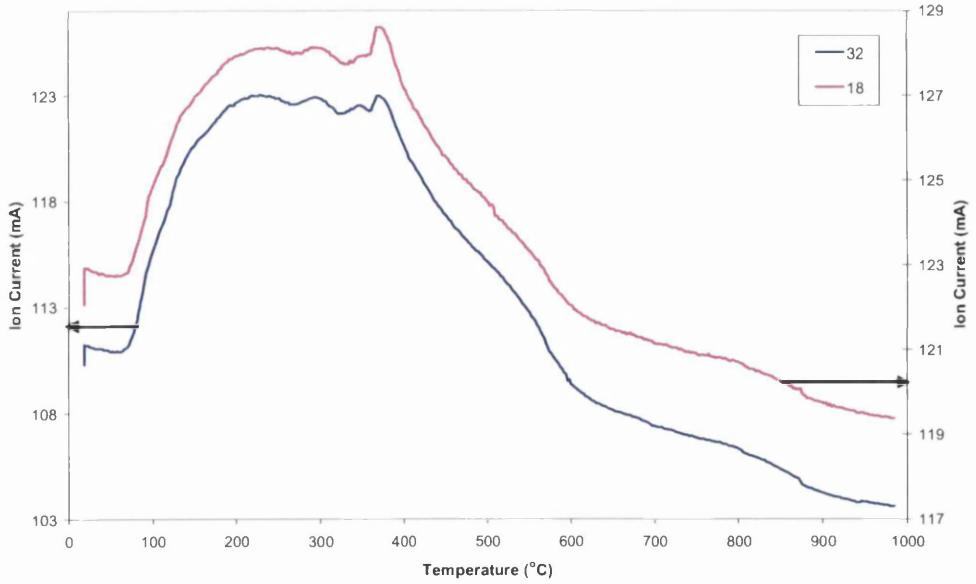

4.4.4.2 Cobalt acetate supported catalysts

4.4.4.2.1 Thermogravimetric analysis (TGA)

Figure 4.78: TGA weight profiles of silica, alumina and 99% silica + 1% titania supported cobalt catalysts in argon.

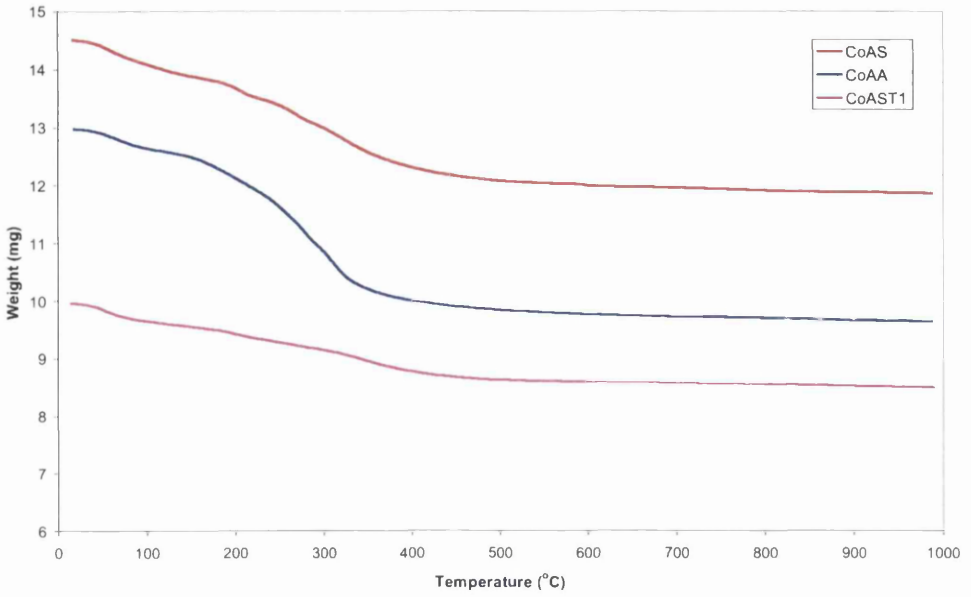

Figure 4.79: TGA derivative weight profiles of silica, alumina and 99% silica + 1% titania supported cobalt catalysts in argon.

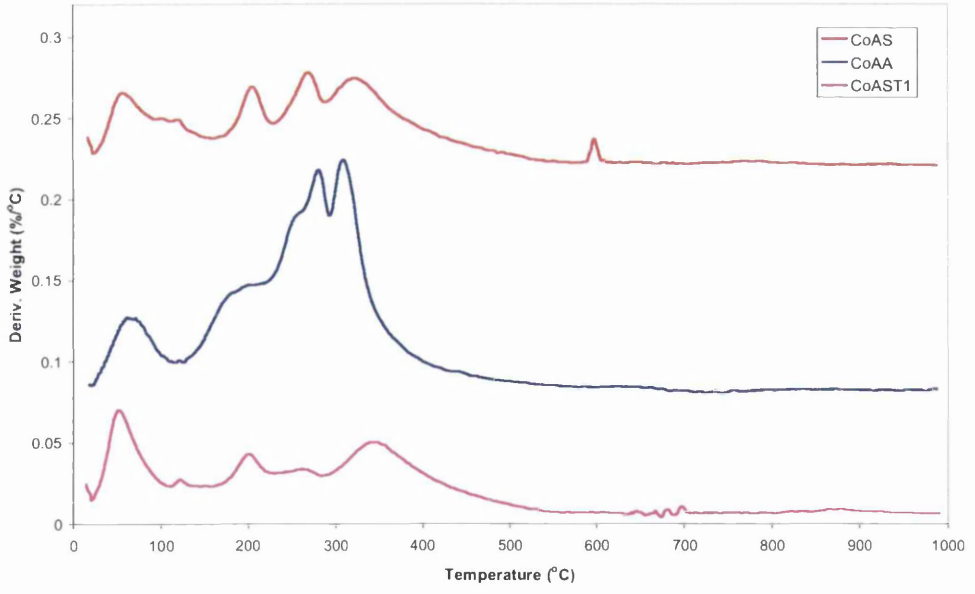

The TGA weight loss and derivative weight profiles, are presented in figures 4.78 and 4.79. From the weight loss curves it can be seen that the majority of weight is lost up to 550°C. For each of the catalysts, this weight loss can be observed as a series of several overlapping peaks in the derivative weight profile. There is very little significant weight loss after this temperature. The profiles for the CoAS and CoAST1are similar however the CoNS curves shows an additional small peak at 600°C.

4.4.4.2.2 Differential Scanning Calorimetry (DSC)

Figure 4.80: DSC heat flow profiles of silica, alumina and 99% silica + 1% titania supported cobalt catalysts in argon.

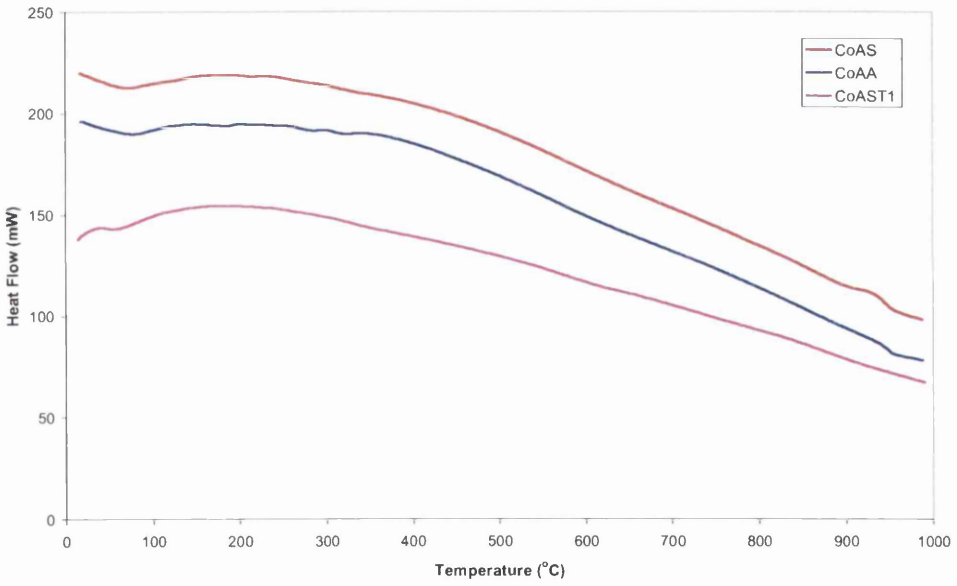

The DSC profile for each of the catalysts is shown in figure 4.80. An endothermic event occurs in all of the catalysts at around 80°C; thereafter there are several inflections seen on the profile for the CoAS and CoAA between 150-400°C. At higher temperatures an exotherm is observed from the DSC trace of CoAS at 935°C, and a small endotherm at 955°C is shown for CoAA.

4.4.3.1.1 Mass spectrometric analysis

Figure 4.81: Mass spectrometric data of H_2 (m/z=2), H_2O (m/z=18) O_2 (m/z=32), CO (m/z=28) and CO_2 (m/z=44) for silica supported cobalt catalyst in argon.

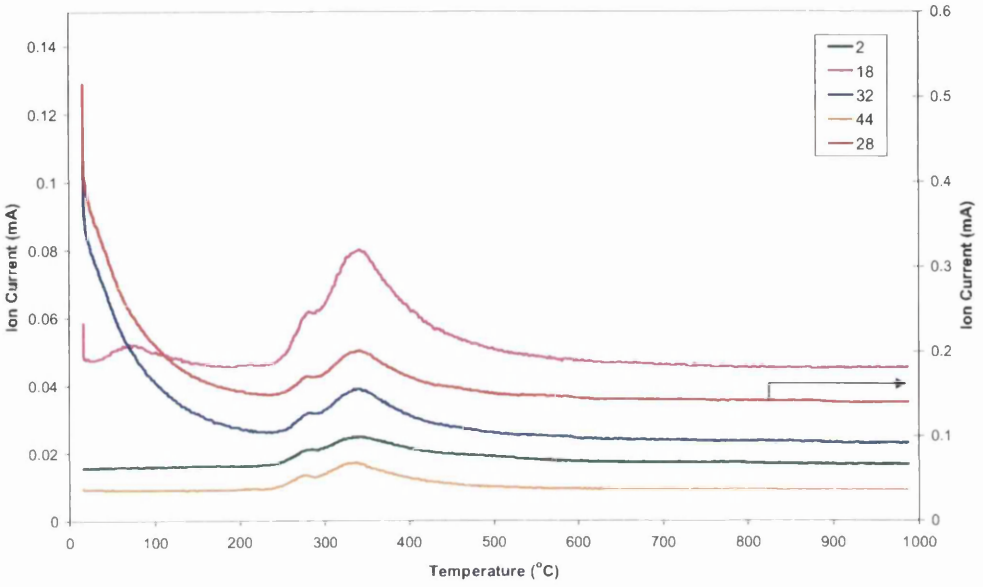

Figure 4.81 shows the evolution of products from the decomposition of the catalysts in argon. The main products during the decomposition in argon were hydrogen, water, carbon monoxide, oxygen and carbon dioxide. The evolution of all the different products occur at the same temperature around 340°C, and show a small shoulder on this main peak for each of the products. Water can also be seen to evolve at 70°C.

Figure 4.82: Mass spectrometric data of H_2 (m/z=2), H_2O (m/z=18) O_2 (m/z=32), CO (m/z=28) and CO_2 (m/z=44) for alumina supported cobalt catalyst in argon.

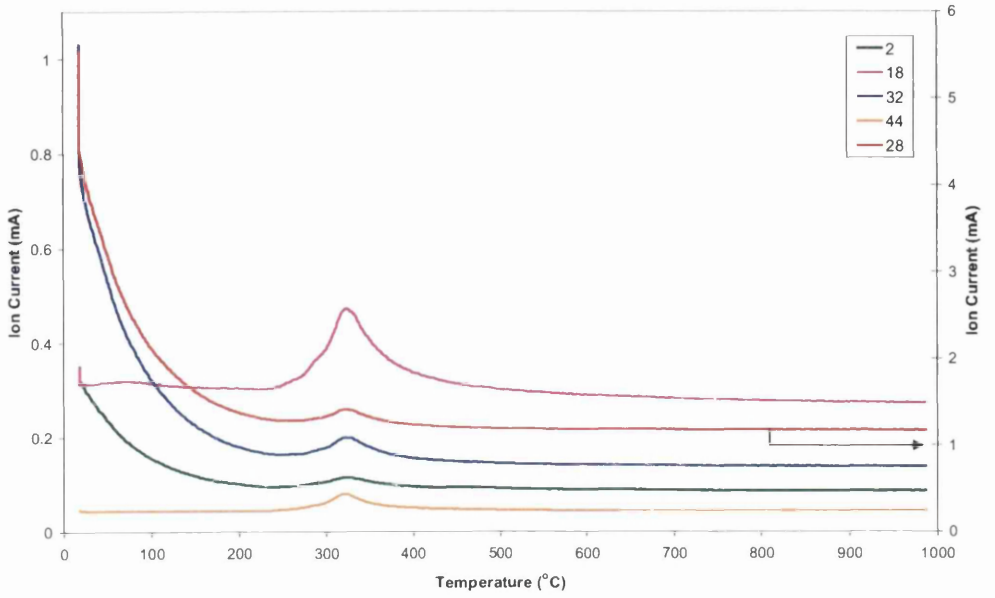

Figure 4.82 shows the products of decomposition for the CoAA catalyst. These all evolve as a broad peak at 326°C, with the exception of small amount of water at 80°C. Again the major products of the decomposition are hydrogen, water, carbon monoxide, oxygen and carbon dioxide.

Figure 4.83: Mass spectrometric data of H_2 (m/z=2), H_2O (m/z=18) O_2 (m/z=32), CO (m/z=28) and CO_2 (m/z=44) for 99% silica + 1% titania supported cobalt catalyst in argon.

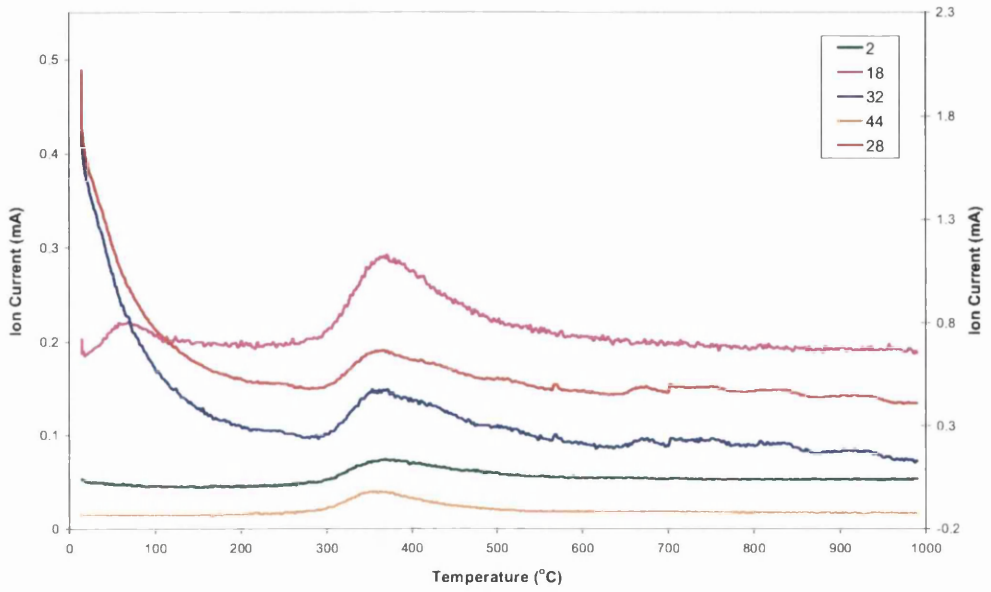

Mass spectrometric data for the decomposition of CoAST1 catalysts is shown in figure 4.83. Water is seen to evolve at 70°C, followed by a main broad peak of evolved gases around 370°C. These gases include hydrogen, water, carbon monoxide, oxygen and carbon dioxide. Several inflections on the mass spectrometric profiles for carbon monoxide and oxygen are seen at higher temperatures.

4.4.4.2.4 Hot-stage X-ray Diffraction (XRD)

Figure 4.84: Hot-stage XRD patterns of cobalt acetate on alumina in argon.
Phases denoted are (¤) Co_3O_4. The XRD pattern is offset for clarity.

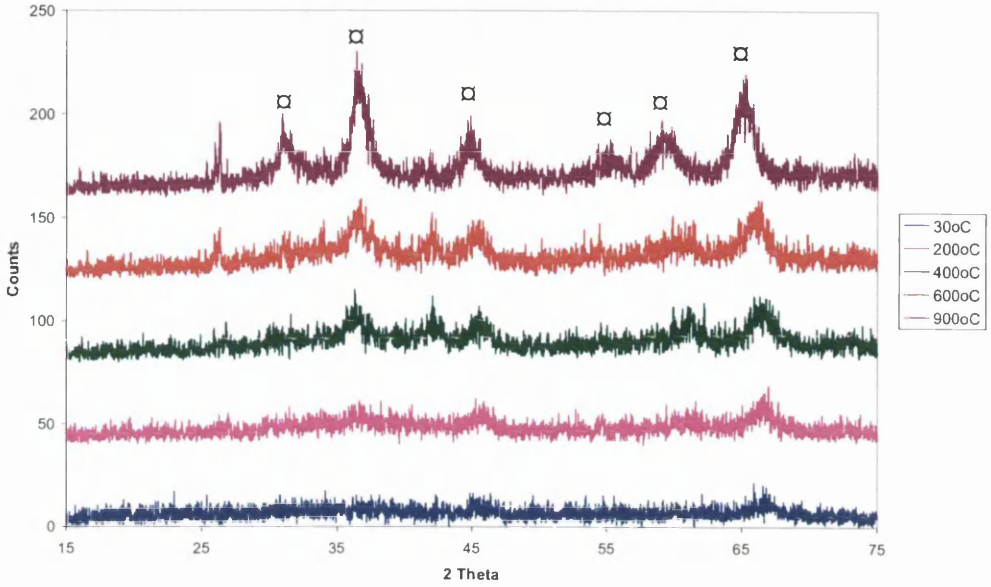

Hot-stage XRD analysis of CoAA catalyst is shown in figure 4.84. The peaks seen indicate the formation of Co_3O_4 particles. The average crystallite size was calculated using the Scherrer formula, by measuring the full width at half maximum of the most intense peak. The average Co_3O_4 crystallite size with temperature is shown in table 4.11.

Table 4.11: Co_3O_4 crystallite size as determined by hot-stage XRD of cobalt acetate on alumina in argon.

Temperature (°C)	Average particle size (nm)
400	13
500	8
600	7
700	5
800	7
900	7

Figure 4.85: Hot-stage XRD patterns of cobalt acetate on 99% silica + 1% titania in argon.
Phases denoted are (*) metallic Co. The XRD pattern is offset for clarity.

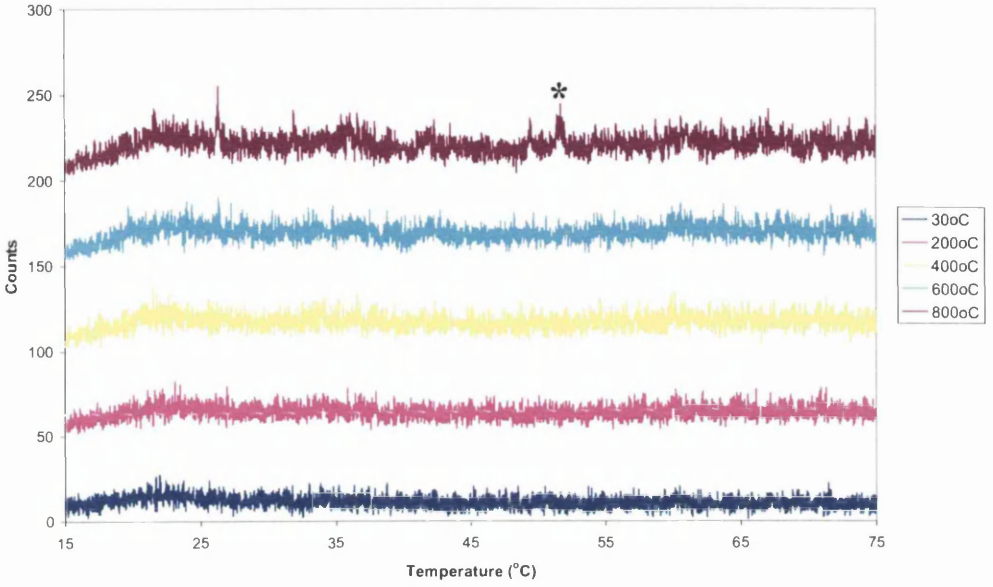

The hot-stage XRD patterns of CoAST1 catalyst are shown in figure 4.85. The sample appears to be mainly amorphous with almost no peaks seen. By 800°C a peak is seen at $2\theta=51.5^{\circ}$ corresponding to metallic cobalt. The crystallite size was calculated to be 14nm at 800°C.

5.0 DISCUSSION

5.1 Cobalt Nitrate

5.1.1 Argon

5.1.1.1 Cobalt nitrate

The decomposition of cobalt nitrate was followed by TGA-DSC together with online MS analysis of gaseous products with the results shown in section 4.3.4.1. Previous reports [22] have shown that the decomposition of cobalt nitrate proceeds as shown below, with the release of nitrogen dioxide, water and oxygen:

$$3[Co(NO_3)_2.6H_2O] \rightarrow Co_3O_4 + 6NO_2 + O_2 + 18H_2O$$

However, in the current study, the decomposition of the cobalt nitrate was accompanied by the evolution of nitrogen monoxide as well as water, oxygen and nitrogen dioxide. All decomposition events were endothermic and from the various techniques adopted the following table can be constructed:

Table 5.1: Weight loss temperatures and gases evolved for cobalt nitrate in argon.

Weight loss temperatures (°C)	Gases evolved
30-105	H_2O
105-243	H_2O, O_2
246	H_2O, O_2, NO, NO_2
271	H_2O, O_2, NO, NO_2
834	O_2, NO

Since the decomposition of cobalt nitrate was carried out in an inert gas, the weight loss corresponded to conversion to the oxide. The temperature at which the decomposition is completed is around 320°C, with two main decomposition events occurring at 246°C and 271°C. This indicates that the decomposition is more complex than the equation above

suggests. Given that the evolution is principally that of nitrogen monoxide, then the following equation maybe a more accurate representation:

$$3[Co(NO_3)_2.6H_2O] \rightarrow Co_3O_4 + 6NO + 18H_2O + 4O_2$$

However, given that a small amount of nitrogen dioxide is also produced, it is possible that decomposition is represented by both of these equations and may occur simultaneously.

From the calculated weight loss, the decomposition was found to proceed to Co_3O_4 by 400°C. Further weight loss at 834°C, accompanied by oxygen release, is due to the decomposition of the spinel oxide to the thermodynamically more stable divalent cobalt oxide[23]. This is represented by the equation shown below:

$$Co_3O_4 \rightarrow 3CoO + \tfrac{1}{2} O_2$$

The calculated experimental weight loss at 890°C is in keeping with the equation above.

5.1.1.2 Supported cobalt nitrate catalysts

Cobalt nitrate was impregnated onto silica, alumina and 99%silica + 1% titania supports in order to gain an insight into the effect of the support on the decomposition of the nitrate precursor. All of the supports have a hydroxylated surface, therefore interaction with the cobalt is expected especially during the decomposition process. The decomposition was followed to 1000°C by TGA-DSC with online MS as well as hot-stage XRD. The data is shown in section 4.3.4.2. From the various techniques adopted the following table can be constructed:

Table 5.2: Nitrate decomposition temperatures and gases evolved for supported cobalt nitrate catalysts in argon.

Catalyst	**Nitrate decomposition temperature (°C)**	**Gases Evolved**
CoNS	193, 220	NO, H_2O, O_2
CoNA	245, 346	NO, H_2O, O_2
CoNST1	304	NO, H_2O, O_2

It can be seen from the table that the change in support results in differences in the nature of the nitrate decomposition. For all the supported catalysts, analysis showed that the decomposition was endothermic, and accompanied by the evolution of gaseous NO, H_2O and O_2. Only a small amount of NO_2 was detected for the decomposition of the CoNS catalyst. The nitrate decomposition for the CoNS is similar to that of the bulk cobalt nitrate, in that the double event still occurs except that the maximum temperatures of the two nitrate decomposition events are reduced by around 50°C. Indicating that the support has a mild catalysing effect on the decomposition, probably due to the interaction of the support hydroxyls with the complex. However, the temperature at which the decomposition is completed was higher than that found with the unsupported compound. Like the cobalt nitrate decomposition, there is also a weight loss at slightly lower temperature of 825°C for the CoNS, and is again accompanied by the evolution of water. There are two possibilities for this event. It may be due to the break down of the spinel oxide to CoO, as seen with the bulk nitrate around the same temperature. However it also may be attributed to the interaction of the Co surface species with the support. It should be stressed that these two options are not mutually exclusive and a combination of both cannot be discounted. Unfortunately due to insufficient material to allow measurements to be performed there is no XRD data to confirm species present above these temperatures.

For the CoNA catalyst, the first nitrate decomposition event is at a similar temperature to that of the bulk metal nitrate however the second peak has shifted 75°C higher. Therefore in contrast to the silica support, which enhanced decomposition, the alumina stabilises a portion of the cobalt nitrate. No NO_2 gas was detected from the decomposition. From the XRD data, it can be seen that, after decomposition, the cobalt is present as the spinel oxide on the support. Therefore although the cobalt used to prepare the catalyst was in the trivalent form, after decomposition it is present as both trivalent and divalent states in the form of Co_3O_4. This is in keeping with the following equation:

$$\mathbf{3[Co(NO_3)_2.6H_2O] \rightarrow Co_3O_4 + 6NO + 18H_2O + 4O_2}$$

At 600°C, both Co_3O_4 and CoO as well as metallic cobalt are all present on the catalyst surface. By 700°C only metallic cobalt and cobalt oxide spinel are detected. It is not clear what the redox process is that converts cobalt oxide to metallic cobalt given that it is run in an inert atmosphere.

In contrast to the CoNST1 catalyst, there is no high temperature weight loss associated with the CoNA. This may be due to the stabilising effect of the alumina support, which is

seen to effect the decomposition events. The alumina may be stabilising the cobalt oxide spinel, shifting its conversion to CoO to a much higher temperature.

For CoNST1 catalyst the decomposition steps were not separated in a way that was seen with the bulk metal nitrate. Instead the decomposition occurs as a broad peak at a higher temperature, with a maximum at 310°C. The temperature at which the decomposition is complete was similarly increased. However weight loss around 860°C is similar to that seen with the pure cobalt nitrate, and is again accompanied by the evolution of oxygen. The possibilities for this event are as discussed with the CoNS catalyst.

The results suggest that the mechanism proposed for the decomposition of bulk cobalt nitrate in the literature [22] is invalid for supported cobalt nitrate. The decomposition on the support surfaces is dominated by the decomposition as depicted below:

$$3[Co(NO_3)_2.6H_2O] \rightarrow Co_3O_4 + 6NO + 18H_2O + 4O_2$$

However over the silica supported sample there is evidence that a small percentage of the cobalt nitrate may follow the decomposition equation detailed in the literature [22]. Following on from the production of Co_3O_4 there is subsequent decomposition to CoO. Hence the complete decomposition is:

$$3[Co(NO_3)_2.6H_2O] \rightarrow Co_3O_4 + 6NO + 18H_2O + 4O_2$$

$$Co_3O_4 \rightarrow 3CoO + \tfrac{1}{2} O_2$$

5.1.2 Oxygen

5.1.2.1 Cobalt nitrate

Results for the decomposition in oxygen of cobalt nitrate are shown in section 4.3.1.1. The oxidative decomposition was followed by TGA-DSC with on-line MS. Water, nitrogen monoxide, nitrogen dioxide and oxygen are the major gaseous products released during cobalt nitrate decomposition in oxygen.

Table 5.3: Weight loss temperatures and gases evolved for cobalt nitrate in oxygen.

Weight loss temperature (°C)	**Gas evolved**
40-216	H_2O, O_2
242	NO, NO_2
266	NO, NO_2
862	O_2

There are two endothermic decomposition events at 242°C and 266°C, corresponding to the evolution of NO and NO_2. Again the weight loss around 862°C is attributed to formation of CoO from the decomposition of the cobalt spinel, Co_3O_4. In keeping with this an evolution of oxygen also occurs at this temperature. Apart from the high temperature weight loss, the decomposition in oxygen is complete by 325°C. Since it is bulk cobalt nitrate, the weight loss corresponds to the conversion to the oxide. The overall weight loss by 500°C, after main decomposition, corresponds to the conversion to Co_3O_4. After the weight loss at 852°C, the measured weight loss (74%,) is identical to the theoretical weight loss expected for the decomposition of fully hydrated $Co(NO_3)_2.6H_2O$ complex to CoO. This suggests a stepwise decomposition of $Co(NO_3)_2.6H_2O$ to Co_3O_4 followed by decomposition of Co_3O_4 to CoO at high temperature. The presence of a low concentration of oxygen in the feed gas is insufficient to stop the thermodynamically driven conversion of Co_3O_4 to CoO. We could expect this conversion to be shifted to much higher temperatures if the concentration of oxygen used was increased.

5.1.2.2 Supported cobalt nitrate catalysts

The effect of the support on the oxidative nitrate decomposition was investigated, with TGA-DSC and online MS following the process as a function of temperature. The results obtained for the supported cobalt nitrate catalysts are shown in section 4.3.1.2.

Table 5.4: Nitrate decomposition temperatures and gases evolved for supported cobalt nitrate catalysts in oxygen.

Catalyst	**Nitrate decomposition temperature (°C)**	**Gases Evolved**
CoNS	200	NO, H_2O, O_2
CoNA	239, 340	NO, H_2O
CoNST1	290	NO, H_2O

From the results obtained, table 5.4 above can be produced. A marked effect of the support on the decomposition profile was observed, not only in terms of the temperature but also in terms of the gases evolved, *i.e.* there was no NO_2 evolved. In the case of the CoNS, most of decomposition occurs in a single event with a maximum rate of evolution of NO at 200°C, compared with the two separate events at higher temperature for the bulk metal nitrate. This is in keeping with the decomposition in argon where the silica support catalysed decomposition at a lower temperature. Although at a slightly higher temperature, the weight loss around 885°C occurs again accompanied by the evolution of oxygen. The two possibilities for this event are as discussed before with the argon in section 5.1.1.2.

The decomposition observed for CoNA still occurs as two separate events, although the temperature of the second peak is around 75°C higher and the completion of decomposition was delayed until around 485°C. Here again the alumina support acts to stabilize the nitrate complex in a manner found with the decomposition in argon.

CoNST1 catalyst decomposition in oxygen is similar to that seen in argon, occurring as a single event over a broad temperature range of c.a 125-455°C. It is clear that the partial processes of decomposition of the bulk metal nitrate are fused due to the influence of the support. From the XRD pattern at 500°C, after main decomposition, cobalt is present as the oxide spinel, Co_3O_4. On heating to 900°C the XRD pattern shows the presence CoO, cobalt

titinate and cobalt silicate. The weight loss and evolution of oxygen at 890°C is in keeping with the XRD pattern at 900°C, since the decomposition of the spinel Co_3O_4 to form the thermodynamically more stable CoO involves the release of oxygen.

Cobalt silicate and cobalt titanate are formed due to the interaction between cobalt surface species and support. It is unclear whether it is the spinel oxide or CoO species that reacts with the support to form cobalt silicate or it is during the decomposition of the spinel that the reaction takes place. Equations for both are shown below. The support interaction with the cobalt oxide spinel involves the stoichiometric release of oxygen. The equations are similar for the interaction of titania and cobalt oxide phases. Evaluating which processes are occurring is fraught with much difficulty. It should be noted though that the equations relating to the decomposition of the spinel oxide to the divalent cobalt and its subsequent reaction with the silica can be combined to produce the first equation.

$$2Co_3O_4 + 3SiO_2 \rightarrow 3Co_2SiO_4 + O_2$$

$$Co_3O_4 \rightarrow 3CoO + \tfrac{1}{2} O_2$$
$$2CoO + SiO_2 \rightarrow Co_2SiO_4$$

From the XRD data, the measured Co_3O_4 crystallite size for the CoNST1 sample are 26 nm at 500°C which is slightly larger than that of the CoNA catalyst which are 18 nm. With the CoNST1 catalyst we observe a significant difference between the decomposition of the pure nitrate and that of the supported complex. This reflects the different interaction between the complex and the support hydroxyl groups and hence the subtle differences in hydroxyl group properties between the different supports.

5.1.3 Hydrogen

5.1.3.1 Cobalt nitrate

TGA-DSC coupled to MS was used to investigate the reduction of cobalt nitrate as a function of temperature. The results are shown in section 4.3.3.1. The table below summarises the weight loss events observed:

Table 5.5: Weight loss temperatures and gases evolved for cobalt nitrate in hydrogen.

Weight loss temperature (°C)	Gas evolved
83	H_2O
122	H_2O
283	H_2, H_2O, NO, O_2, NO_2
366	H_2, H_2O, NO, O_2, NO_2
383-475	H_2O
506-625	H_2O
661-1000	H_2O

From the table the decomposition of the nitrate precursor can be seen clearly to occur as two separate events at 283°C and 366°C. These events are endothermic and are accompanied by the evolution of hydrogen, water, nitrogen monoxide, oxygen and nitrogen dioxide. Uptake of hydrogen and evolution of water are observed in three main events at approximately 407°C, 547°C and 911°C. These last three peaks are mostly likely to represent the sequential reduction of cobalt oxides to metallic cobalt.

5.1.3.2 Supported cobalt nitrate catalysts

Reduction of the supported cobalt nitrate catalysts was followed by TGA-DSC coupled to on-line MS. From this, decomposition of nitrate precursor and reduction of cobalt oxide to cobalt metal could be observed. The weight loss temperatures and gases evolved for these events are shown in table 5.6 below:

Table 5.6: Weight loss temperatures and gases evolved for supported cobalt nitrate catalysts in hydrogen.

Catalyst	Weight loss temperatures (°C)	Gas evolved
CoNS	186, 217, 241 283, 418, 812	H_2O, NO H_2O
CoNA	254 322, 556	H_2O, NO, N_2O H_2O
CoNST1	217 296, 565	H_2O, NO H_2O

Reduction of the CoNS catalyst is clearly a complex process. Decomposition occurs as three overlapping events at temperatures much lower than those observed for the double

decomposition event for the cobalt nitrate. NO_2 was only detected for two of the three nitrate decomposition events. Several peaks ranging from 283°C to 812°C accompanied by the uptake of hydrogen, corresponding to the evolution of water may be attributed to the reduction of the cobalt oxide species. These events are similar to that of the unsupported cobalt nitrate in that the reduction still occurs as three events, however, the maximum of these peaks is approximately 100°C lower in temperature. This suggests that similar to the effect seen with the nitrate decomposition in argon and oxygen, the silica support is causing the reduction to occur at a lower temperature. It is possible that this effect could be related to the dispersion of the cobalt species on the silica support compared with the bulk metal nitrate. This will increase the surface area of the cobalt complex, making more surface sites available and therefore causing reduction to occur more rapidly. Unfortunately, due to the poor separation of peaks and lack of XRD data, attribution of reduction events to specific reduction steps is not possible.

The reduction profile for the CoNA catalyst is much less complex. Decomposition of the nitrate occurs as a single event at a temperature much lower than the two decomposition events of unsupported cobalt nitrate. Therefore, in contrast to the treatments in argon and oxygen, where the alumina stabilized the cobalt nitrate, the support decreases the temperature of decomposition. Two reduction peaks corresponding to the uptake of hydrogen and evolution of water are observed at 322°C and 556°C. From previous studies [ref] these two events are most likely to represent a two-step reduction of Co_3O_4 to metallic cobalt. In quantifying these results, it is known that there is a direct relationship between the amount of hydrogen consumed and the amount of metal contained in the sample. Using this, it is possible to determine the oxidation state of the metal in the reaction. Integration of the two peak areas for the uptake of hydrogen gave a ratio of ~1:3 which could then be interpreted by the following equations:

$$Co_3O_4 + H_2 \rightarrow 3CoO + H_2O \qquad \text{moles } H_2 = 1$$

$$3CoO + 3H_2 \rightarrow 3Co^0 + 3H_2O \qquad \text{moles } H_2 = 3$$

It can be seen that a two-step reduction fits in well with the hydrogen consumption ratio for the CoNA catalyst in this study. This confirms that the reduction of Co_3O_4 proceeds in a stepwise manner possibly involving complete conversion to CoO prior to subsequent

reduction to metallic cobalt. The first peak attributed to the reduction of the trivalent Co to the divalent Co, and the second larger peak being the reduction of CoO to metallic Co.

The XRD pattern of CoNA at 300°C, after the nitrate decomposition, shows the presence of Co_3O_4 and CoO. It is thought that the Co_3O_4 is the product of the nitrate decomposition and since the first reduction peak begins before 300°C, that the CoO present is a consequence of the reduction of the spinel oxide. From the XRD pattern at 400°C, Co_3O_4 and CoO species are observed. At this temperature, the second reduction event has begun, therefore suggesting that not all the Co_3O_4 is reduced to CoO before the start of the second step of reduction. From 500-900°C, the presence of metallic cobalt is detected, however, some Co_3O_4 still remains.

For the CoNST1 catalyst, decomposition of the nitrate precursor occurs, as with the treatment in argon and oxygen, as a single event. It is observed at a lower temperature than both the decomposition events seen with unsupported cobalt nitrate. Similarly the reduction peaks occurring at 296°C and 565°C are at much lower temperatures. The second broad reduction seems to be overlapping with another event at 800-1000°C. It is thought this may be due to high temperature reduction of species cobalt silicate or cobalt titanate formed by diffusion of cobalt ions into the support lattice. From XRD at 300°C, after decomposition, Co_3O_4 is detected. The first reduction event occurs at this temperature, and is considered to be the reduction of the spinel oxide to the divalent cobalt. In keeping with this CoO is also present on the XRD pattern. By 400°C, as well as CoO, peaks indicating the presence of metallic cobalt are present. The second reduction event, has begun by this temperature, which is due to the reduction of CoO to metallic cobalt. At 900°C, cobalt metal is the only species present on the catalysts surface.

5.1.4 Hydrogen after calcination in oxygen (treatment 2)

5.1.4.1 Cobalt nitrate supported catalysts

Results from the reduction of supported cobalt nitrate catalyst after treatment in oxygen to 500°C are shown in section 4.3.2. This was carried out in an attempt to provide insight into the effect of reduction of the catalyst after calcination. The reduction was followed by TGA-DSC with on-line MS as well as hot-stage XRD to elucidate the steps observed. From the results, table 5.7 below can be constructed:

Table 5.7: Reduction temperatures and gases evolved for supported cobalt nitrate catalysts in hydrogen after calcination in oxygen.

Catalyst	Temperature (°C)	Gas evolved
CoNS	322, 417	H_2O
CoNA	354, 607	H_2O
CoNST1	331, 477	H_2O

For all of the supported cobalt nitrate catalysts, two reduction events are observed with the uptake of hydrogen and evolution of water. These events are all at lower temperatures than the reduction events for the cobalt nitrate. It should be mentioned that for some of the catalysts, the second broad reduction process seems to comprise of more than one peak. The different shoulders are likely to be due to the variation in oxide particle size and interaction with the support. Again, although the precise identity is not clear, the broad peaks above 750°C associated with the CoNS and CoNST1 catalyst profiles are attributed to the reduction of cobalt species that are in intimate interaction with the support, e.g., cobalt silicate/titanate. As before, the hydrogen consumption of the reduction events observed, corresponds to the stoichiometry of the two steps thought to be involved (Co_3O_4 → CoO → Co metal). This can be seen more clearly with better separation of events due to the decomposition of the nitrate occurring during the calcinations. Hot-stage XRD data is consistent with idea of the reduction occurring in a step-wise manner. From the XRD pattern for the CoNA at 200°C, before the first reduction peak, only Co_3O_4 is detected. At 300-400°C, during the first reduction peak, CoO is also present. By 500°C, during the second reduction event, metallic cobalt is detected. The hot-stage XRD for CoNST1catalyst is again consistent for the reduction, however, by 900°C as well as cobalt

metal, there is still some CoO present that has not been reduced. The CoNS catalyst shows the lowest reduction temperatures, this implies easier reduction, and therefore the weakest metal-support interactions.

5.2 Acetate

5.2.1 Argon

5.2.1.1 Cobalt acetate

Decomposition of cobalt acetate was followed by TGA-DSC with species evolved being identified by MS. The results are shown in section 4.4.4.1. The table below shows decomposition events and evolved species:

Table 5.8: Weight loss temperatures and gases evolved for cobalt acetate in argon.

Weight loss temperature (°C)	Evolved gas
83	H_2O
122	H_2O
283	H_2, H_2O, CO, CO_2, O_2
364	H_2, H_2O, CO, CO_2, O_2

From the table, it can be seen that the acetate decomposition occurs as two events at 283°C and 364°C. Since the decomposition is of the bulk cobalt acetate with no support, the total weight loss corresponds to the conversion of the oxide. In agreement with previous studies [14], weight loss calculations showed that decomposition of cobalt acetate proceeded to the oxide spinel, Co_3O_4, as the final product. All decomposition events were found to be endothermic. It is a noticeable difference that even though cobalt nitrate and cobalt acetate decompose to Co_3O_4 , the Co_3O_4 formed from the acetate does not convert to CoO at the temperature found for Co_3O_4 formed from the nitrate and the literature [23].

5.2.1.2 Supported cobalt acetate catalysts

The effect of the support on the acetate decomposition was investigated by TGA-DSC with on-line MS. The results are shown in section 4.4.4.2. Table 5.9 below shows the acetate decomposition temperatures and gases evolved for the supported catalysts:

Table 5.9: Acetate decomposition temperatures and gases evolved for supported cobalt acetate catalysts in argon.

Catalyst	Acetate decomposition temperature (°C)	Gas evolved
CoAS	286, 340	H_2, H_2O, O_2, CO, CO_2
CoAA	326	H_2, H_2O, O_2, CO, CO_2
CoAST1	370	H_2, H_2O, O_2, CO, CO_2

All the supports investigated had an effect on the profile of decomposition in terms of the temperatures involved. For CoAS decomposition is similar to cobalt acetate in that it occurs, although overlapping, as two events. The gases evolved were unchanged, however while the temperature of the first peak was unaffected, the maximum of the second peak was increased by around 25°C. In contrast to CoNS catalyst in argon, here the silica support acts to stabilize a fraction of the acetate complex.

Decomposition for the CoAA catalyst occurs as a single event at a temperature in the middle of the two decomposition events for cobalt acetate. Decomposition as with the bulk cobalt acetate is endothermic. The XRD patterns for CoAA confirm that as with the bulk acetate, Co_3O_4 is the product of the decomposition. In a manner similar to that of the nitrate supported catalyst CoNST1, decomposition occurs as a single event with a maximum temperature greater than the two events seen for the cobalt precursor. The hot-stage XRD patterns are amorphous until 800°C, where cobalt metal is detected. However, given that the catalyst is run in an inert atmosphere, it is not clear what the redox process is that converts cobalt oxide into metallic cobalt.

This highlights the difference between the two precursors. With the cobalt nitrate there is conversion of Co_3O_4 to CoO but no metallic cobalt formed, in contrast to this, with the cobalt acetate no conversion to CoO is present however metallic cobalt is formed.

5.2.2 Oxygen

5.2.2.1 Cobalt acetate

Results for the decomposition in oxygen of cobalt acetate are shown in section 4.4.1.1. Chemical species evolved during thermal treatment have been identified by TGA-DSC coupled to MS. The main decomposition events were all endothermic and are summarised in table 5.10 below:

Table 5.10: Weight loss temperatures and gases evolved for cobalt acetate in oxygen.

Weight loss temperature (°C)	**Gases evolved**
83	H_2O
123	H_2O
193	CO, CO_2
276	H_2O, CO, CO_2, O_2, H_2
364	H_2O, CO, CO_2, O_2, H_2
860	O_2

In addition to these endothermic events, a large exothermic event occurs between 388°C and 447°C, and is accompanied by the simultaneous uptake of oxygen and evolution of water, oxygen, carbon monoxide and carbon dioxide. However, the TGA data for this event suggest a weight gain. Previous reports [14] have observed a highly exothermic event in cobalt acetate decomposition and attributed it to the acetate combustion as shown the equation below:

$$3[Co(CH_3COO)_2.4H_2O] + 12.5\ O_2 \rightarrow Co_3O_4 + 12\ CO_2 + 21H_2O$$

However, the current study found that combustion of the acetate also involved the evolution of carbon monoxide. This suggests that the decomposition of cobalt acetate is more complex than the equation suggests. However, there is a difference between our experimental conditions and those used to form the equation above. The significantly lower concentration of oxygen used in this study may contribute to the formed carbon monoxide and hydrogen not being fully oxidised through to carbon dioxide and water.

Again the high temperature weight loss at 860°C is attributed to decomposition of the spinel oxide to the more stable CoO, accompanied by the evolution of oxygen.

5.2.2.2 Supported cobalt acetate catalysts.

Supported cobalt acetate catalysts decomposition in oxygen was investigated by TGA-DSC with coupled MS as a function of temperature. The results are shown in section 4.4.1.2. Table 5.11 below shows the decomposition steps and the gases evolved:

Table 5.11: Acetate decomposition temperatures and gases evolved for supported cobalt acetate catalysts in oxygen.

Catalyst	**Decomposition weight loss temperatures (°C)**	**Gases evolved**
CoAS	230	H_2O, CO, O_2, CO_2
	304, 336	H_2, H_2O, CO, O_2, CO_2
CoAA	320	H_2, H_2O, CO, O_2, CO_2
CoAST1	230	H_2O, CO, CO_2, O_2
	330, 355	H_2, H_2O, CO, O_2, CO_2

The decomposition of CoAS occurs as three exothermic events, with those at 304°C and 366°C overlapping and appearing almost as a broad single event. Compared with unsupported cobalt acetate, the two main decomposition events have converged, with the event at 304°C shifted 28°C higher, and the event at 336°C shifted 28°C lower.

The decomposition of the CoAA catalyst occurs as a broad event centred at 320°C and looks to consist of several overlapping peaks. The maximum of the CoAA decomposition event lies exactly between the main two decomposition events of the cobalt acetate. This suggests that the presence of the alumina has acted to combine these two separate events. XRD confirms that Co_3O_4 was the cobalt species present after the CoAA decomposition.

The profile of CoAST1 is similar to that of the CoAS catalyst, with decomposition occurring as three exothermic events. Again, the events at 330°C and 355°C are overlapping, almost appearing as one broad event. The main decomposition events have moved towards each other in terms of temperature, however, the first event has shifted considerably more than the second in this case.

5.2.3 Hydrogen (treatment 3)

5.2.3.1 Cobalt acetate

Reduction of cobalt acetate was followed by TGA-DSC coupled to on-line MS. The results are shown in section 4.4.3.1. Table 5.12 below shows the main weight loss events that occurred and the gases evolved:

Table5.12: Weight loss temperatures and gases evolved for cobalt acetate in hydrogen.

Weight loss temperature (°C)	Gas evolved
82	H_2O
122	H_2O
282	H_2O, O_2, CO_2
367	H_2O, O_2, CO, CO_2
388-489	H_2O
489-615	H_2O

From the table it can be seen that the acetate precursors decomposition in hydrogen occurs as two separate events centred at 282°C and 367°C. For both events, analysis showed that the decomposition was accompanied by the evolution of water, oxygen, carbon dioxide. Carbon monoxide was also detected for the second decomposition event. The events ranging from 388-615°C occur as two overlapping peaks and are accompanied by the uptake of hydrogen coinciding with the evolution of water, and are most likely to be associated with the reduction of the cobalt oxide to metallic cobalt. There is also a small weight loss event at around 873°C, however there was no evolved gas detected. From calculations, it appears that the cobalt is present as Co_3O_4 after acetate decomposition.

5.2.3.2 Supported cobalt acetate catalysts

Reduction of the supported acetate catalysts was followed by TGA-DSC coupled to online MS. The results are shown in section 4.4.3.2. Table 5.13 below shows the major weight losses and the gases evolved for these events:

Table 5.13: Weight loss temperatures and gases evolved for supported cobalt acetate catalysts in hydrogen.

Catalysts	Weight loss temperatures (°C)	Gas Evolved
CoAS	60	H_2O
	109	H_2O, CO_2
	129	H_2O, CO_2
	212	H_2O, CO_2
	272	H_2O, CO_2, H_2, O_2, CO
	338	H_2O, CO_2, H_2, O_2, CO
	637	O_2, CO
	956	H_2O
CoAA	71	H_2O
	188	H_2O
	282	H_2, H_2O, CO, O_2, CO_2
	317	H_2, H_2O, CO, CO_2, O_2
	360	H_2, H_2O, CO, CO_2, O_2
	500	H_2, CO_2
	538-737	H_2O
	above 737	H_2O
CoAST1	64	H_2O
	126	H_2O
	203	H_2O, CO_2, CO
	271	H_2O, O_2, CO_2, H_2, CO
	342	H_2O, O2, CO2, H_2
	553-649	H_2O, O_2
	649-988	H_2O, O_2

From the results it is clear that the reduction profile of the supported cobalt catalysts is complex with many overlapping events, this is also reflected in table 5.13 above. For the CoAS catalyst, decomposition occurs over a large temperature range involving several overlapping events ranging from 109°C to 637°C. The gases evolved vary with temperature, however they are unchanged compared with that of the unsupported cobalt acetate. Simultaneous uptake of hydrogen and evolution of water occurs with a maximum at 955°C, and is most likely due to the reduction of cobalt oxide to metallic cobalt. A shoulder is apparent around 850°C on reduction events suggesting, that like with the cobalt acetate, the reduction occurs in two steps. The reduction of the supported catalysts occurs at a much higher temperature than that of the bulk cobalt acetate and with much less separation between the two events. From the XRD metallic cobalt is detected at 700°C and 800°C.

For the CoAA, apart from the decomposition event occurring at 500°C, the temperature range for the precursor decomposition events is very similar to that of the bulk cobalt acetate. The gases evolved during decomposition are unchanged, however the decomposition occurs as three separate events compared with the two events for the cobalt

acetate. There is also an additional decomposition event occurring at 500°C, in this instance accompanied only by the evolution of hydrogen and carbon monoxide. This may suggest that the alumina support stabilises a portion of the acetate complex. Although at much higher temperatures, the reduction of CoAA catalyst like the bulk cobalt acetate occurs as two events. Peaks on the XRD patterns from 500°C indicate the presence of metallic cobalt. This suggests that the reduction to cobalt metal has begun at a slightly earlier temperature than the TGA data would suggest.

For the CoAST1 catalysts, decomposition occurs over a slightly lower temperature range. The gases evolved remained unchanged, although compared with the cobalt acetate, decomposition occurs with an additional event. Reduction again occurs as two events, although at higher temperatures than seen with the unsupported cobalt acetate. The XRD data confirms that metallic cobalt was present at 800°C and 900°C, suggesting that the second reduction peak is associated with the reduction to cobalt metal.

The lack of reduction associated with the cobalt acetate catalysts may suggest the formation of cobalt support oxides, such as cobalt silicate, that are only reducible at the upper temperature limits of the applied conditions.

5.2.4 Hydrogen after calcination in oxygen (treatment 2)

5.2.4.1 Supported cobalt acetate catalysts

Results from the cobalt acetate supported catalysts after treatment in oxygen to 500°C are shown in section 4.4.2.1. As mentioned before with the cobalt nitrate supported catalysts, this treatment was carried out to investigated the effect of reduction of the catalyst after calcination. The reduction was followed by TGA-DSC with on-line MS as well as hot-stage XRD to elucidate the steps observed. From the results, table 5.14 below can be constructed:

Table 5.14: Weight loss temperatures and gases evolved for supported cobalt acetate catalysts in hydrogen after calcination in oxygen.

Catalyst	Weight loss temperature (°C)	Gases Evolved
CoAS	246-400	H_2O
	400-703	H_2O
	above 703	H_2O
CoAA	317	H_2O
	369	H_2O
	466-698	H_2O
	698-779	H_2O
	above 779	H_2O
CoAST1	262-429	H_2O
	429-660	H_2O
	above 660	H_2O

All the weight losses for each of the catalyst is accompanied by the uptake of hydrogen and the evolution of water with the heat flow data for each of the catalysts relatively featureless. For CoAS, there appear to be two reduction events followed by a continuous weight loss region above 703°C. The lack of XRD data, due to insufficient material, makes attribution of the reduction peaks difficult. However it is clear that the reduction begins around 140°C lower for the supported catalyst compared with that of the cobalt acetate. For the CoAA, reduction occurs as several events again with a continuous weight loss region above 700°C. From the hot-stage XRD data, the presence of metallic cobalt is detected at 500°C. This may suggest that peak starting at 466°C is associated with the reduction of cobalt oxide to metallic cobalt. Further peaks at higher temperatures are then likely to be due to the variation in oxide particle size and interaction with the support. The above 779°C may be ascribed to the reduction of cobalt alumina species. For the CoAST1 reduction is similar to the CoAS, with two reduction events followed by a continuous

weight loss region above 660°C. The hot-stage XRD data confirm the presence of metallic cobalt at 700°C, suggesting that it is the event above 660°C that is ascribed to the reduction of cobalt oxide to metallic cobalt. Unfortunately, unlike with the cobalt nitrate supported catalysts, the stoichiometry of the reduction process is difficult to elucidate form the mass spectrometric data.

6.0 CONCLUSIONS

Throughout this research project, the experimental work was carried out with the aim of compiling information regarding the effect of both the support and the precursor on structural and chemical properties of cobalt supported catalysts. Valuable insights into both concerns were obtained and are summarised in this section.

6.1 Support effect

From characterisation carried out using TGA-DSC coupled to an online mass spectrometer, it was discovered that the support had a significant effect on both the decomposition and reduction of supported cobalt catalysts. The silica support had a mild catalysing effect on the catalyst decomposition whereas the alumina was found to stabilise portions of the precursor. The 99% silica + 1% titania support fused the decomposition events into one single broad event. In all the catalysts Co_3O_4 was found to be the cobalt species present after decomposition. In all of the supported catalysts the reducibility was increased in comparison with the bulk cobalt salts. Pre-calcination of the catalysts further increased reducibility. Using TGA and XRD analysis, the reduction to was found to occur as a step wise process, involving the conversion to CoO before being reduced to metallic cobalt. The most easily reduced catalyst was the CoNS, therefore suggesting that the silica had the least interaction with the cobalt metal.

6.2 Precursor effects

The effect of the precursor was examined using cobalt nitrate and cobalt acetate salts, and the various techniques carried out highlighted a number of differences. While decomposition events of the supported nitrate catalysts occurred as distinct events, those prepared from the acetate salts observed fused decomposition events, with the exception of the CoAS in oxygen. Furthermore, the cobalt acetate decomposition is highly exothermic compared with that of the cobalt nitrate catalysts, and also proceeds at higher temperatures. Reduction of the supported cobalt oxide species occurs as two distinctive effects on cobalt nitrate catalysts whereas with the cobalt acetate catalysts it is more complex, comprising of several overlapping peaks.

Further worthwhile investigations could involve T.E.M analysis to confirm the size of the particles calculated from the hot-stage XRD. As well as this it would be useful to confirm the cobalt species present by means of temperature programmed UV-visible analysis.

7.0 REFERENCES

[1] J.H. Clark, *Catalysis of organic reagents by supported inorganic reagents*, 1836 **21**

[2] Level 3 Heterogeneous Catalysis Course; S D Jackson 2004.

[3] M. Bowker; *The basis and applications of heterogeneous catalysis*, Oxford Chemistry Primers. 1998, Oxford: Oxford science.

[4] P Concepción, C. López, A. Martínez, V.F. Puntes *J. Catal.*, 2004, **228,** 321

[5] W. Raróg-Pilecka, E. Miśkiewicz, M. Matyszek, Z. Kaszkur, L. Kępiński, Z. Kowalczyk, *J. Catal.*, 2006, **237,** 207

[6] R. Riva, H. Miessner, R.Vitali, G. Del Piero, *Appl. Catal. A: General*, 2000, **196**, 111

[7] M. Voß, D. Borgmann, G.Welder, *J. Catal.*, 2002, **212**, 10

[8] S. Storsæter, B. Tøtdal, J.C. Walmsley, B.S. Tanem, A. Holmen, *J. Catal.*, 2005, **236**, 139

[9] G. Jacobs, T.K. Das, Y. Zhang, J. Li, G. Racoillet, B. H. Davis *Appl. Catal. A: General*, 2002, **233**, 263

[10] A.M. Saib, M. Claeys, E. van Steen, *Catal. Today,* 2002, **71**, 395

[11] J. van de Loosdretch, M. van der Haar, A.M. van der Kraan, A.J. van Dillen, J.W. Gens Appl. *Catal. A: General*, 1997, **150**, 365

[12] A. Martínez, C. López, F. Márquez, I. Díaz, *J. Catal.*, 2003, **220**, 486

[13] J. Panpranot, S. Kaewkun, P.Praserthdam, J.G. Goodwin, Jr., *Catalysis Letters*, 2003, **91**, 95

[14] J-S. Giradon, A.S.Lermontov, L. Gengembre, P.A. Chernavskii, A. Griboval-Constant, A.Y. Khodakov, *J. of Catal*, 2005, **230**, 339

[15] H. Schulz, *Appl. Catal A: General*, 1999, **186**, 3

[16] M.E. Dry, *Catal Today*, 2002, **71**, 227

[17] Promotional Effects in Co-based Fischer-Tropsch catalysis, Catalysis, Royal Society of Chemistry, Volume 19, 2006

[18] B. Ernst, S. Libs, P. Chaumette, A. Kiennemann, *Appl. Catal A:General*, 1999, **186**, 145

[19]*Fundamentals of Industrial Catalytic Processes*, Wiley-Interscience, New Jersey, 2006

[20] R. Oukaci, A.H. Singleton, J.G. Goodwin Jr, *Appl. Catal. A:General*, 1999, **186**, 129

[21] A.Y. Khodakov, R.Bechara, A. Griboval-Constant, *Appl. Catal. A:General,* 2003, **254**, 273

[22] T. Cersi, S. Békássy, G. Kenessey, G. Liptay, F. Figueras, *Thermochim. Acta*, 1996, **288**, 137

[23] *Handbook of chemistry and physics,* CRC press, Florida, 1986, p. B-87